SUPPLEMENTARY INFORMATION

Antifungal mono- and dimeric nitrogenous bisabolenes from an unknown sponge of the order Bubarida from Futuna Islands

Maria Miguel-Gordo,[a] Maggie M. Reddy,[a] Pilar Sánchez,[b] Jordan J. Buckley,[a] Thomas A. Mackenzie,[b] Laurence K. Jennings,[a] Fernando Reyes[b], Kevin Calabro,[a] and Olivier P. Thomas*[a]

[a.] Marine Biodiscovery Laboratory, School of Chemistry and Ryan Institute, National University of Ireland Galway, University Road, Galway H91 TK33, Ireland

[b.] Fundación MEDINA, Centro de Excelencia en Investigación de Medicamentos Innovadores en Andalucía, Parque Tecnológico de Ciencias de la Salud, Avenida del Conocimiento 34, Armilla, Granada E-18016, Spain.

Contents

SUPPLEMENTARY INFORMATION

Biological description of the samples

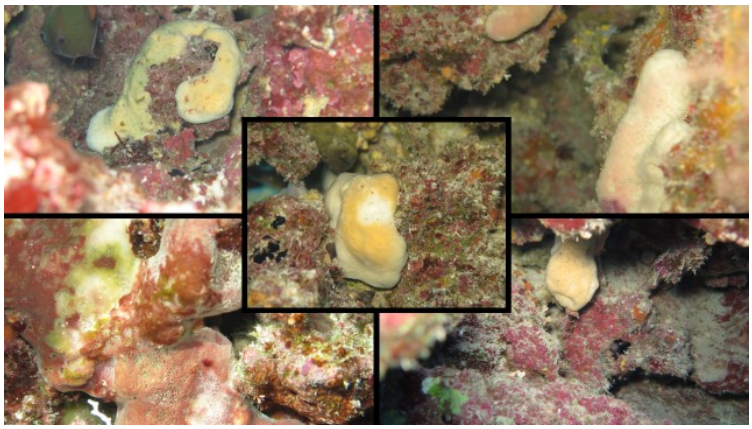

In situ underwater photographs of sponge specimens of the order Bubarida.

Three samples (Fu05-01, Fu07-05 and Fu07-06) were selected for DNA analyses. Samples were stored in 96% ethanol and subsamples were carefully dissected to avoid epiphytes. DNA was isolated from approximately 10 mg of tissue using the Qiagen DNeasy Blood and Tissue kit (Manchester, UK). Methods followed the manufacturers protocol but with the addition of proteinase k and slightly extended incubation periods. The quality and quantity of DNA extracts were assessed and diluted appropriately (1:10-1:100). The standard barcoding gene for sponges, a partial region of the 28s rDNA gene, was amplified using the primers C2-D2 (Chombard et al. 1998). PCRs were carried out in 25 µl reactions consisting of 12.5 µl DreamTaq Hot Start Green PCR Master Mix (Thermo Fischer Scientific, Ireland), 0.1-0.5 µM of each primer, 1 µl BSA (BioSciences, Ireland) and nuclease-free PCR water. Thermal profiles followed those of Morrow et al. 2012 and the annealing temperature determined following successive temperature gradients. PCR products were cleaned with ExoSAP-IT™ (BioSciences, Ireland) as per the manufacture's recommendations. PCR products were sequenced using an ABI 3730 XL sequencer at LGC Genomics (Berlin, Germany).

Sequences were validated on BLAST (Basic Local Alignment Search Tool) and closely related taxa were sourced from the initial BLAST search and the literature. The alignment was edited in Geneious 10.2.4 (Biomatters Ltd, New Zealand) and an appropriate model of evolution determined using jModelTest v. 2.0.[1] Bayesian Inference (BI) and Maximum Likelihood (ML) phylogenetic trees were generated using Mr Bayes v. 3.2.6,[2] and RAxML BlackBox (https://raxml-ng.vital-it.ch/#/). For the BI analysis trees were run for 1 million generations using MCMC and hot and cold chains. The stationarity of trees was assessed with Tracer v. 1.5.[3] The first 25 % of all trees were discarded as burn-in and the remaining trees used to estimate PP support values. For the ML analysis, the GTR model of evolution was used, and all other parameters set as standard. Support values were estimated from 100 bootstrap pseudoreplicates. All support values were indicated at the internode of well-supported clades (>0.85,75%). The tree was rooted on its midpoint.

[1] D. Darriba, G. L. Taboada, R. Doallo and D. Posada, Nat. Methods, 2012, 9, 772-772.
[2] F. Ronquist and J. P. Huelsenbeck, Bioinformatics, 2003, 19, 1572-1574.
[3] A. Rambaut, A. J. Drummond, D. Xie, G. Baele and M. A. Suchard, Syst. Biol., 2018, 67, 901-904.

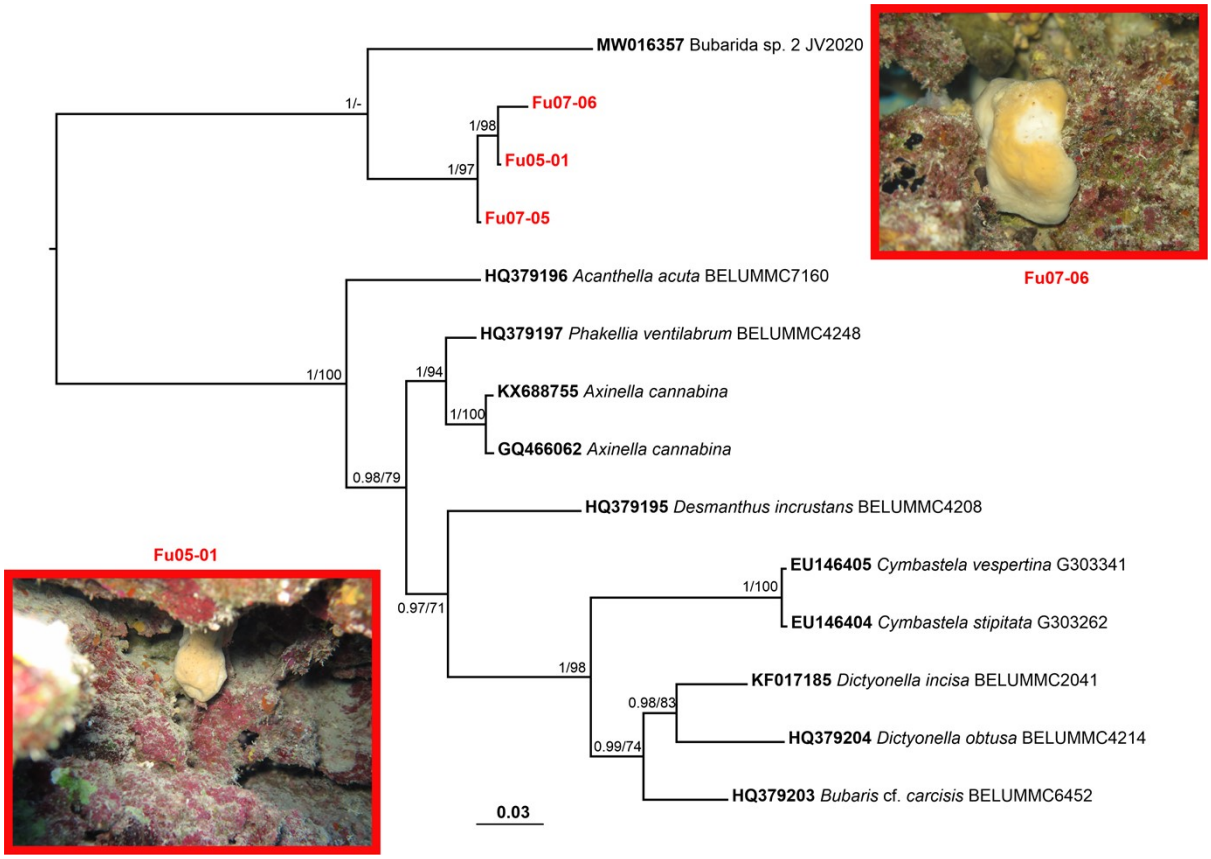

All three specimens were resolved within a single well-supported clade (PP: 1; BP: 97). This clade was sister to a recently identified specimen collected from Hawaii, Bubarida sp. 2 JV-2020.[4] These taxa combined were resolved within a larger clade shared with taxa currently assigned to the order Bubarida such as species of *Acanthella*, *Dictyonella*, *Bubaris*.

[4] J. Vicente, M. K. Webb, G. Paulay, W. Rakchai, M. A. Timmers, C. P. Jury, K. Bahr and R. J. Toonen, Coral Reefs, 2021, DOI: 10.1007/s00338-021-02109-7.

Biological activity assays

Table S1. MIC values (µg/mL) for the compounds isolated from the order Bubarida sponge against microbial pathogens.

Compounds	MIC [µg/mL]								
	C. albicans ATCC64124	*C. glabrata* ATCC2001	*C. krusei* ATCC6258	*C. parapsilosis* ATCC22019	*C. tropicalis* ATCC750	*A. fumigatus* ATCC46645	*A. baumannii* *ATCC19606*	*E. coli* ATCC25922	MSSA ATCC29213
Bubaridin A (**1**)	> 64	> 64	> 64	> 64	> 64	>32	>32	> 64	> 64
Bubaridin B (**2**)	> 32	> 32	> 32	> 32	> 32	>32	>32	> 32	> 32
Bubaridin D (**4**)	> 32	> 32	> 32	> 32	> 32	>32	>32	> 32	> 32
Bubaridin E (**5**)	> 48	> 48	> 48	> 48	> 48	>48	>48	> 48	> 48
Bubaridin F (**6**)	> 48	> 48	> 48	> 48	> 48	> 48	>48	> 48	> 48
Trans -dimer theonellin isocyanide (**7**)	32	1	> 64	8	> 64	32-64	>64	> 64	> 64
Cis -dimer theonellin isocyanide (**8**)	> 64	16-32	> 64	> 64	> 64	>32	>64	> 64	> 64
Cis -dimer theonellin formamide (**9**)	> 64	> 64	> 64	> 64	> 64	>64	>32	> 64	> 64
N,*N*'-bis[(6*R*,7*S*)-7-amino-7,8-dihydro-α-bisabolen-7-yl]	> 64	32	> 64	> 64	> 64	>64	>64	> 64	> 64
Aureol	> 64	> 64	> 64	> 64	> 64	>64	>64	> 64	16
Theonellin formamide	> 48	> 48	> 48	> 48	> 48	>48	>48	> 48	> 48
Control	2-4	2-4	2-4	4	4	2	8	0.25	1
	Anfotericin B						Aztreonam	Colistin	Vancomycin

Table S2. AC_{50} (µg/mL) activity for cytotoxicity against multiple human cell lines

Compounds	AC_{50} [µg/mL]				
	A549	A2058	HepG2	MCF-7	MiaPaca-2
Trans -dimer theonellin isocyanide (**7**)	> 20	13.5 [12.56-14.62]	> 20	> 20	> 20
Cis -dimer theonellin isocyanide (**8**)	> 20	> 20	> 20	> 20	> 20
Cis -dimer theonellin formamide (**9**)	> 20	> 20	> 20	> 20	> 20
N,*N*'-bis[(6*R*,7*S*)-7-amino-7,8-dihydro-α-bisabolen-7-yl]	> 20	> 20	> 20	> 20	> 20

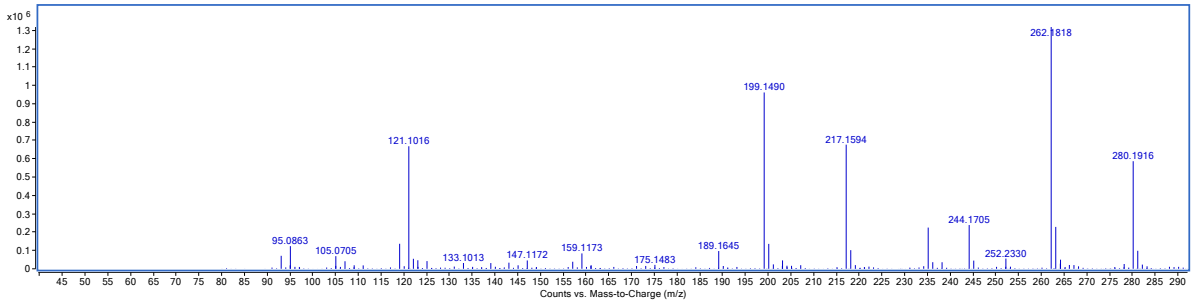

Figure S1. (+)-HRESIMS spectrum of bubaridin A (***rac*-1**)

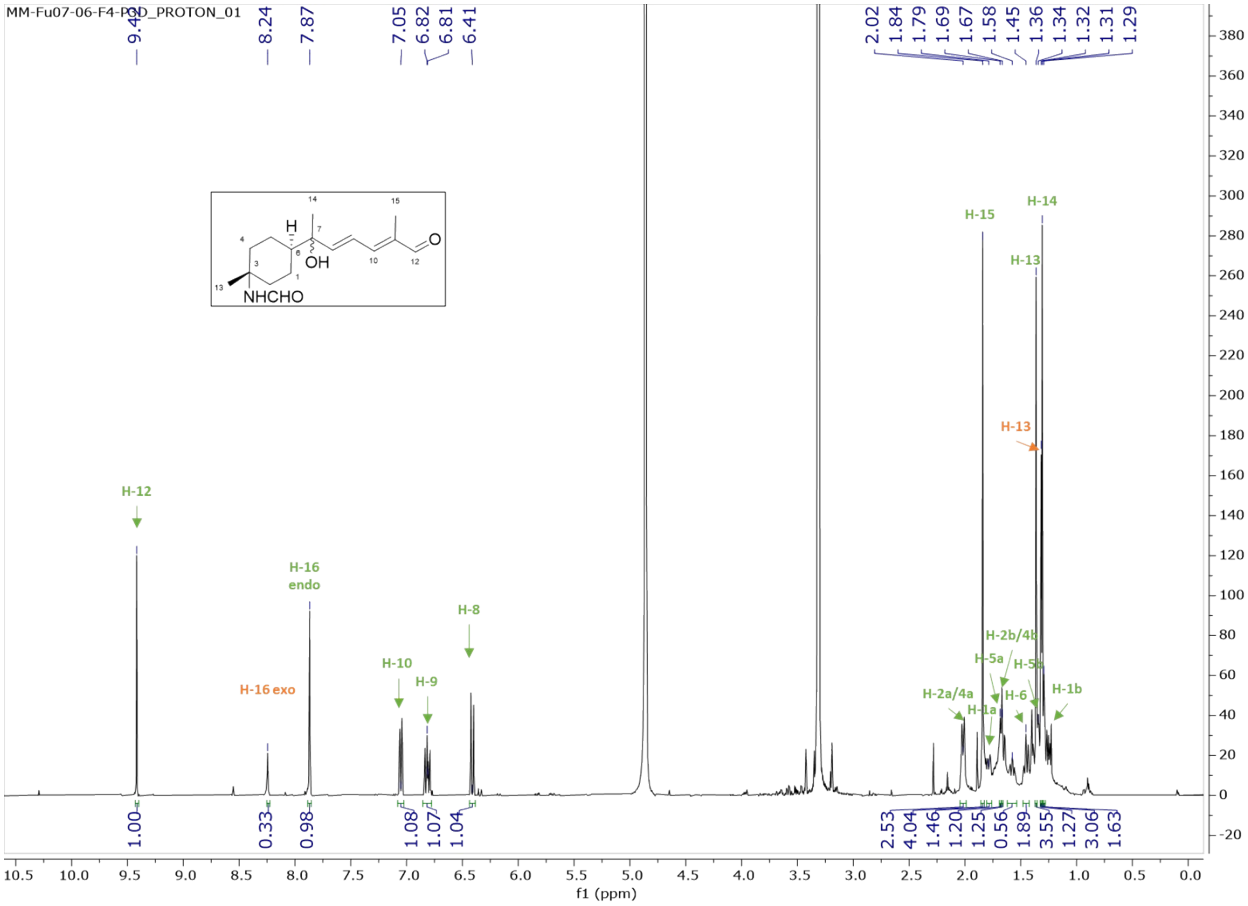

Figure S2. ^{1}H-NMR spectrum of bubaridin A (***rac*-1**) at 600 MHz in CD_3OD

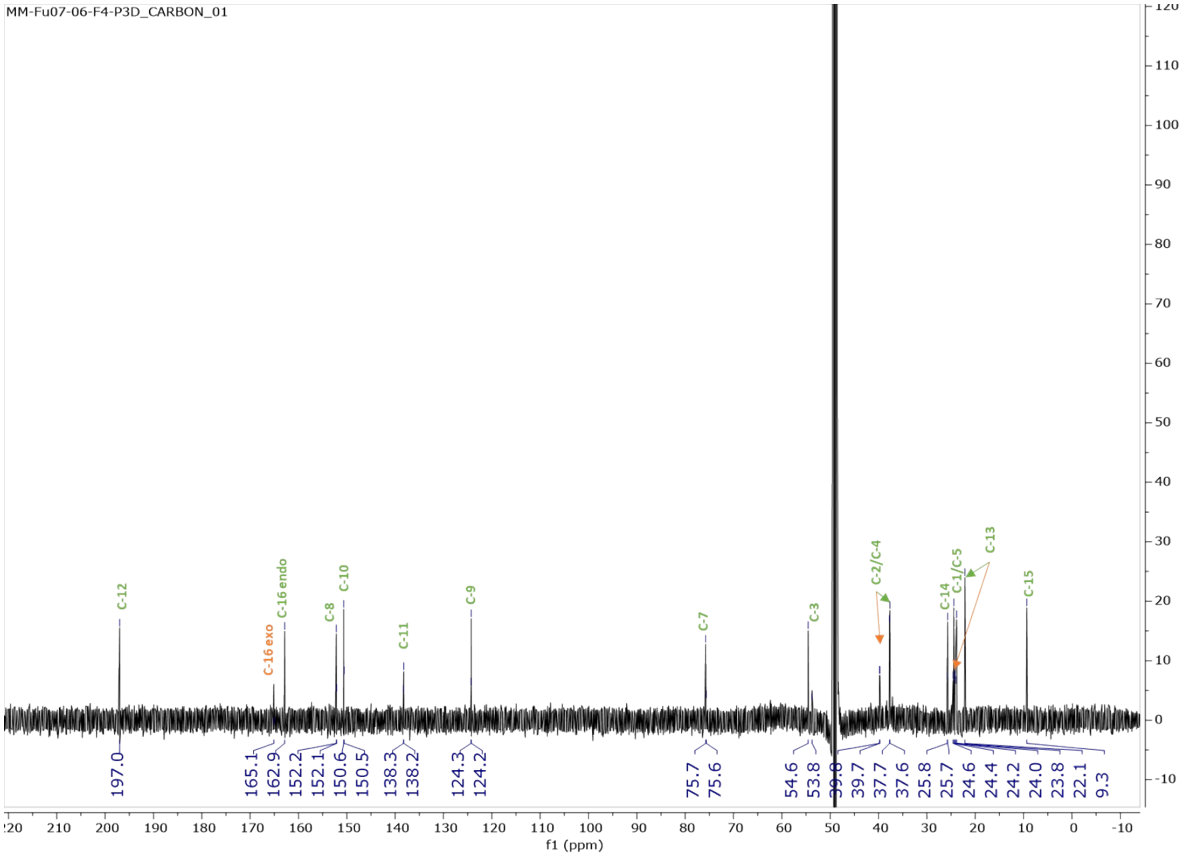

Figure S3. ^{1}H-NMR spectrum of bubaridin A (***rac*-1**) at 150 MHz in CD_3OD

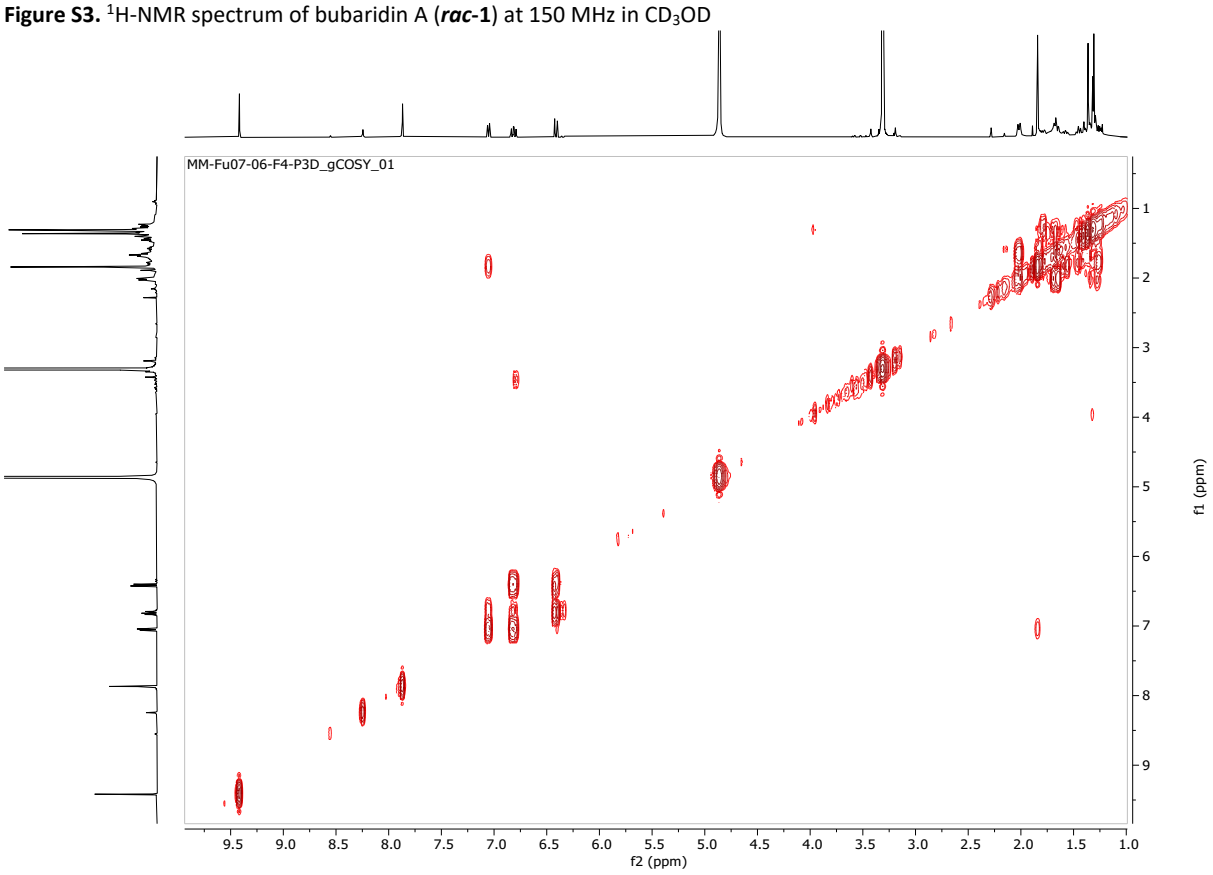

Figure S4. COSY spectrum of bubaridin A (***rac*-1**) at 600 MHz in CD_3OD

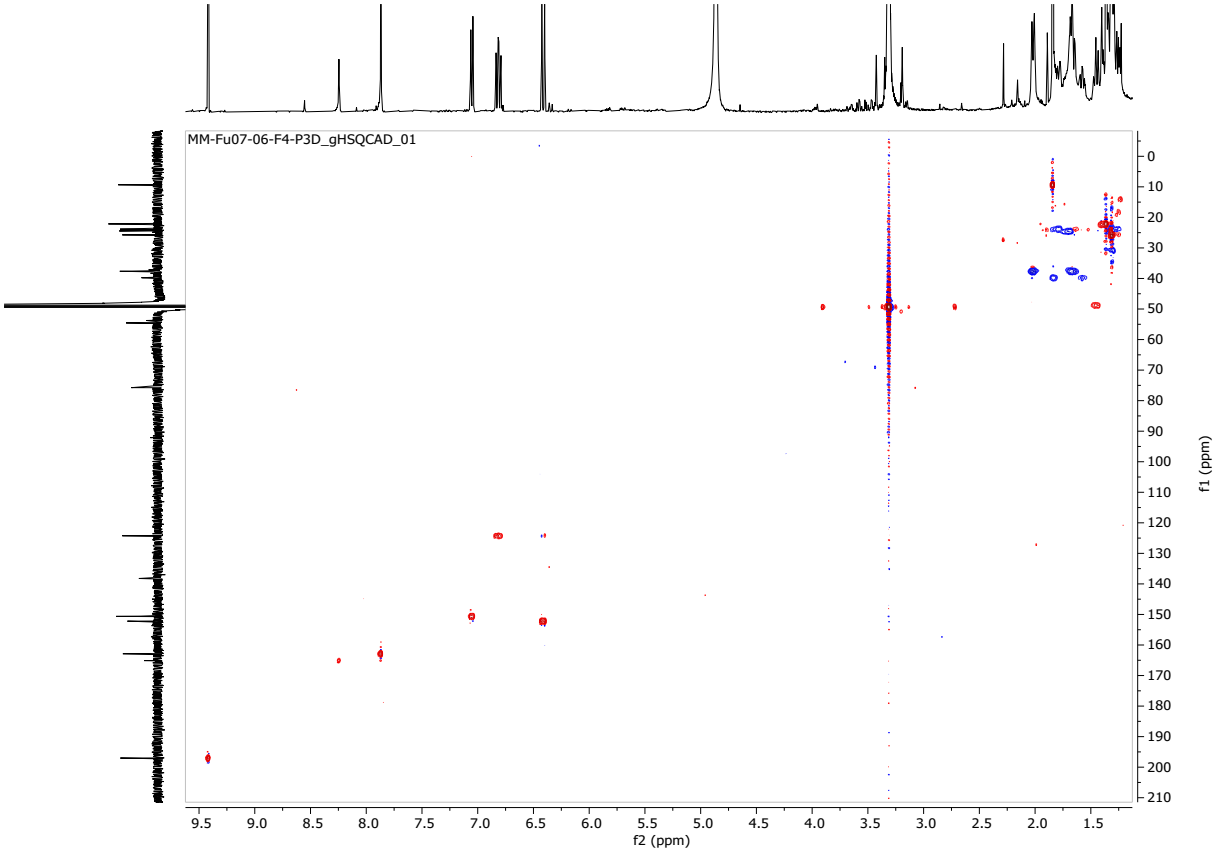

Figure S5. HSQC spectrum of bubaridin A (***rac*-1**) at 600 MHz in CD_3OD

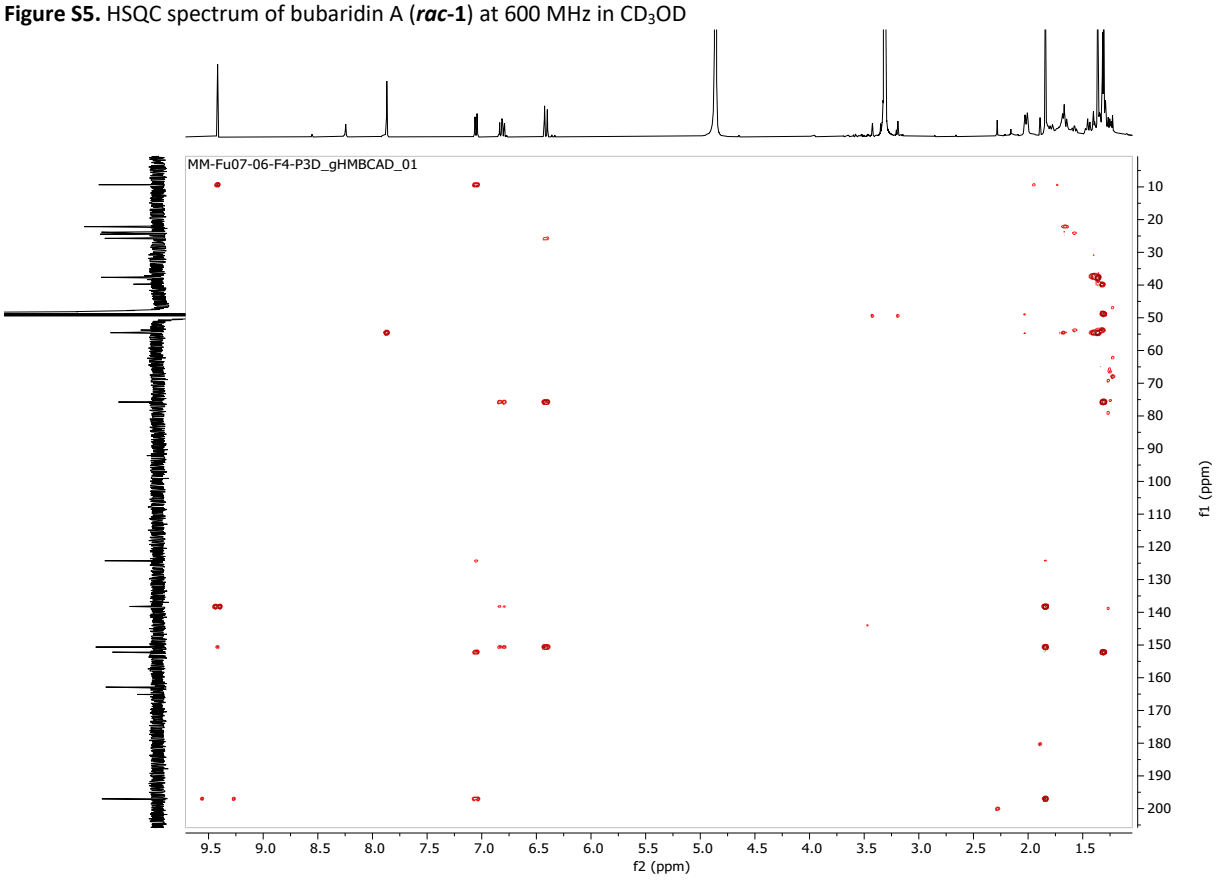

Figure S6. HMBC spectrum of bubaridin A (***rac*-1**) at 600 MHz in CD_3OD

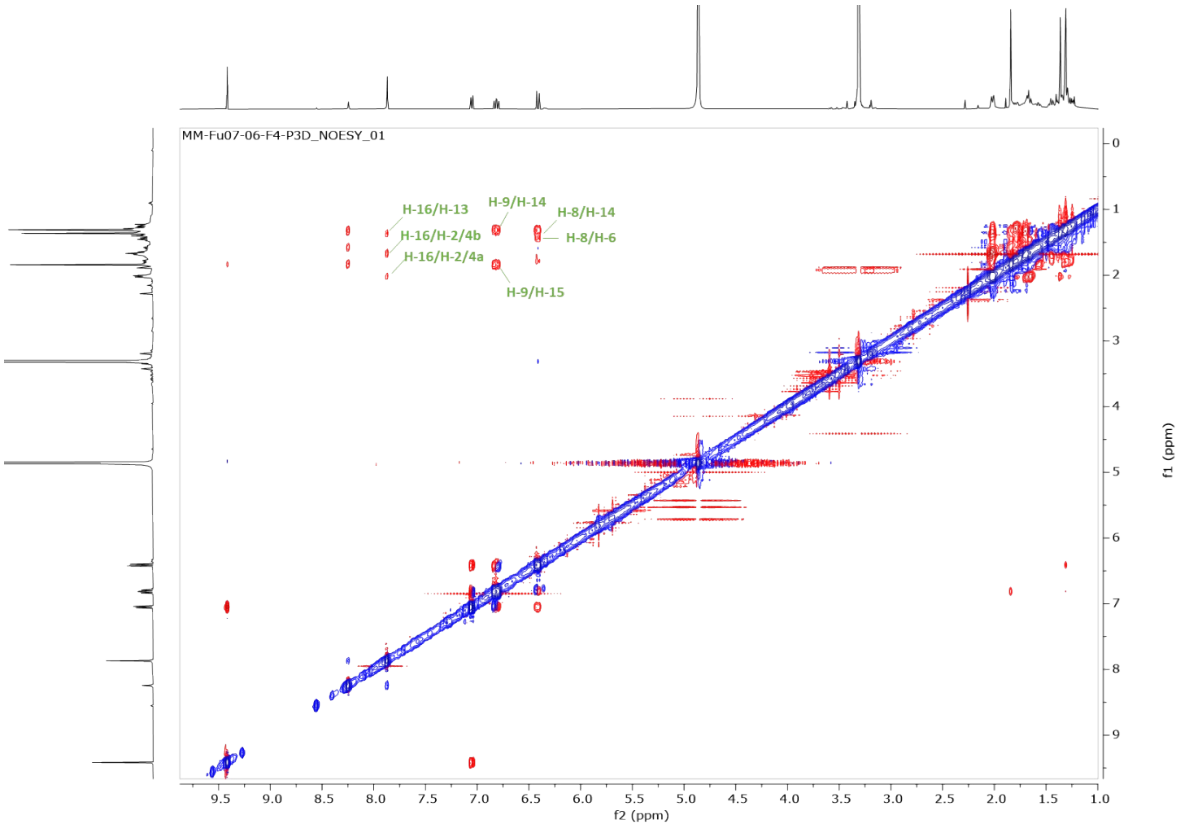

Figure S7. NOESY spectrum of bubaridin A (***rac*-1**) at 600 MHz in CD_3OD

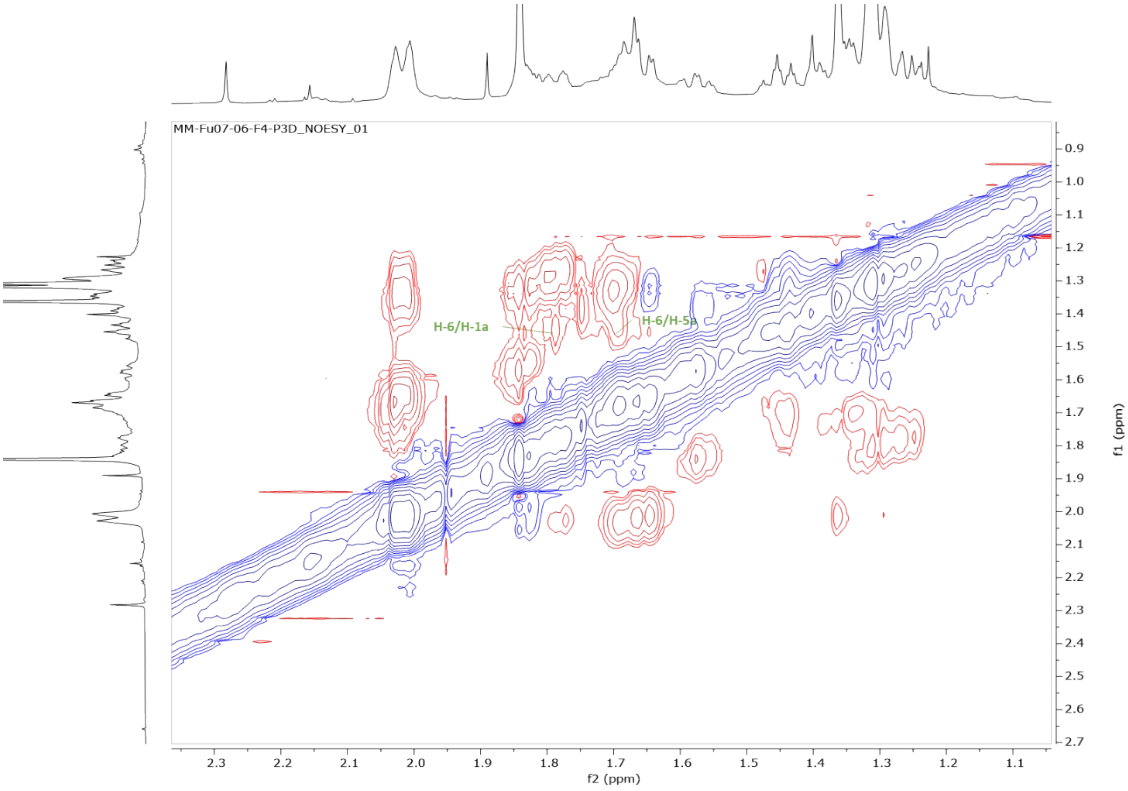

Figure S8. NOESY spectrum of bubaridin A (***rac*-1**) at 600 MHz in CD_3OD

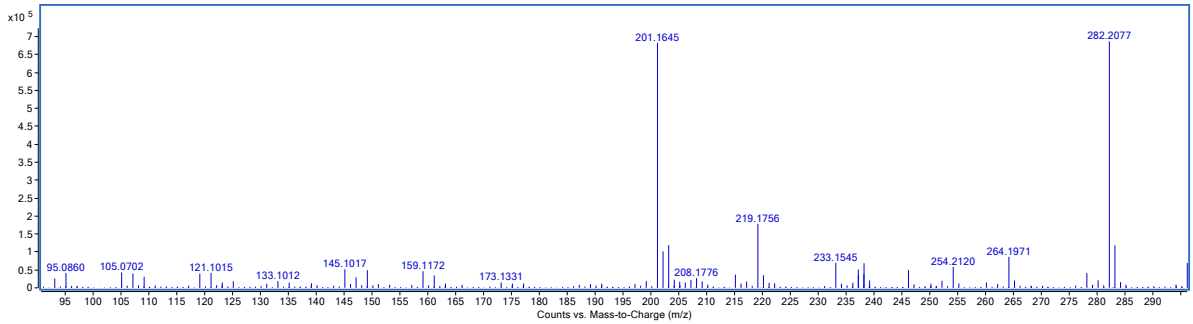

Figure S9. (+)-HRESIMS spectrum of bubaridin B (***rac*-2**)

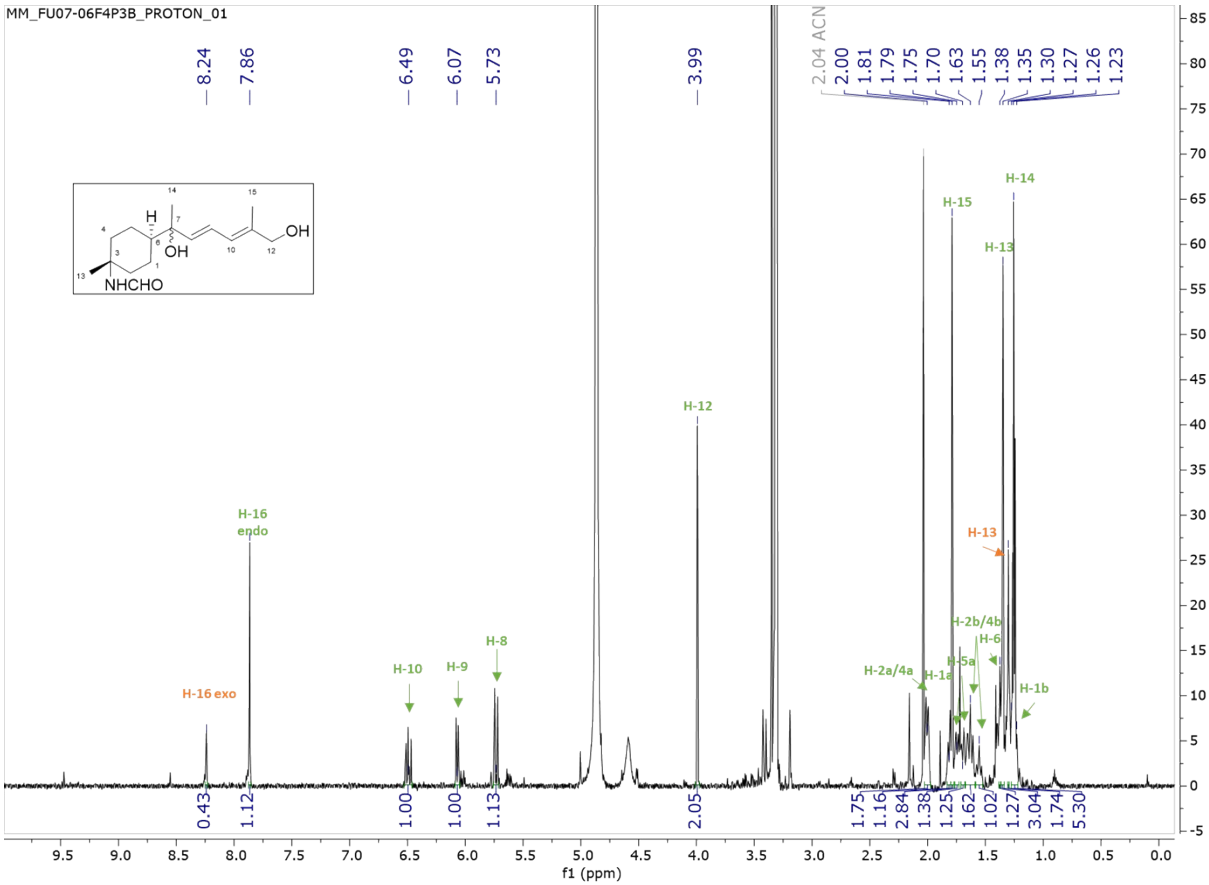

Figure S10. ^{1}H-NMR spectrum of bubaridin B (***rac*-2**) at 600 MHz in CD_3OD

SUPPLEMENTARY INFORMATION

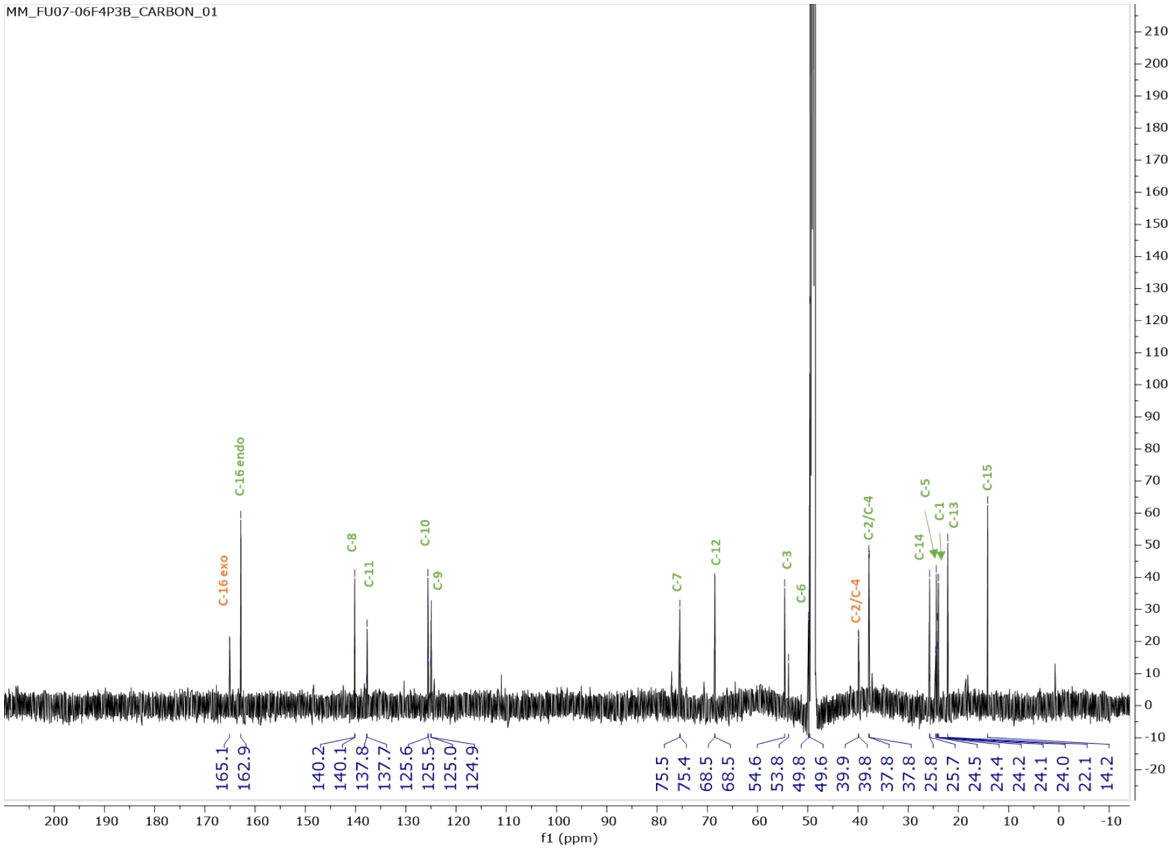

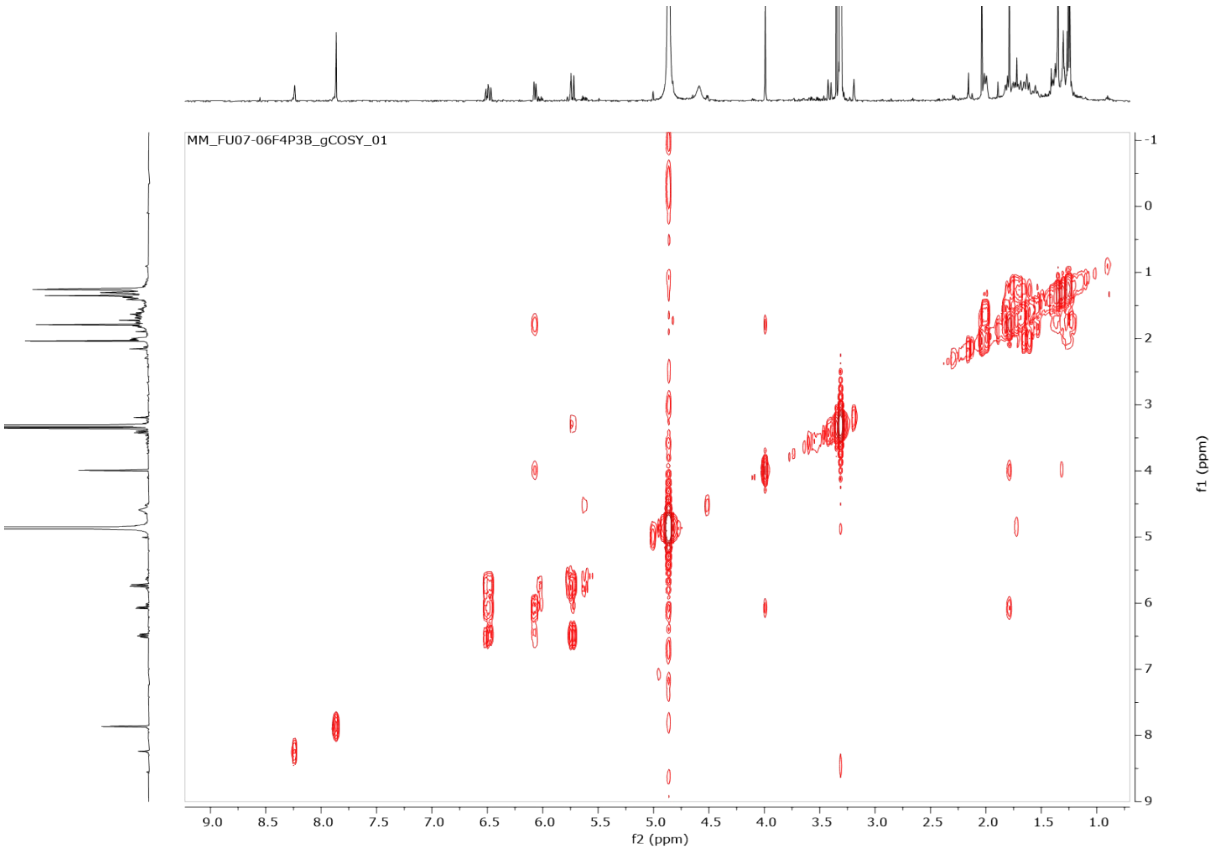

Figure S11. ^{13}C-NMR spectrum of bubaridin B (***rac*-2**) at 150 MHz in CD_3OD

Figure S12. COSY spectrum of bubaridin B (***rac*-2**) at 600MHz in CD_3OD

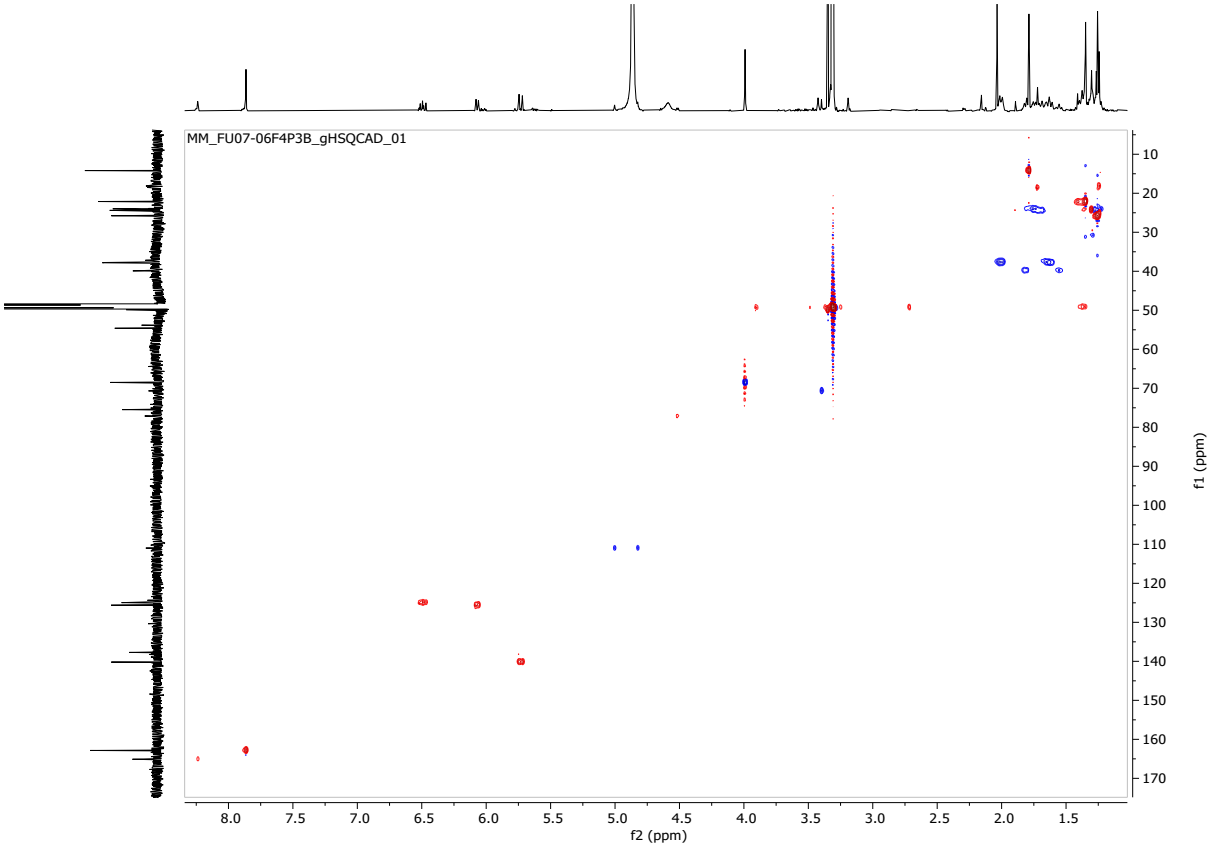

Figure S13. HSQC spectrum of bubaridin B (***rac*-2**) at 600MHz in CD_3OD

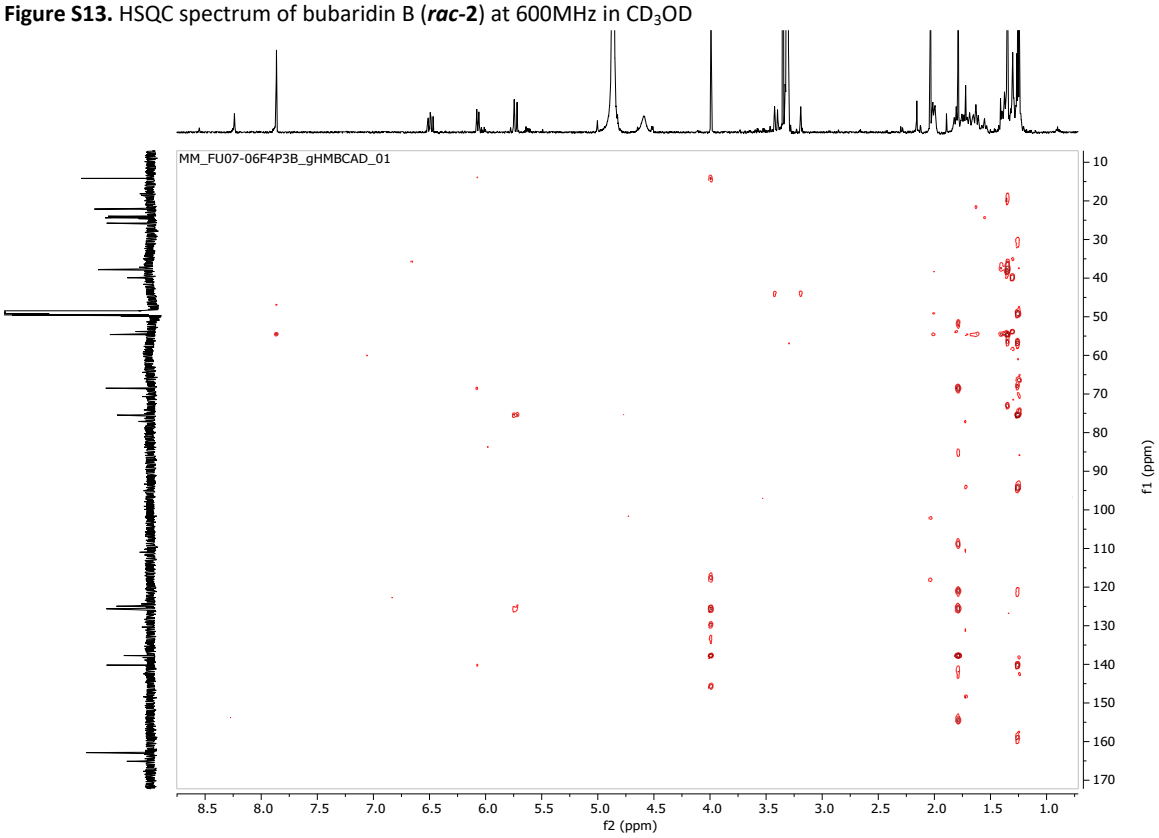

Figure S14. HMBC spectrum of bubaridin B (***rac*-2**) at 600MHz in CD_3OD

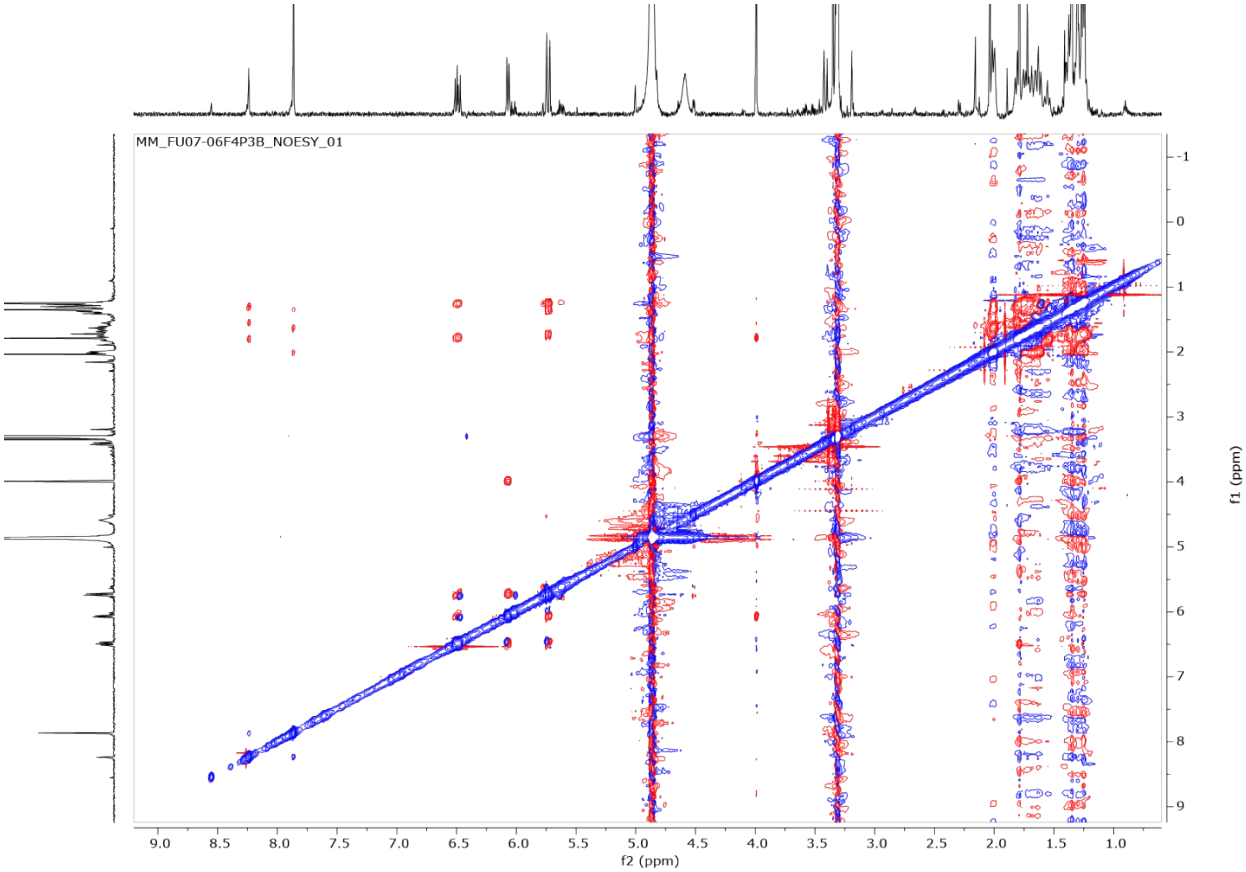

Figure S15. NOESY spectrum of bubaridin B (***rac*-2**) at 600MHz in CD_3OD

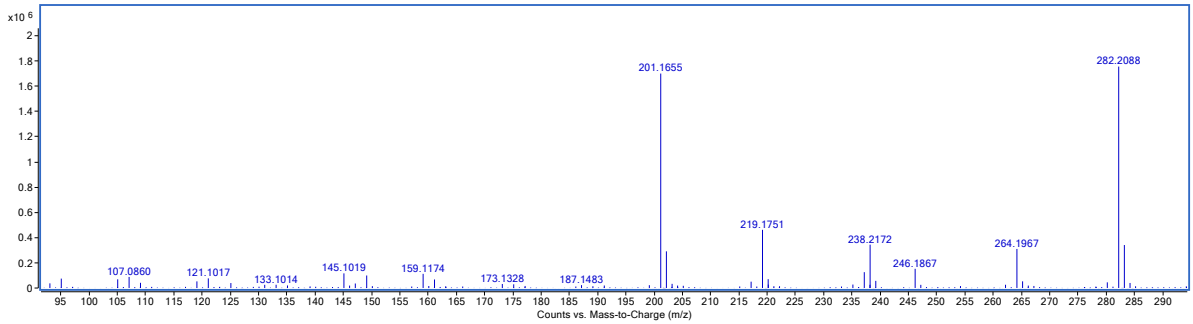

Figure S16. (+)-HRESIMS spectrum of bubaridin C (***rac*-3**)

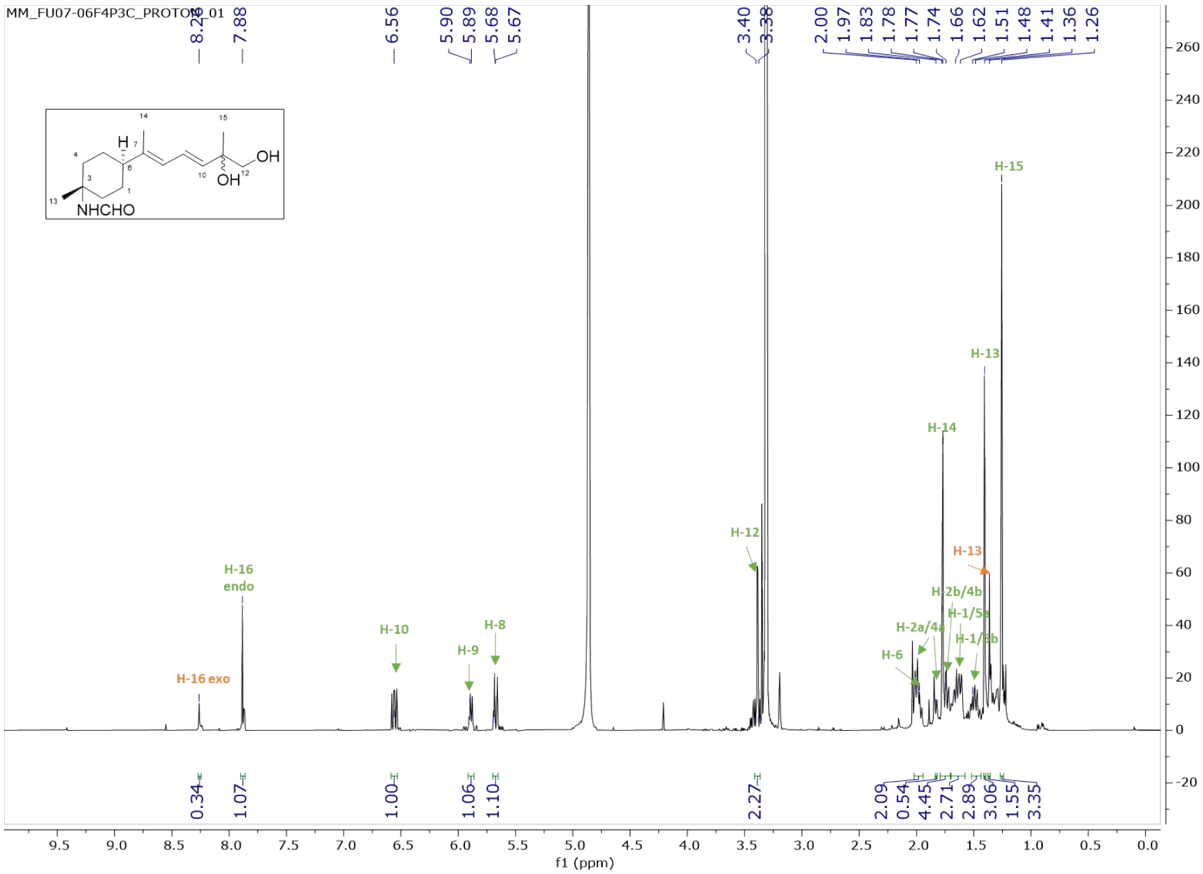

Figure S17. ^{1}H-NMR spectrum of bubaridin C (***rac*-3**) at 600MHz in CD_3OD

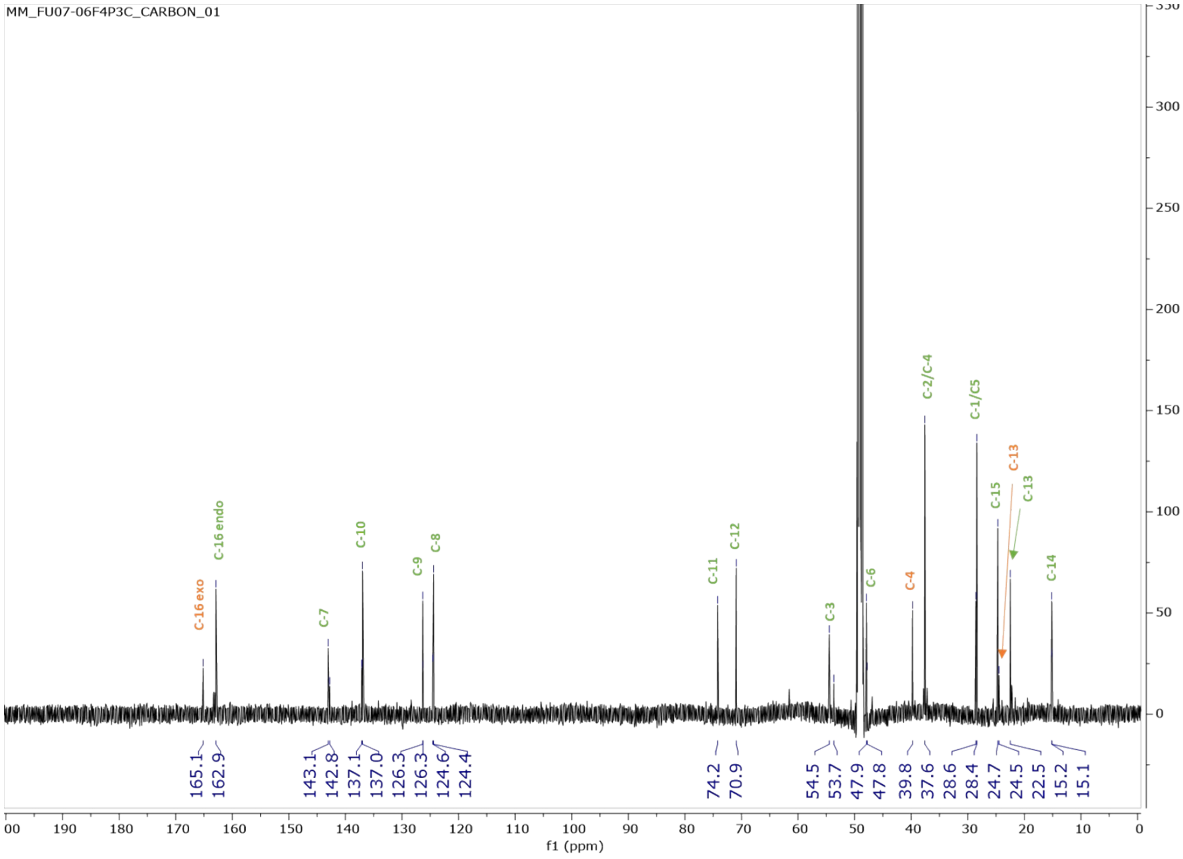

Figure S18. ^{13}C-NMR spectrum of bubaridin C (***rac*-3**) at 600MHz in CD_3OD

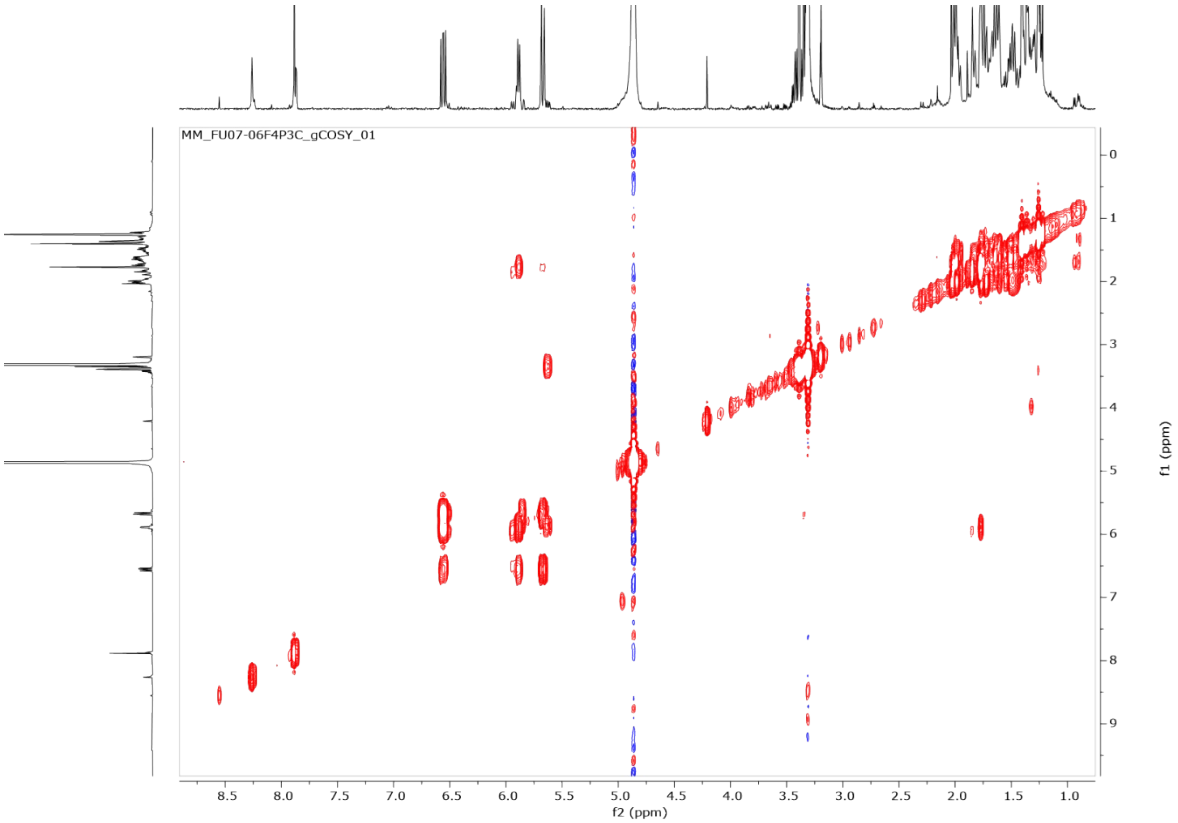

Figure S19. COSY spectrum of bubaridin C (***rac*-3**) at 600MHz in CD_3OD

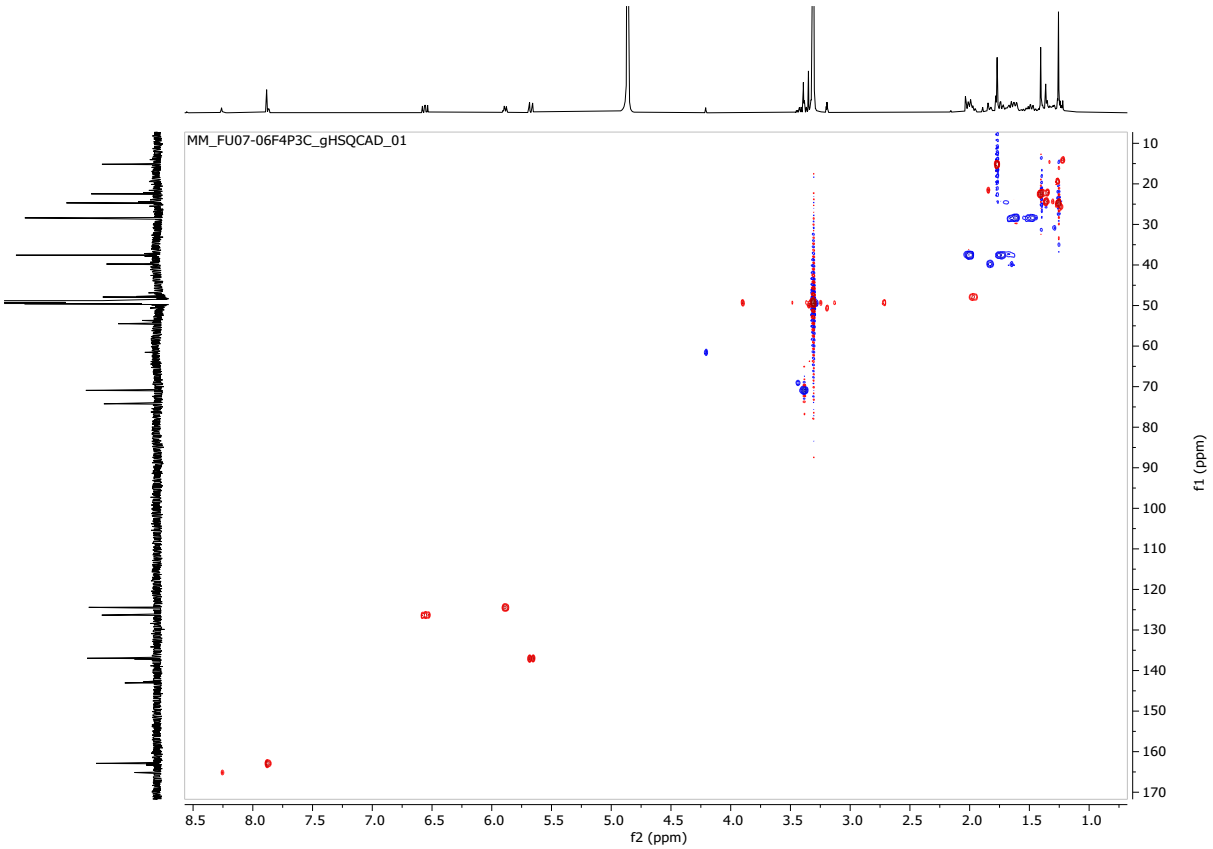

Figure S20. HSQC spectrum of bubaridin C (***rac*-3**) at 600MHz in CD_3OD

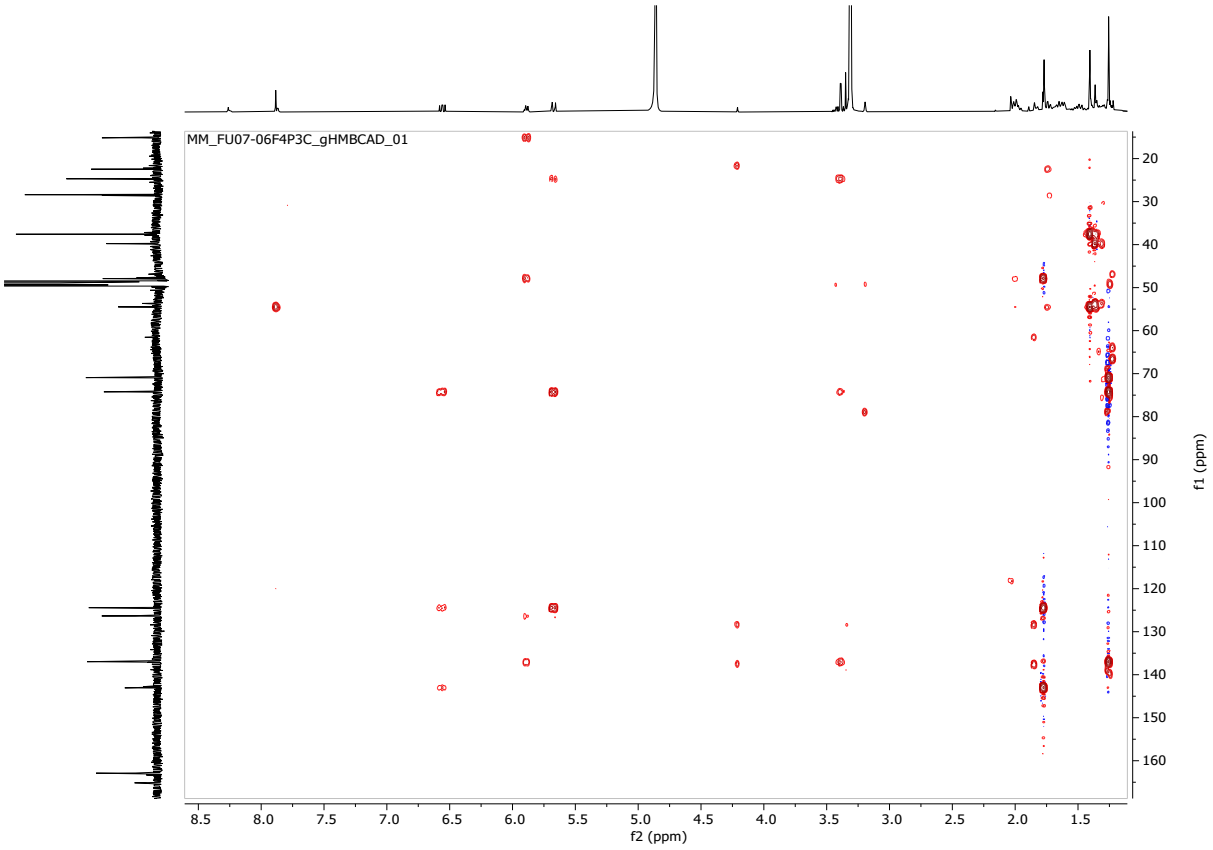

Figure S21. HMBC spectrum of bubaridin C (***rac*-3**) at 600MHz in CD_3OD

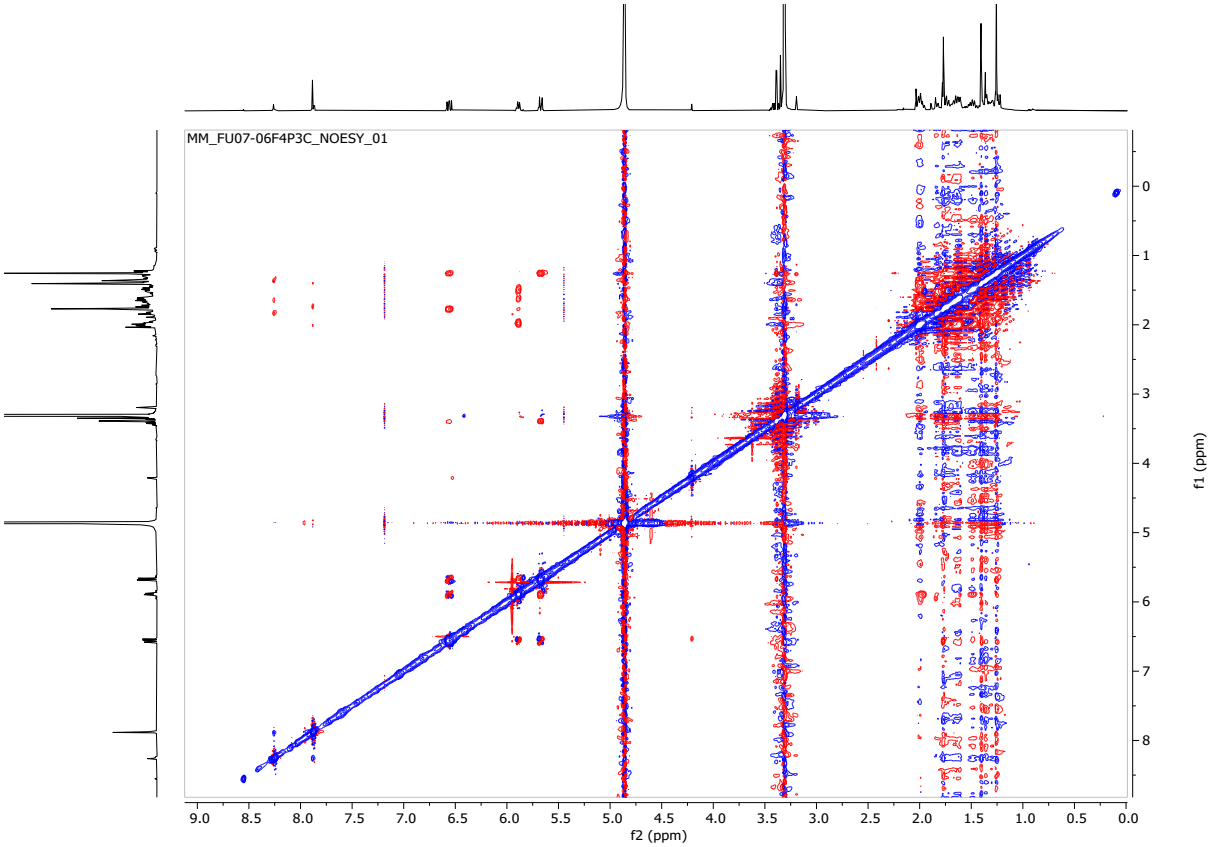

Figure S22. NOESY spectrum of bubaridin C (***rac*-3**) at 600MHz in CD_3OD

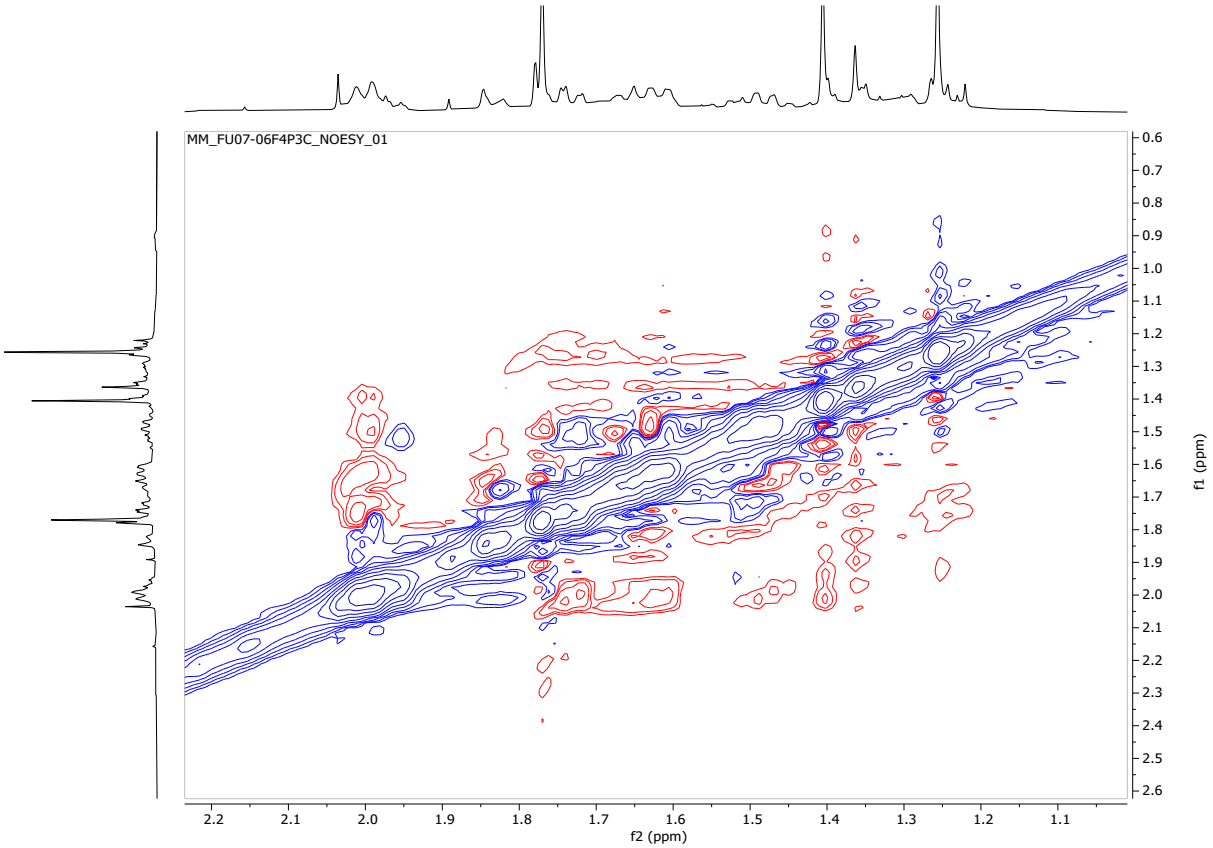

Figure S23. NOESY spectrum of bubaridin C (***rac*-3**) at 600MHz in CD_3OD

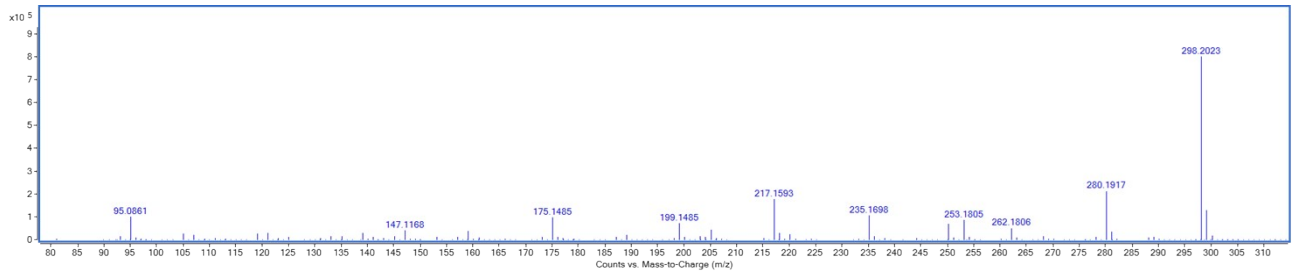

Figure S24. (+)-HRESIMS spectrum of bubaridin D and 11-*epi*-bubaridin D (***rac*-4 and *rac-epi*-4**)

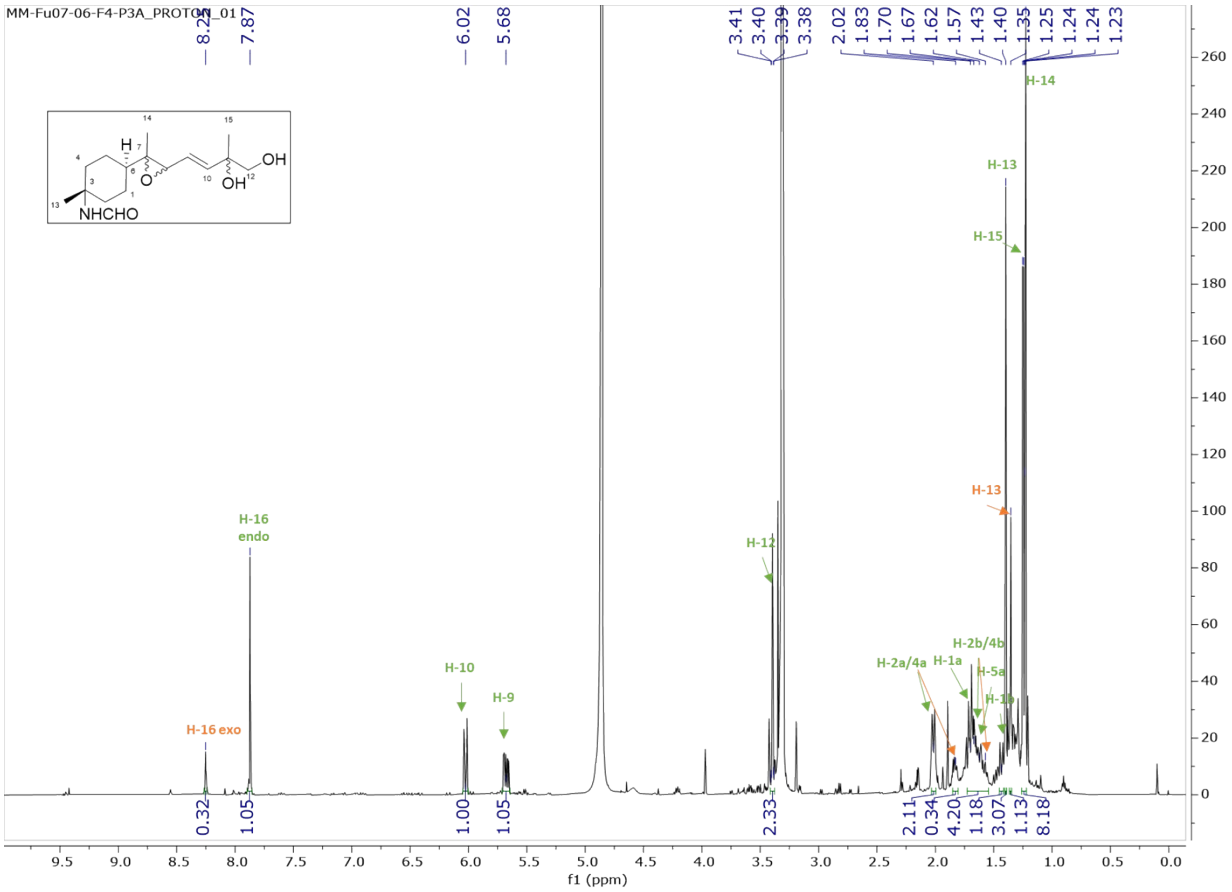

Figure S25. ^{1}H-NMR spectrum of bubaridin D and 11-*epi*-bubaridin D (***rac*-4 and *rac-epi*-4**) at 600MHz in CD_3OD

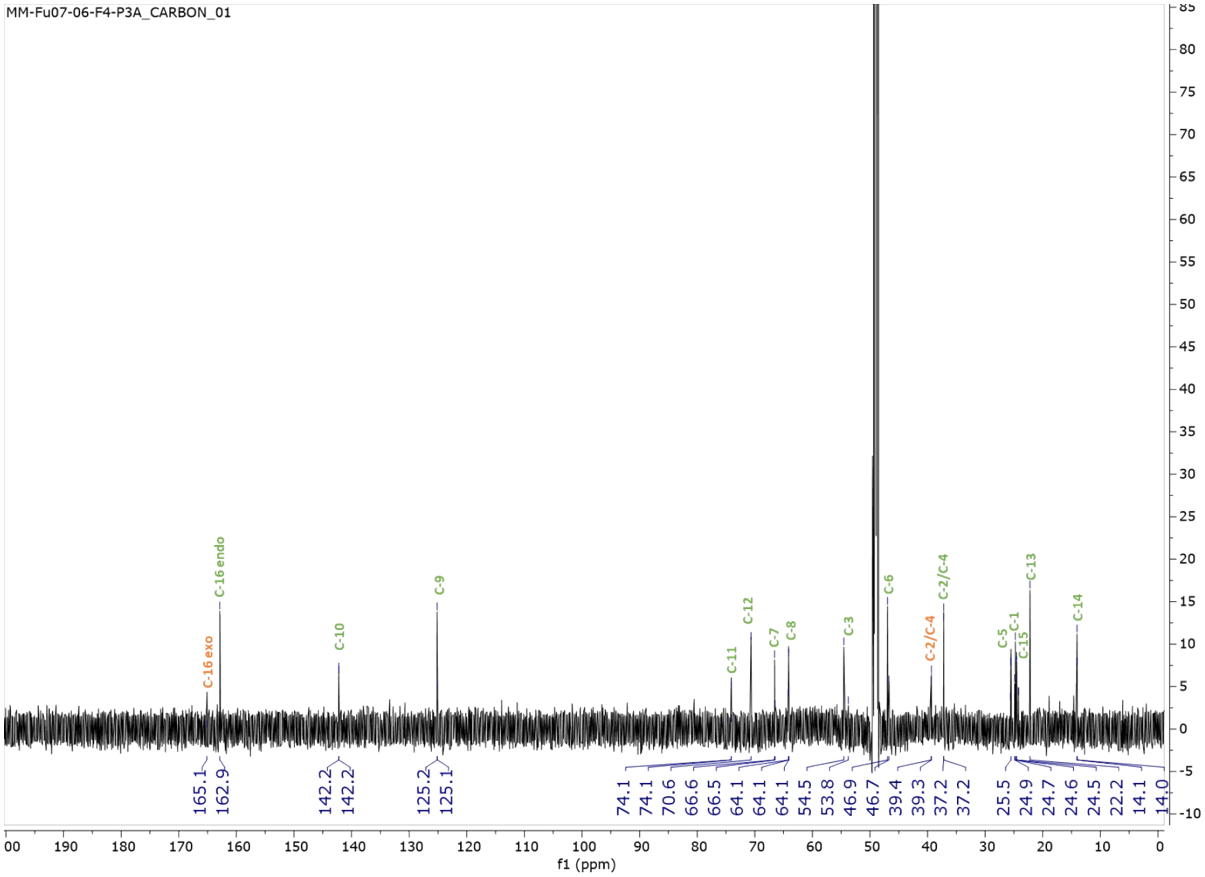

Figure S26. ^{13}C-NMR spectrum of bubaridin D and 11-*epi*-bubaridin D (***rac*-4 and *rac-epi*-4**) at 150 MHz in CD_3OD

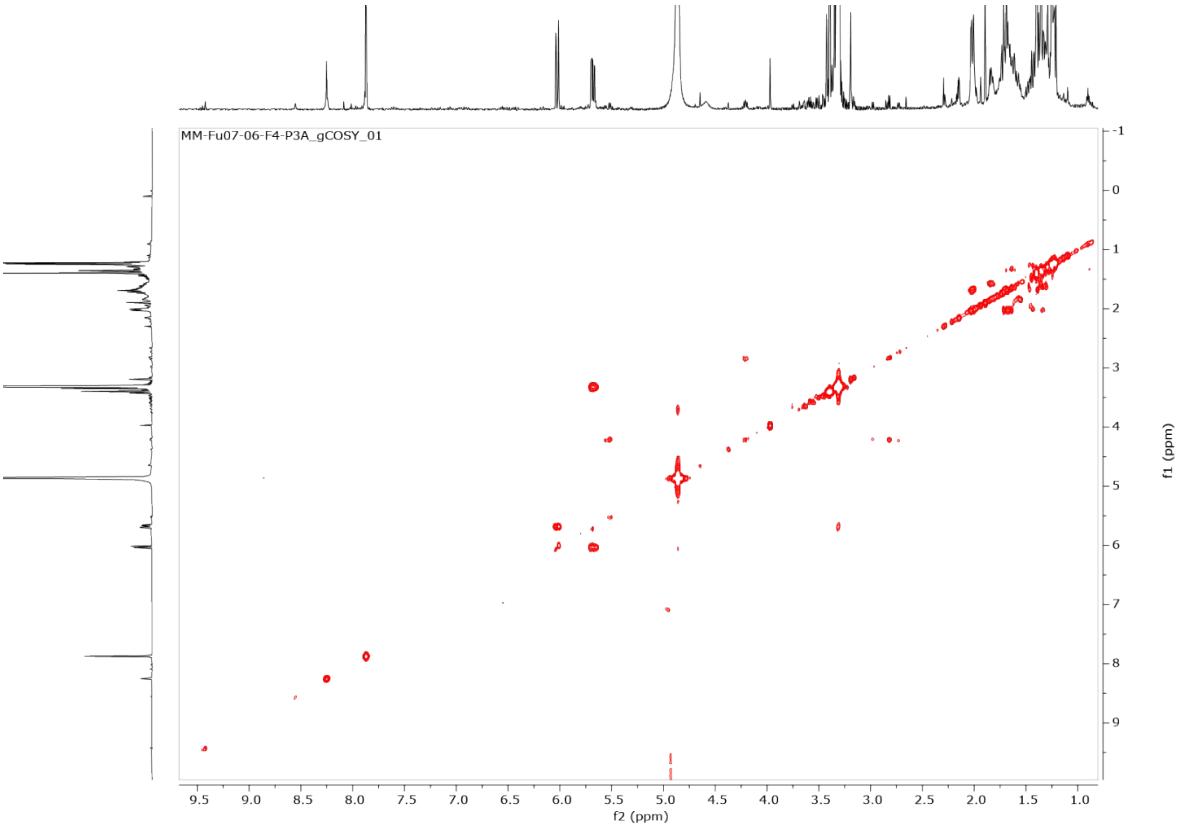

Figure S27. COSY spectrum of bubaridin D and 11-*epi*-bubaridin D (***rac*-4 and *rac-epi*-4**) at 600 MHz in CD_3OD

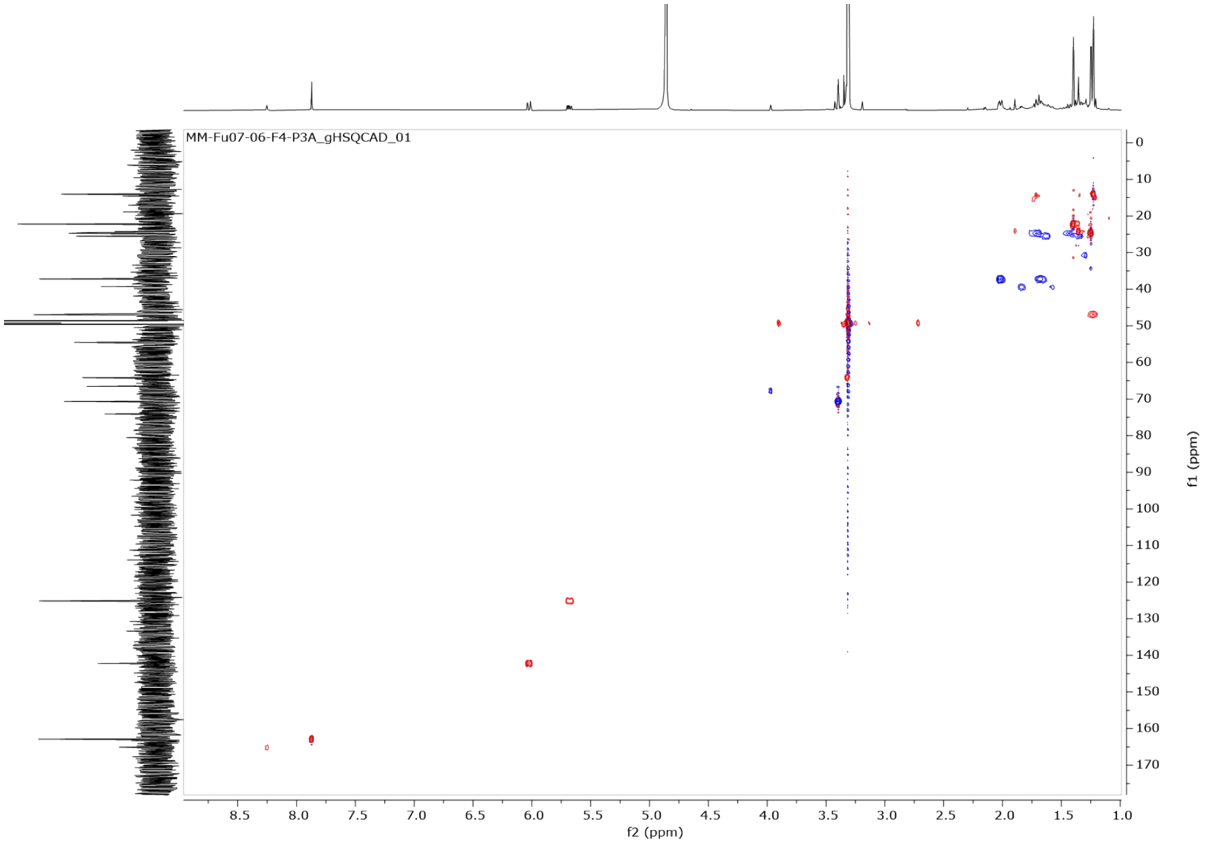

Figure S28. HSQC spectrum of bubaridin D and 11-*epi*-bubaridin D (***rac*-4 and *rac-epi*-4**) at 600 MHz in CD_3OD

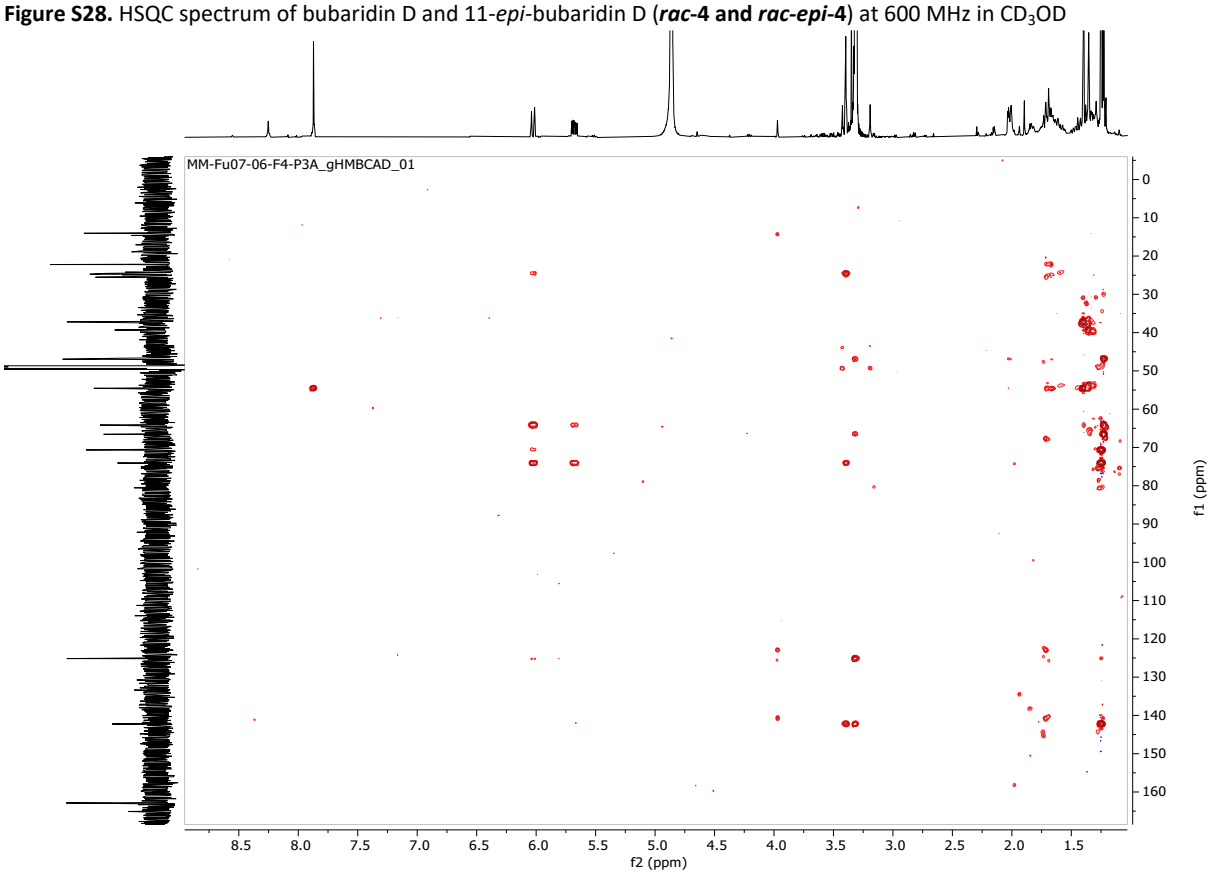

Figure S29. HMBC spectrum of bubaridin D and 11-*epi*-bubaridin D (***rac*-4 and *rac-epi*-4**) at 600 MHz in CD_3OD

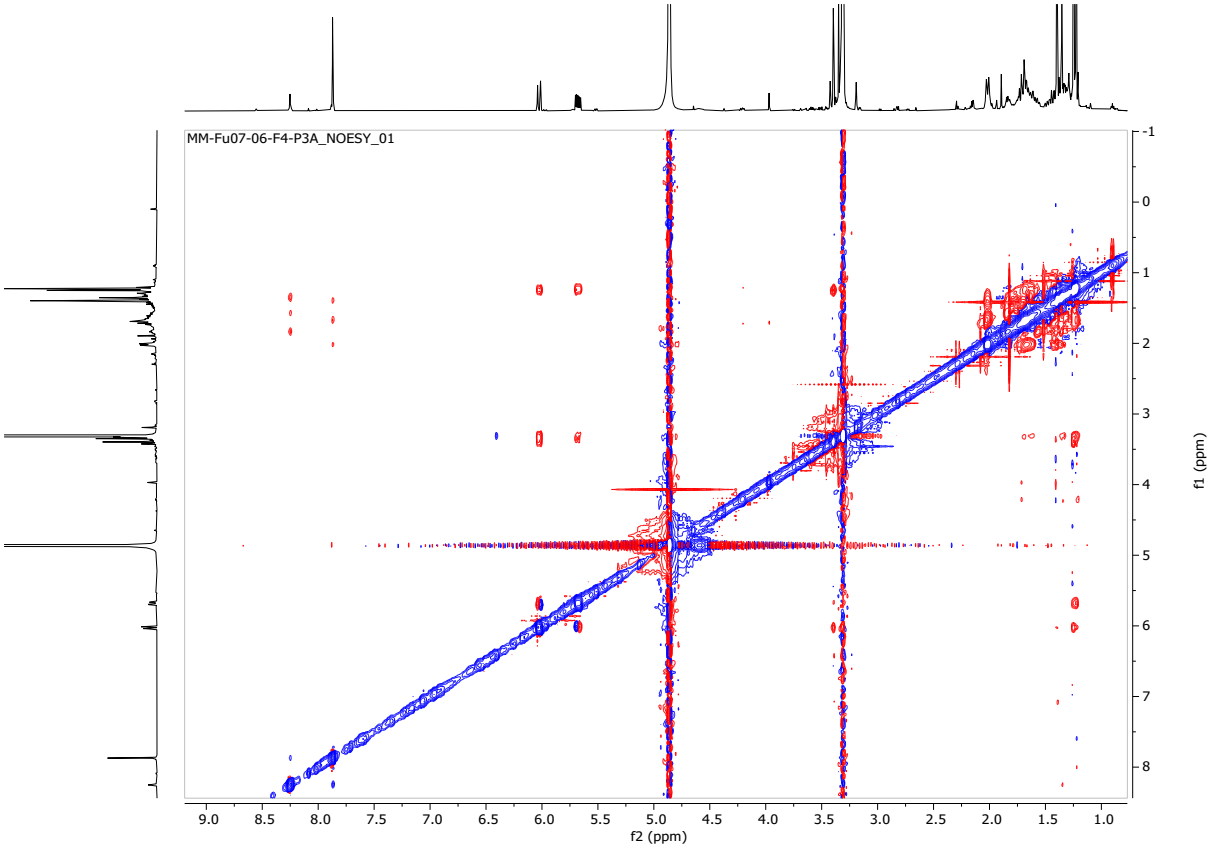

Figure S30. HMBC spectrum of bubaridin D and 11-*epi*-bubaridin D (***rac*-4 and *rac-epi*-4**) at 600 MHz in CD_3OD

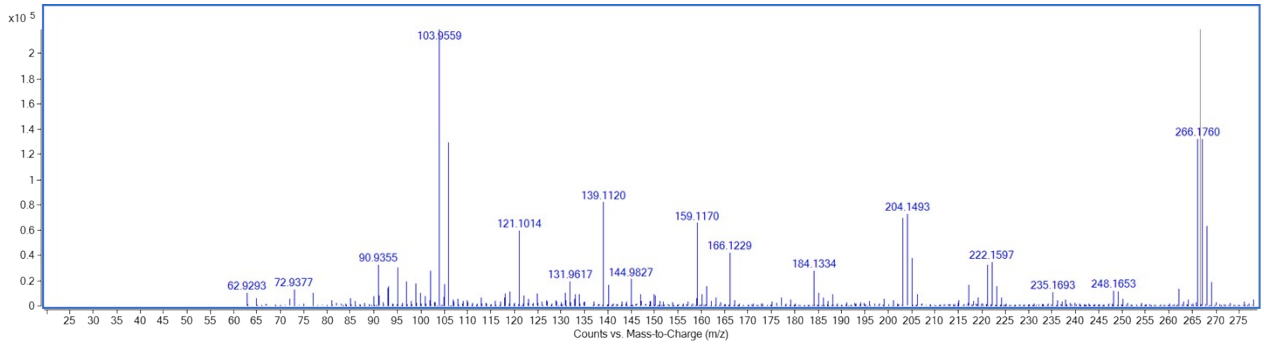

Figure S31. (+)-HRESIMS spectrum of bubaridin E (***rac*-5**)

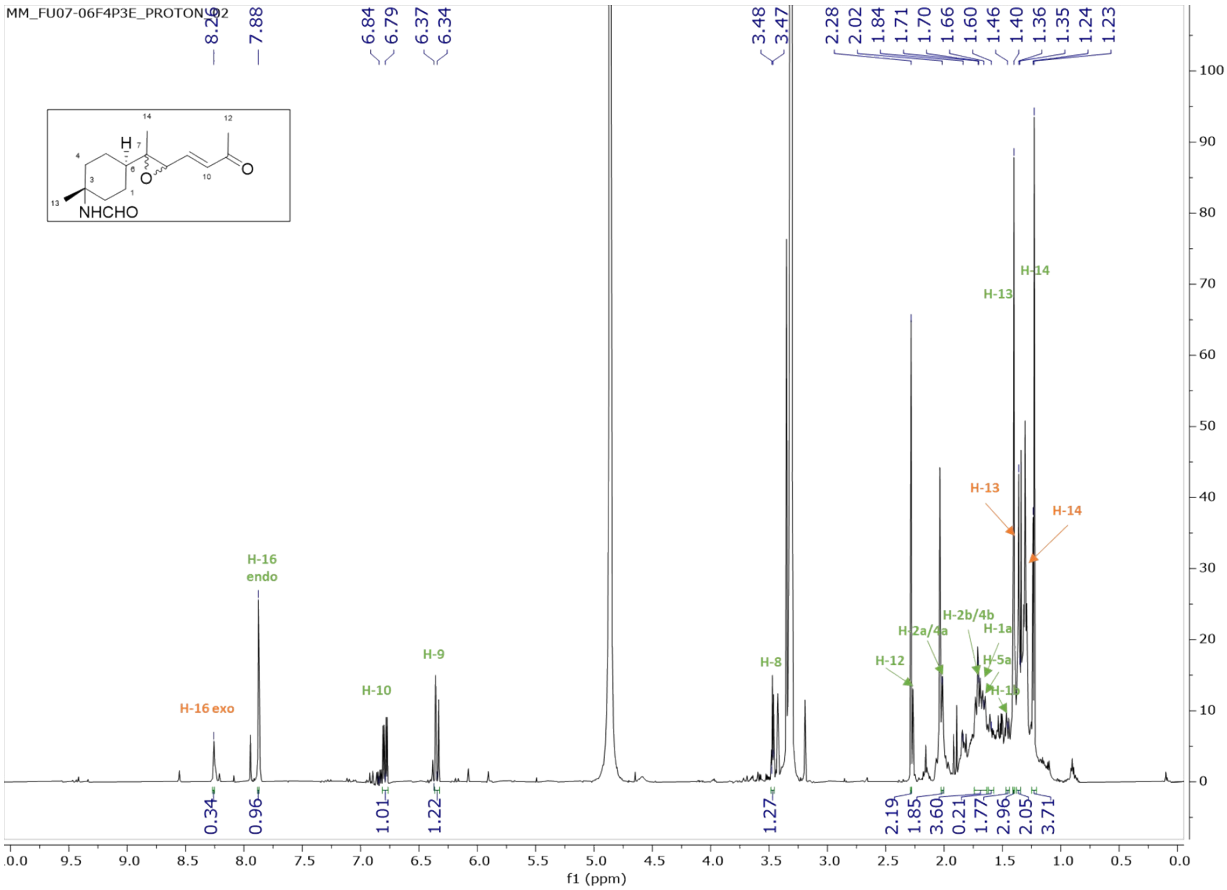

Figure S32. ^{1}H-NMR spectrum of bubaridin E (***rac*-5**) at 600 MHz in CD_3OD

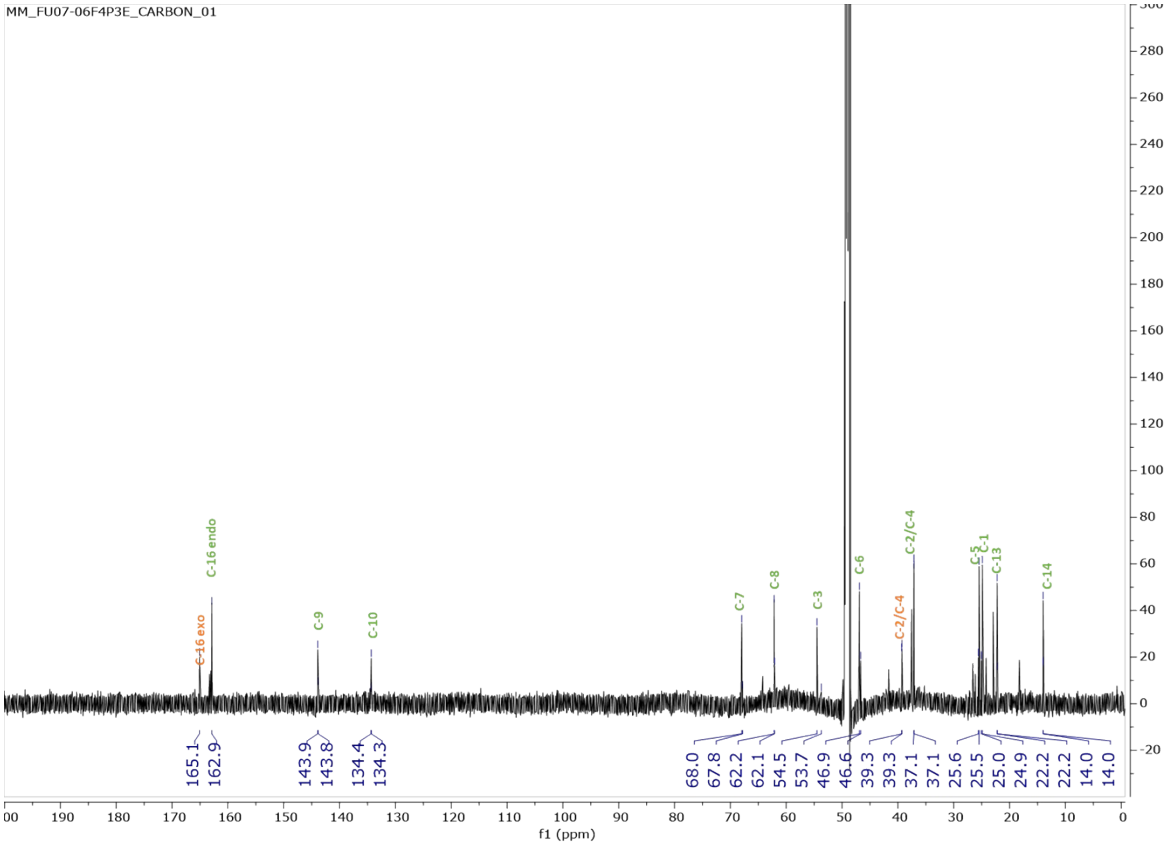

Figure S33. ^{13}C-NMR spectrum of bubaridin E (***rac*-5**) at 600 MHz in CD_3OD

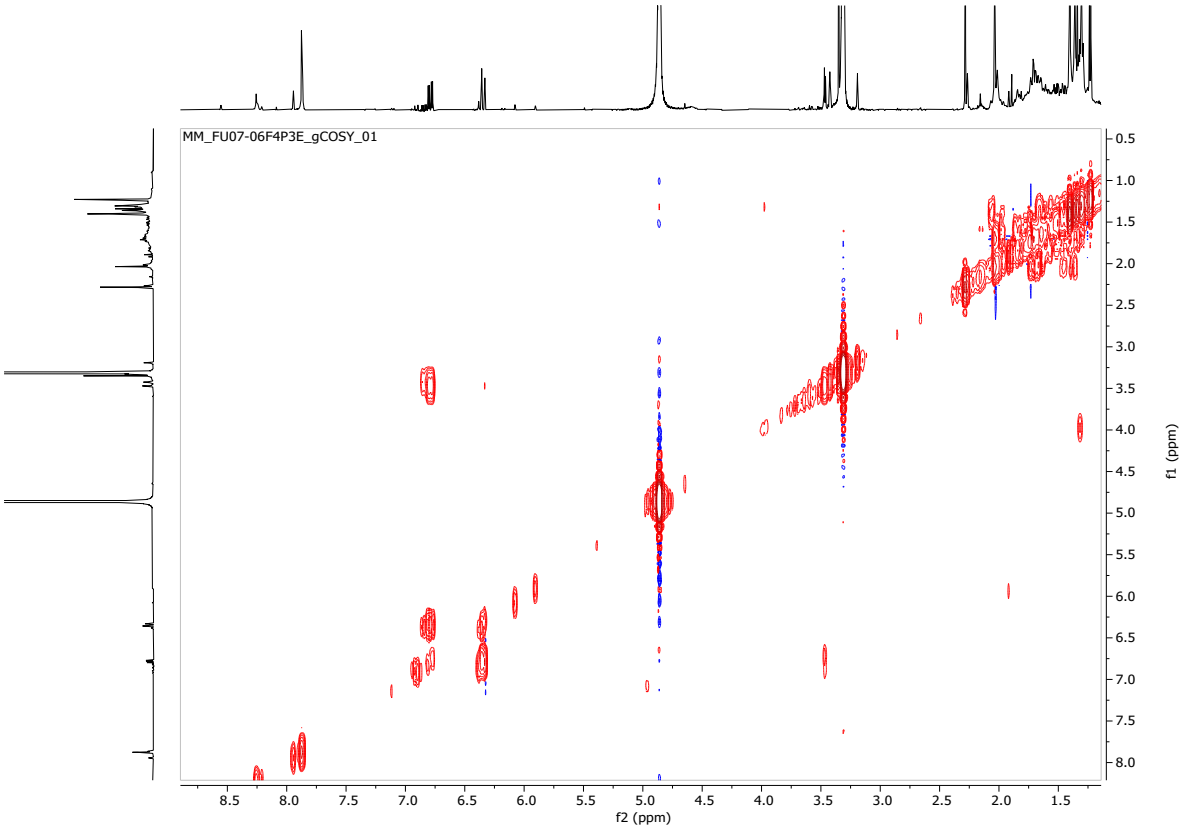

Figure S34. COSY spectrum of bubaridin E (***rac*-5**) at 600 MHz in CD_3OD

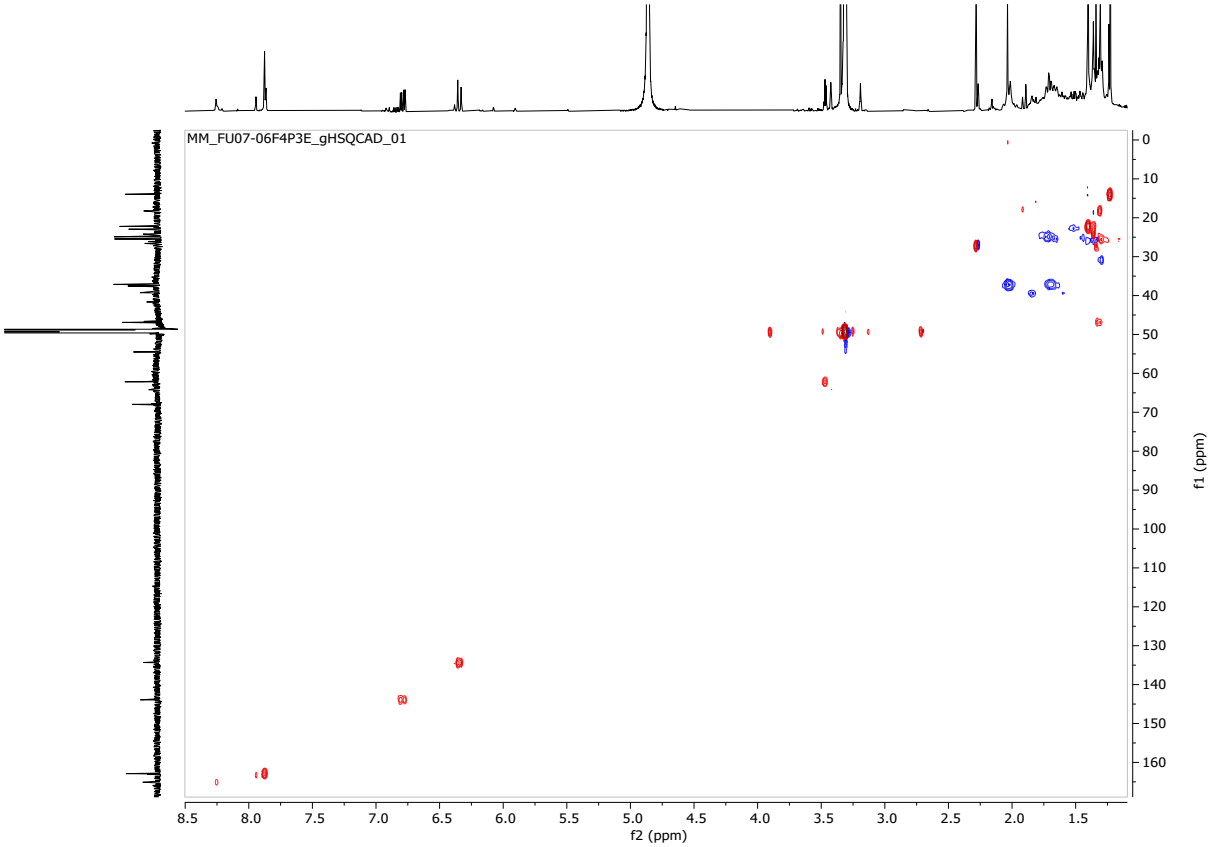

Figure S35. HSQC spectrum of bubaridin E (***rac*-5**)at 600 MHz in CD_3OD

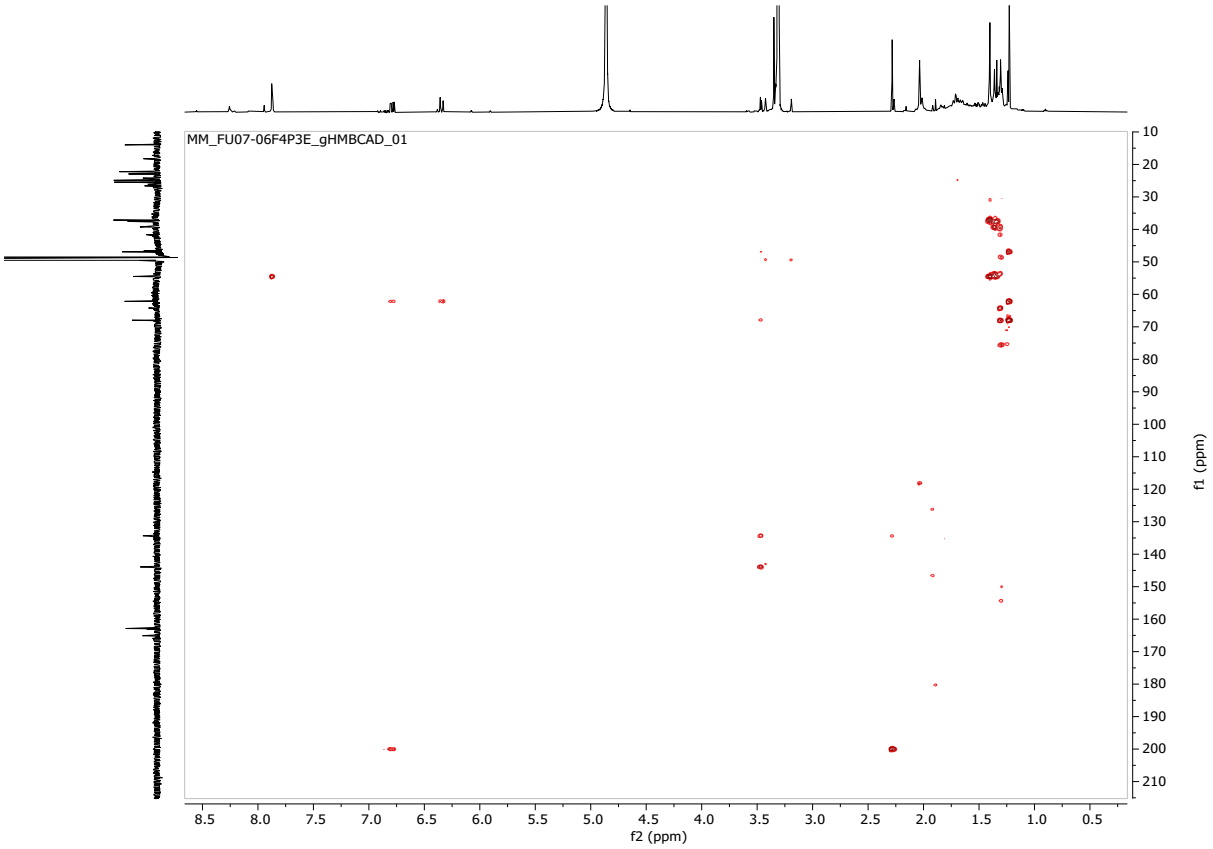

Figure S36. HMBC spectrum of bubaridin E (***rac*-5**)at 600 MHz in CD_3OD

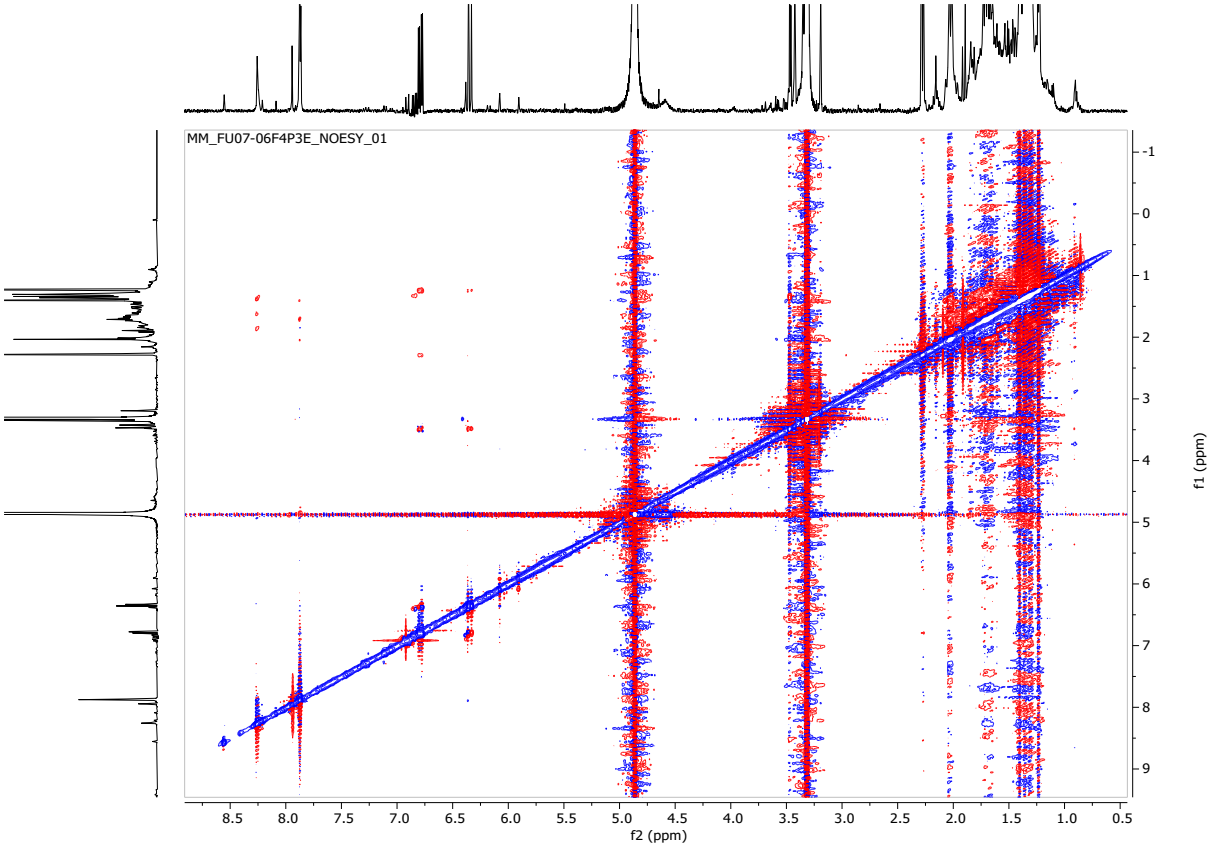

Figure S37. NOESY spectrum of bubaridin E (***rac*-5**) at 600 MHz in CD_3OD

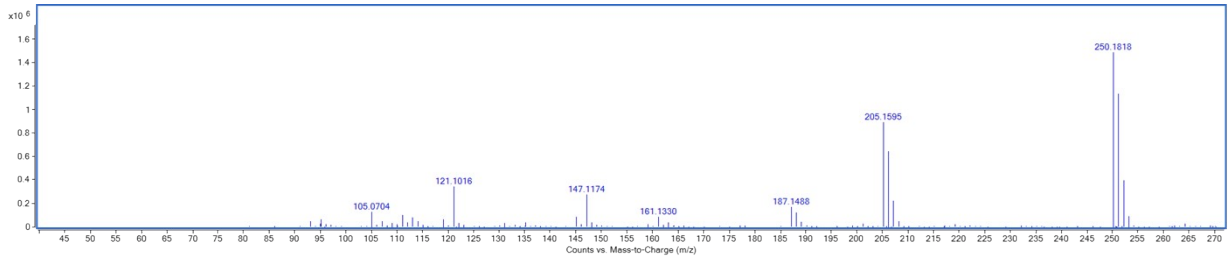

Figure S38. (+)-HRESIMS spectrum of bubaridin F (***rac*-6**)

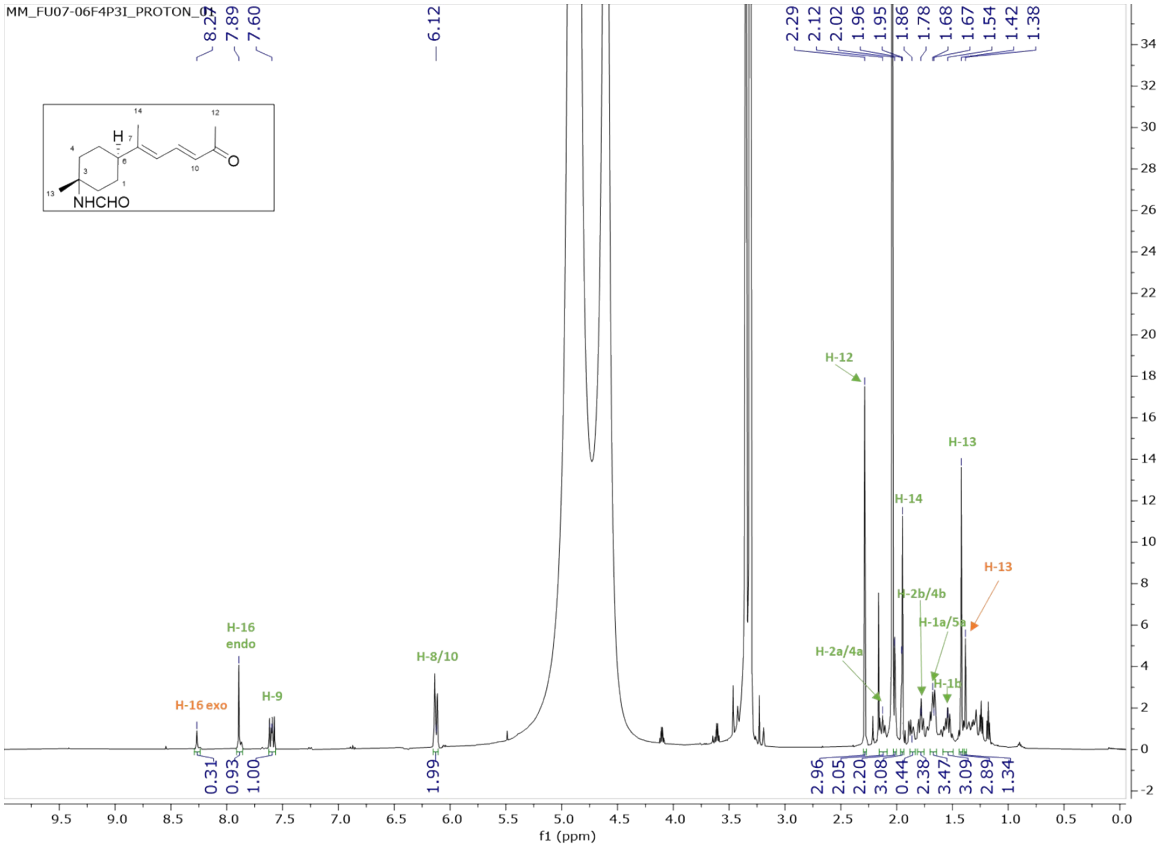

Figure S39. ^{1}H-NMR spectrum of bubaridin F (***rac*-6**) at 600 MHz in CD_3OD

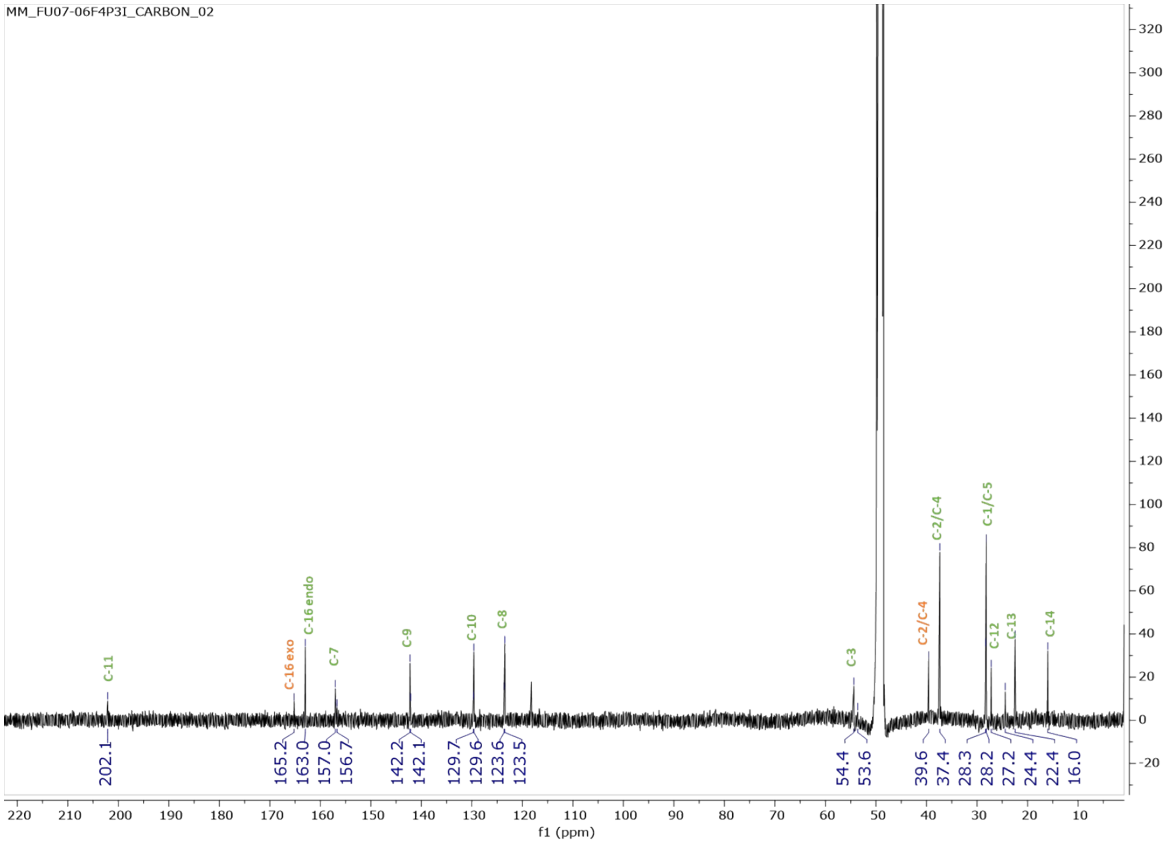

Figure S40. ^{13}C-NMR spectrum of bubaridin F (***rac*-6**) at 150 MHz in CD_3OD

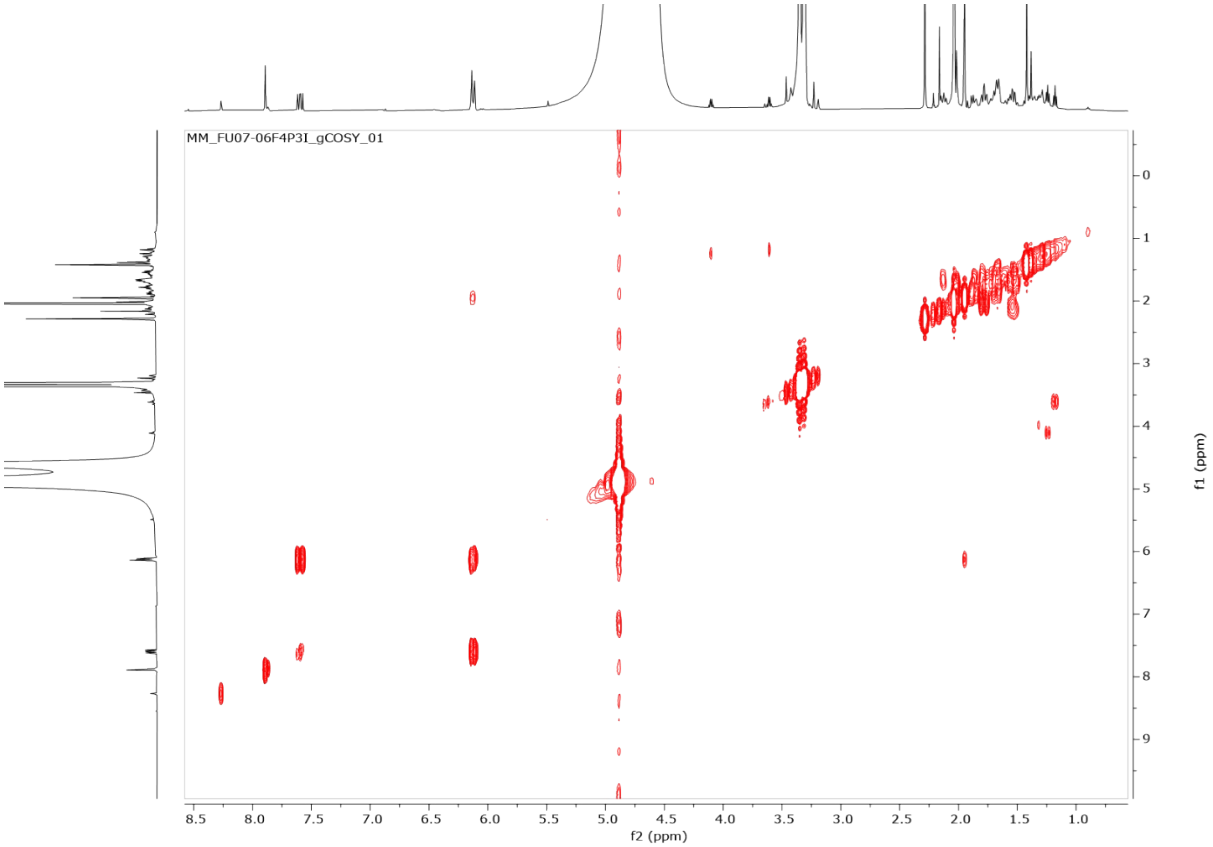

Figure S41. COSY spectrum of bubaridin F (***rac*-6**) at 600 MHz in CD_3OD

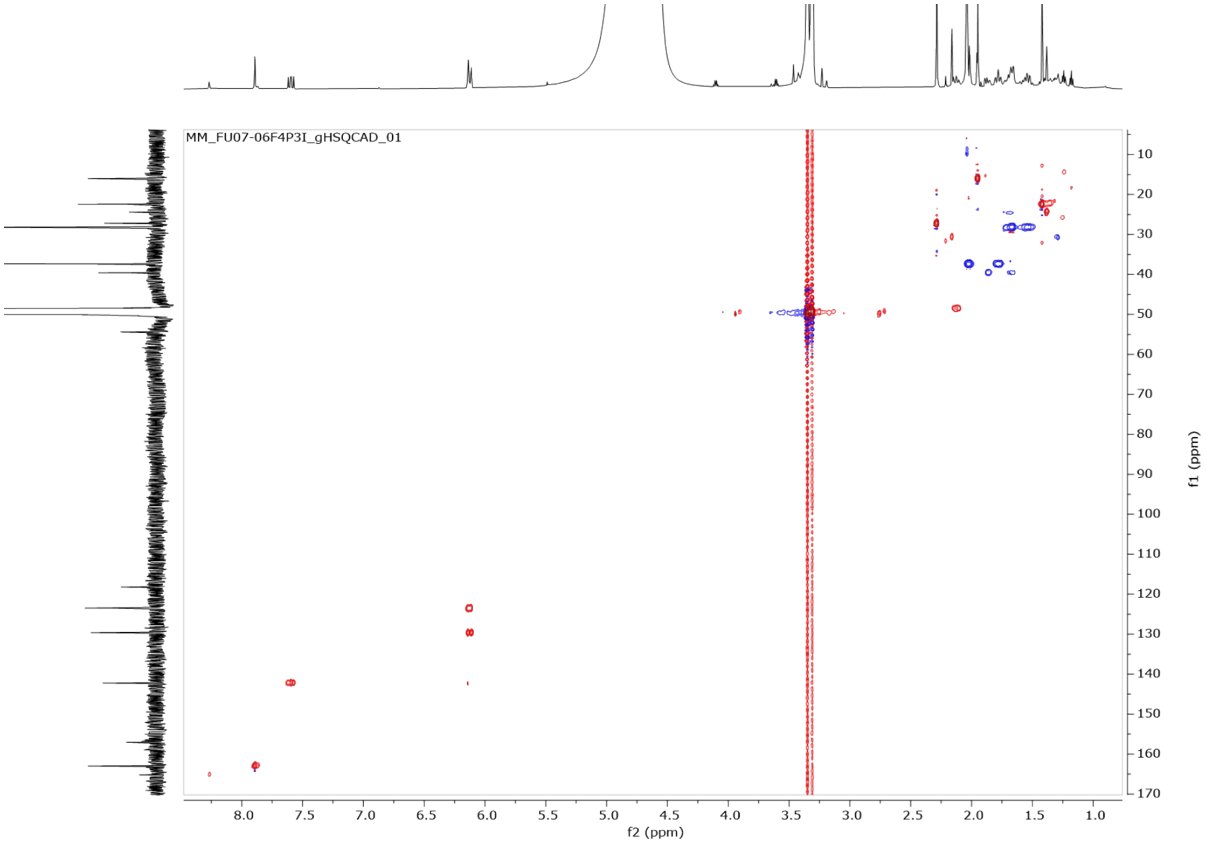

Figure S42. HSQC spectrum of bubaridin F (***rac*-6**) at 600 MHz in CD_3OD

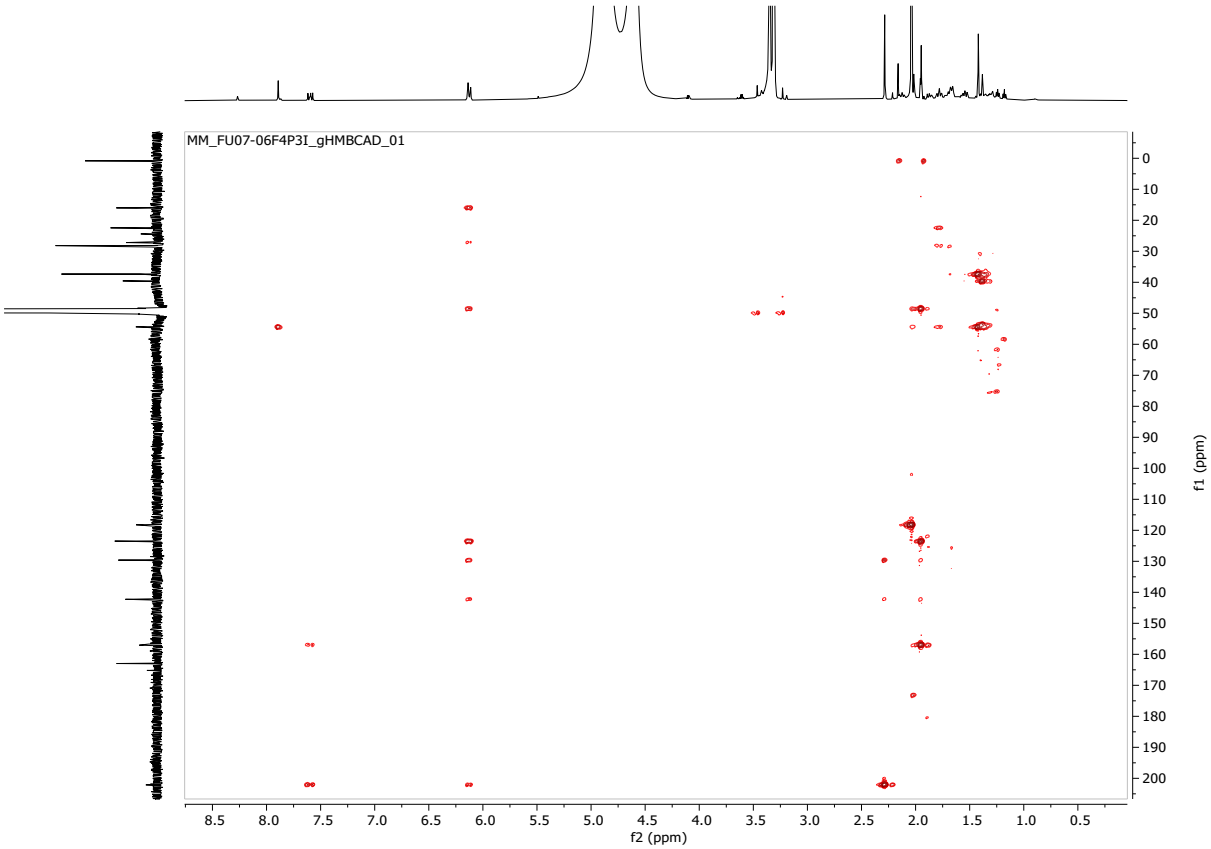

Figure S43. HMBC spectrum of bubaridin F (***rac*-6**) at 600 MHz in CD_3OD

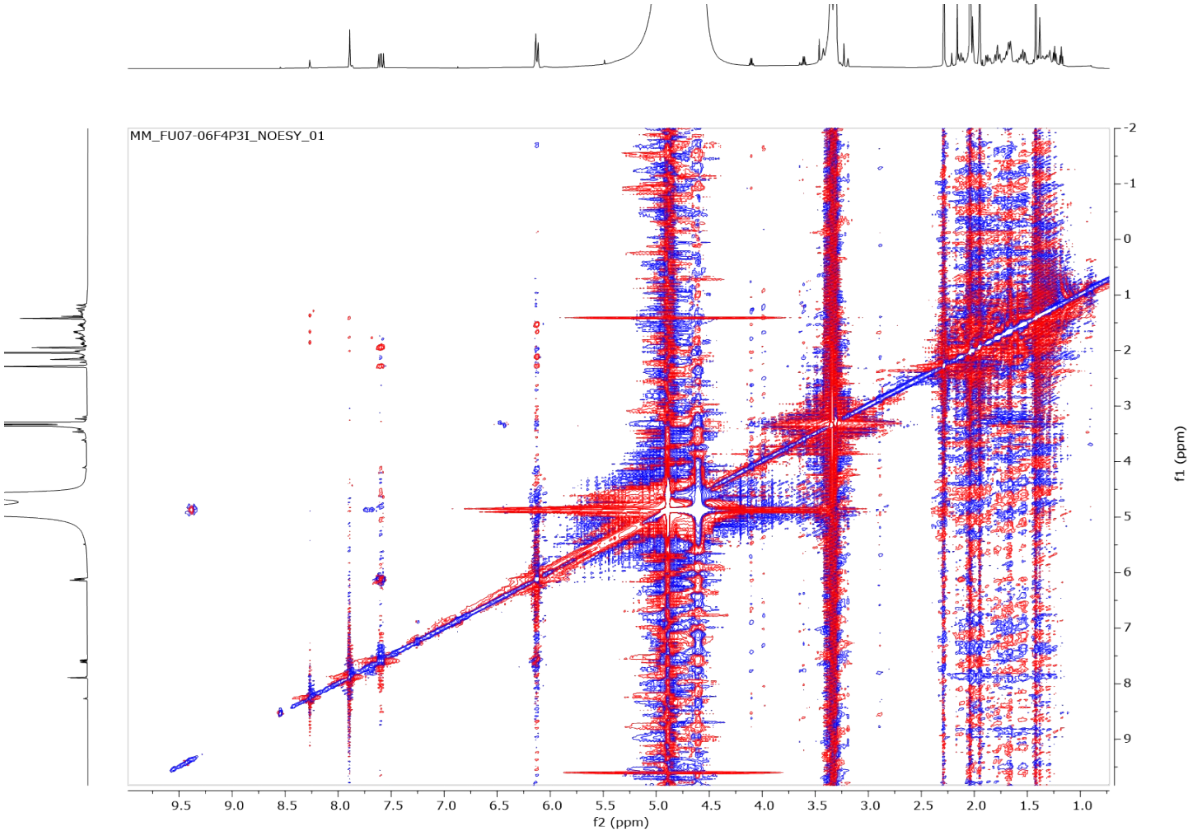

Figure S44. NOESY spectrum of bubaridin F (***rac*-6**) at 600 MHz in CD_3OD

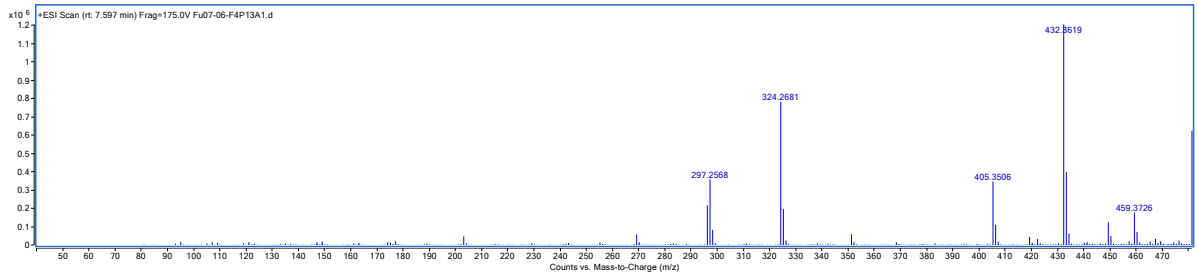

Figure S45. (+)-HRESIMS spectrum of *trans*-dimer theonellin isocyanide (***rac*-7**)

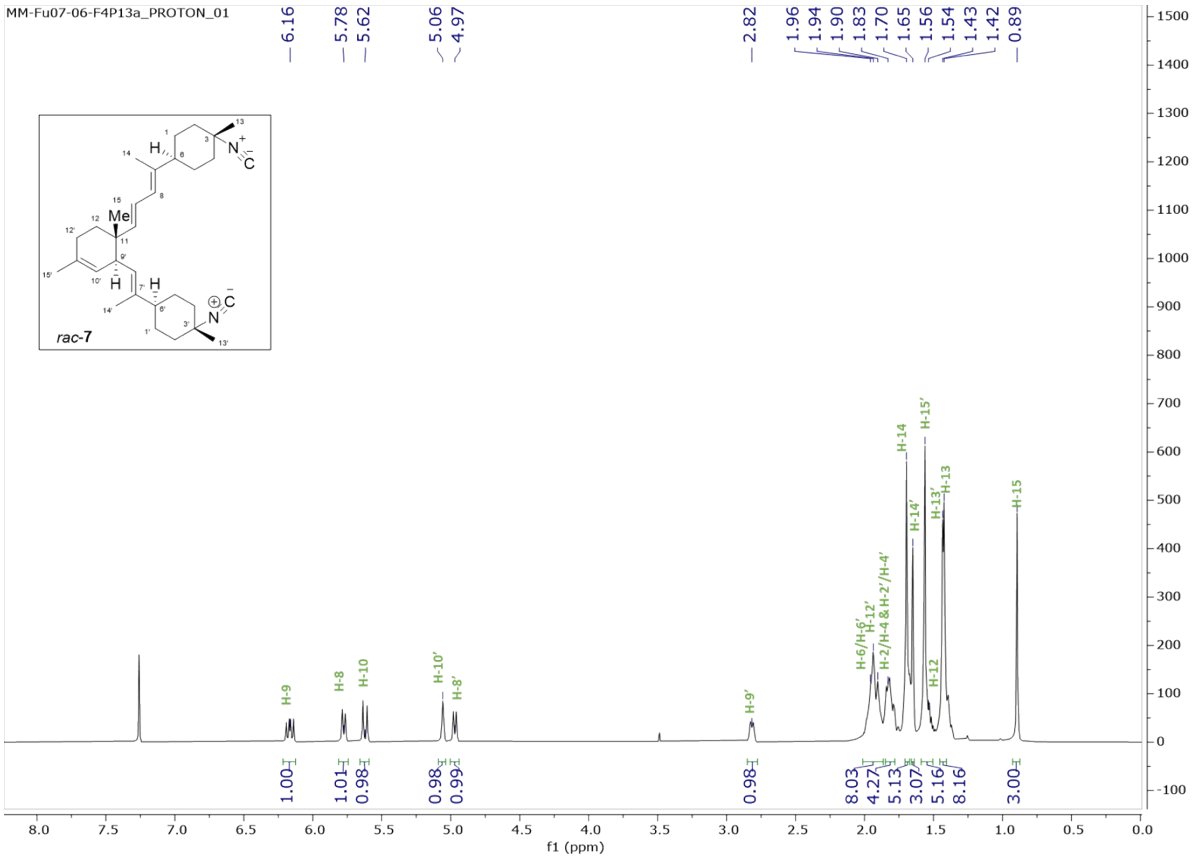

Figure S46. ^{1}H-NMR spectrum of *trans*-dimer theonellin isocyanide (***rac*-7**) at 600 MHz in $CDCl_3$

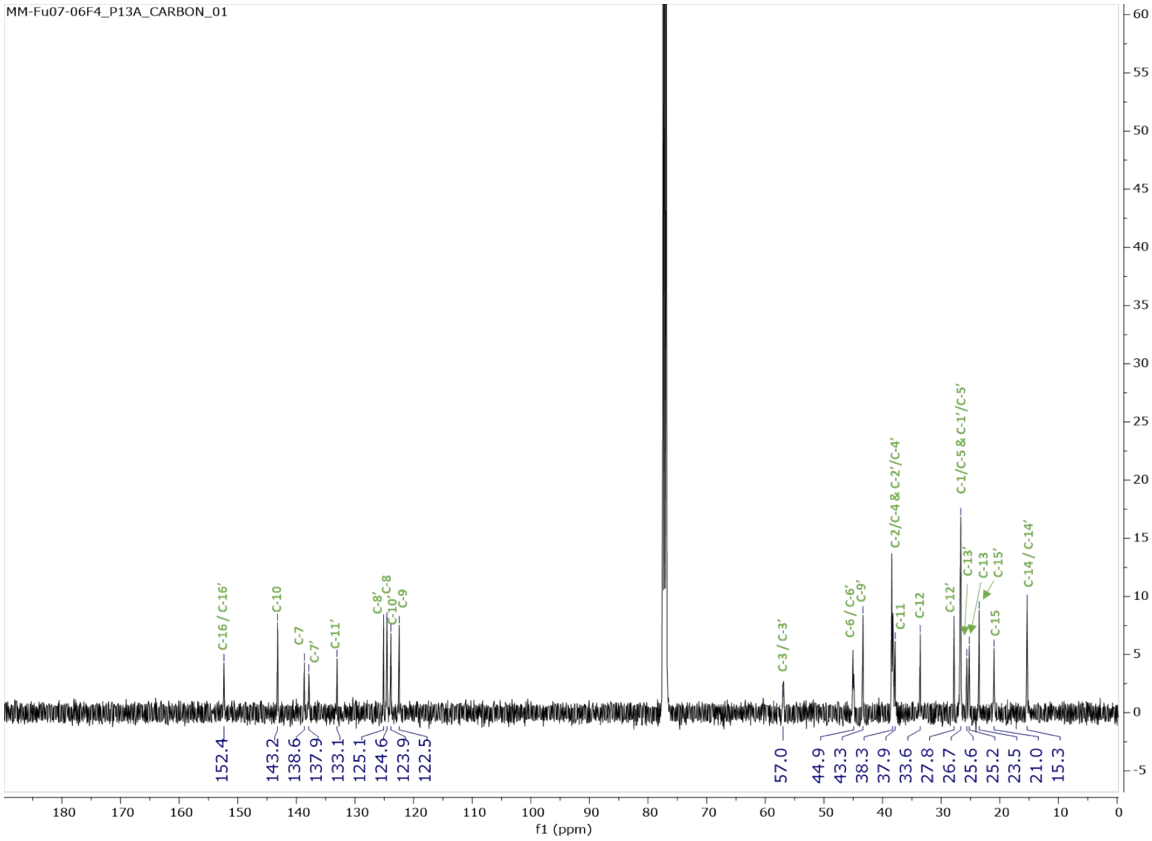

Figure S47. ^{13}C-NMR spectrum of *trans*-dimer theonellin isocyanide (***rac*-7**) at 600 MHz in $CDCl_3$

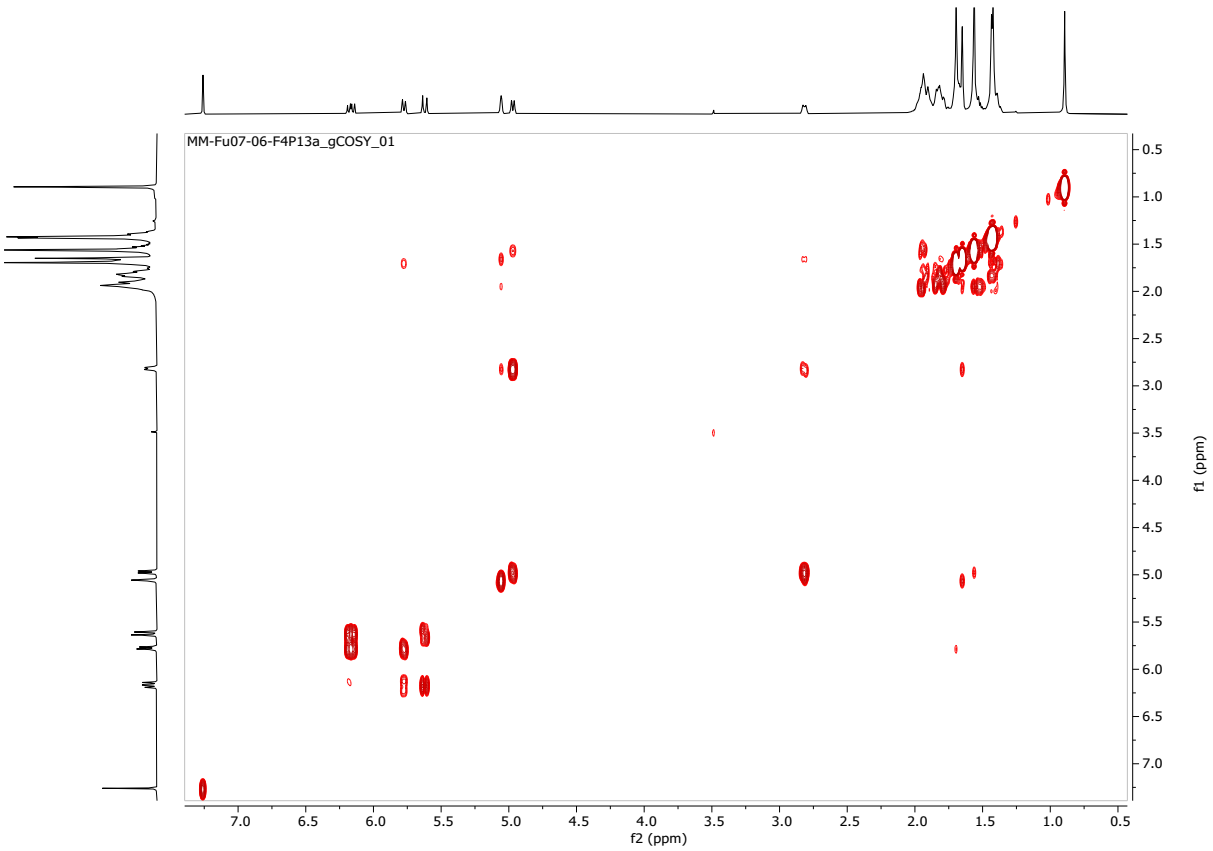

Figure S48. COSY spectrum of *trans*-dimer theonellin isocyanide (***rac*-7**) at 600 MHz in $CDCl_3$

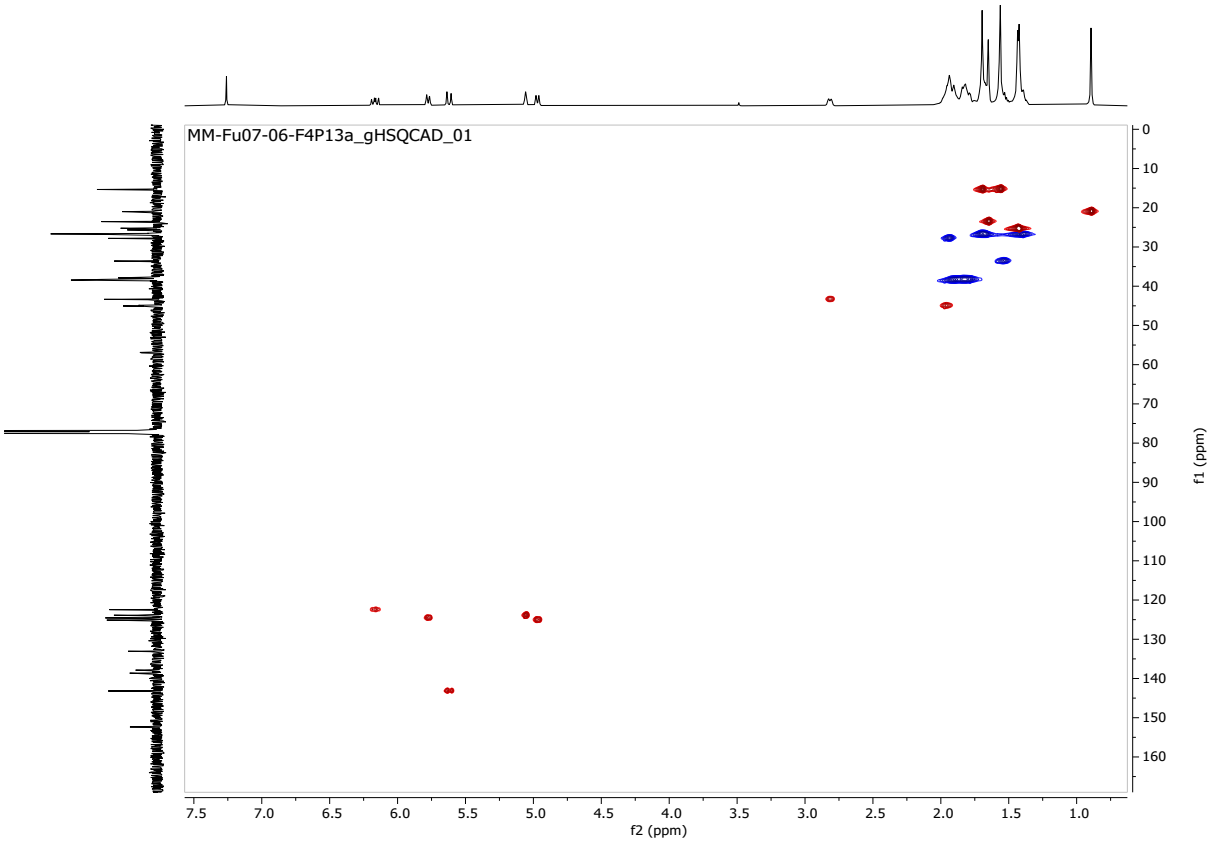

Figure S49. HSQC spectrum of *trans*-dimer theonellin isocyanide (***rac*-7**) at 600 MHz in $CDCl_3$

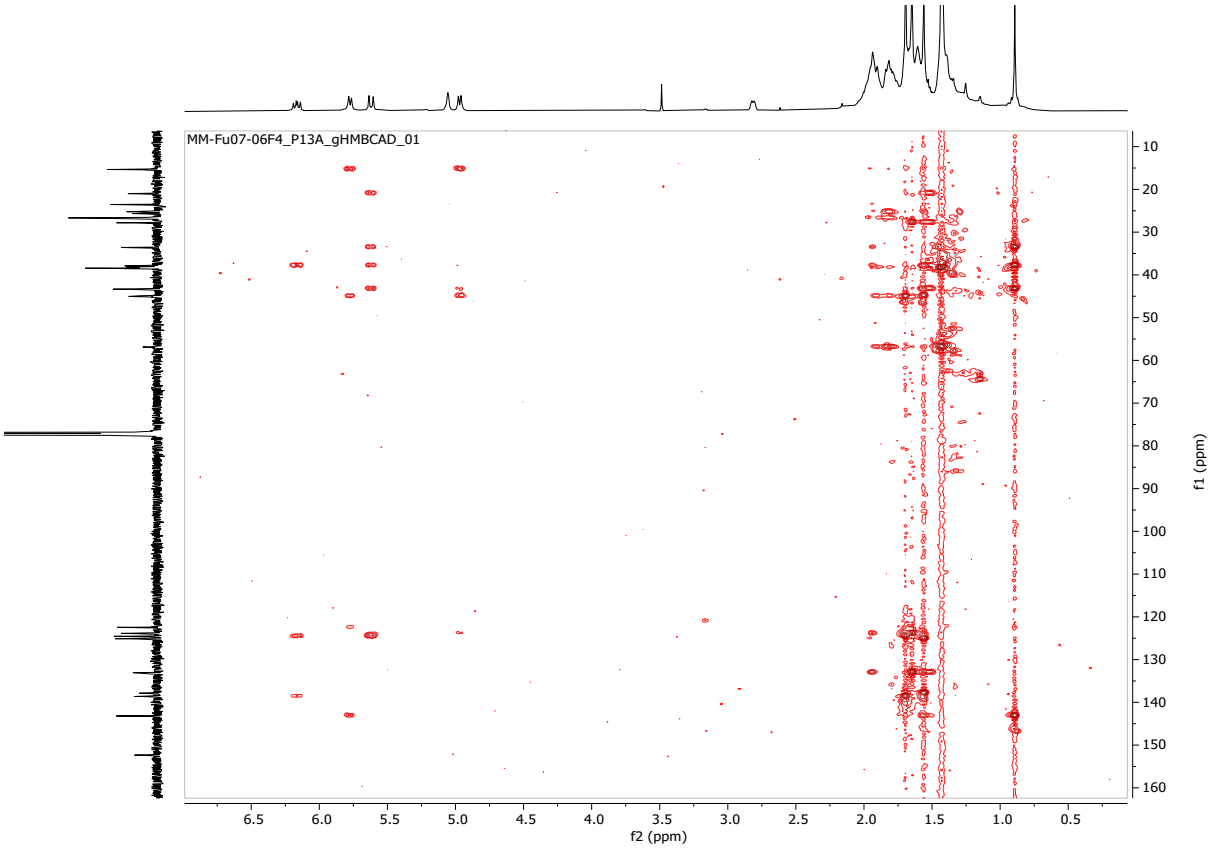

Figure S50. HMBC spectrum of *trans*-dimer theonellin isocyanide (***rac*-7**) at 600 MHz in $CDCl_3$

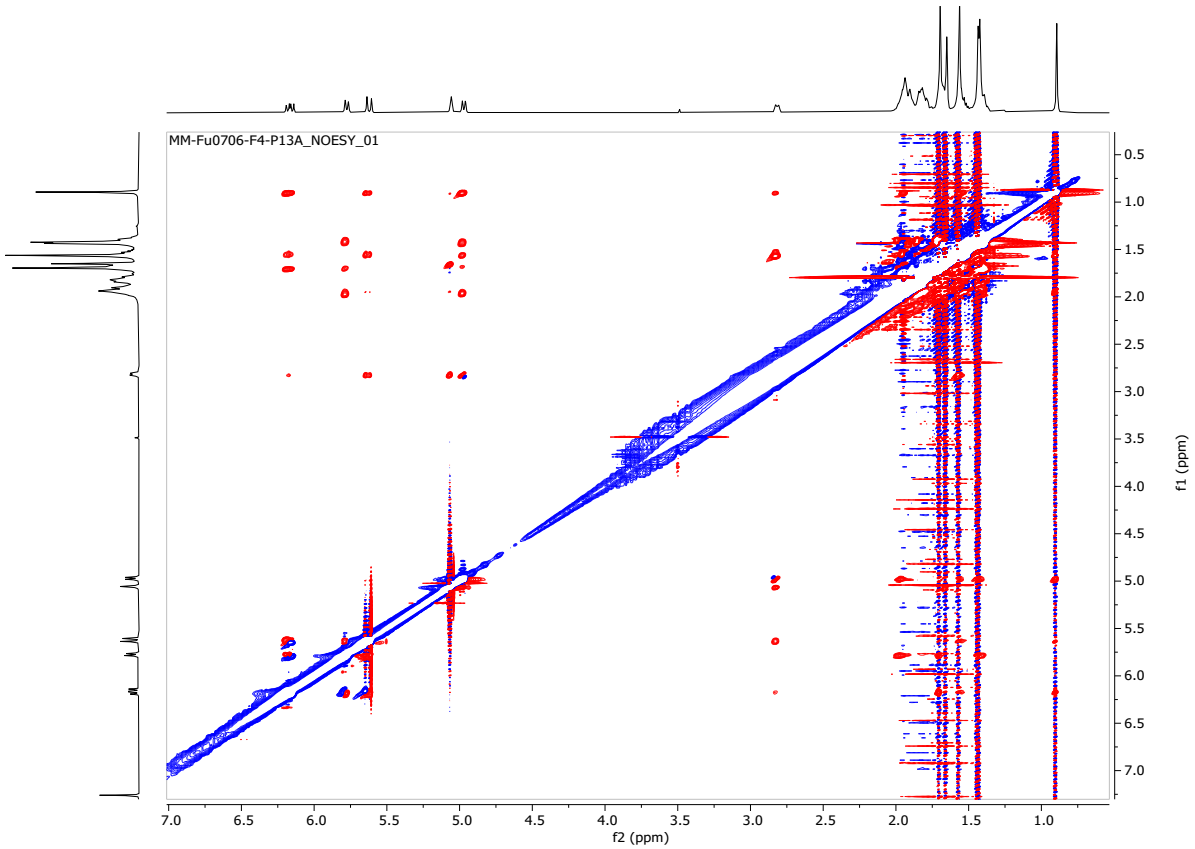

Figure S51. NOESY spectrum of *trans*-dimer theonellin isocyanide (***rac*-7**) at 600 MHz in $CDCl_3$

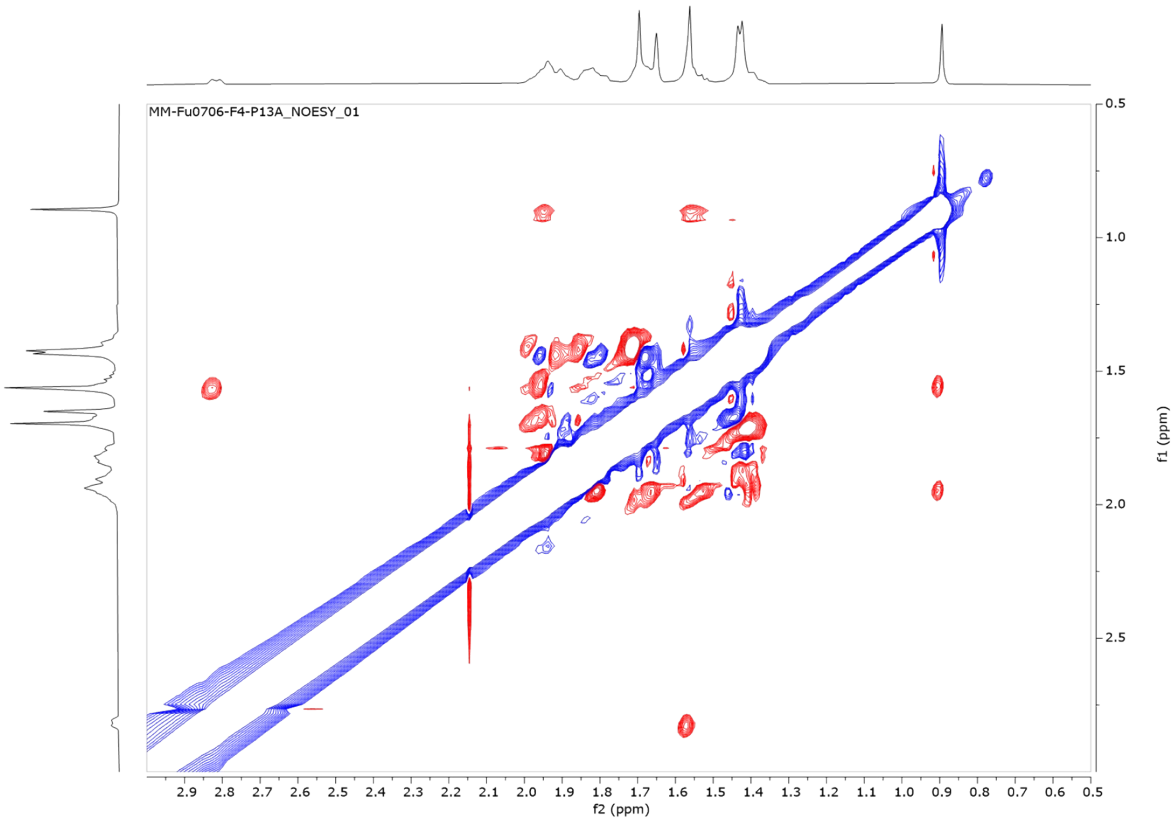

Figure S52. NOESY spectrum of *trans*-dimer theonellin isocyanide (***rac*-7**) at 600 MHz in $CDCl_3$

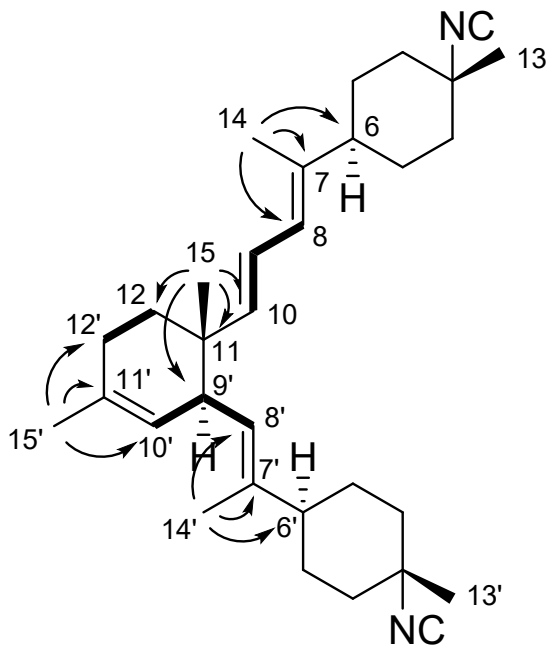

Figure S53. key COSY and HMBC (H to C) correlations for **7**

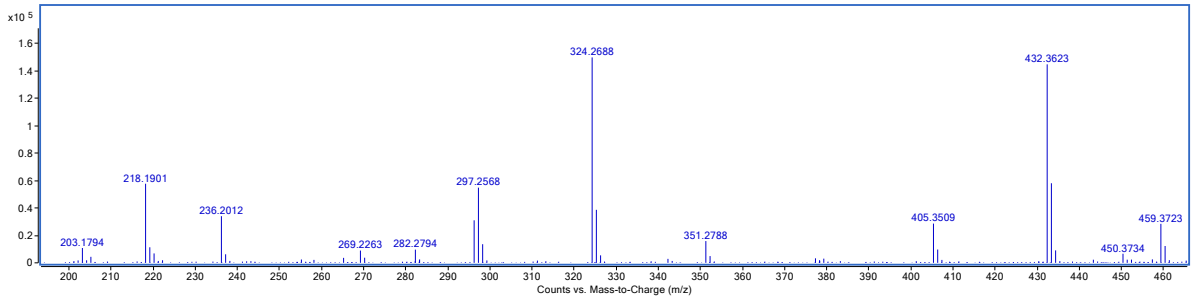

Figure S54. (+)-HRESIMS spectrum of *cis*-dimer theonellin isocyanide (***rac*-8**)

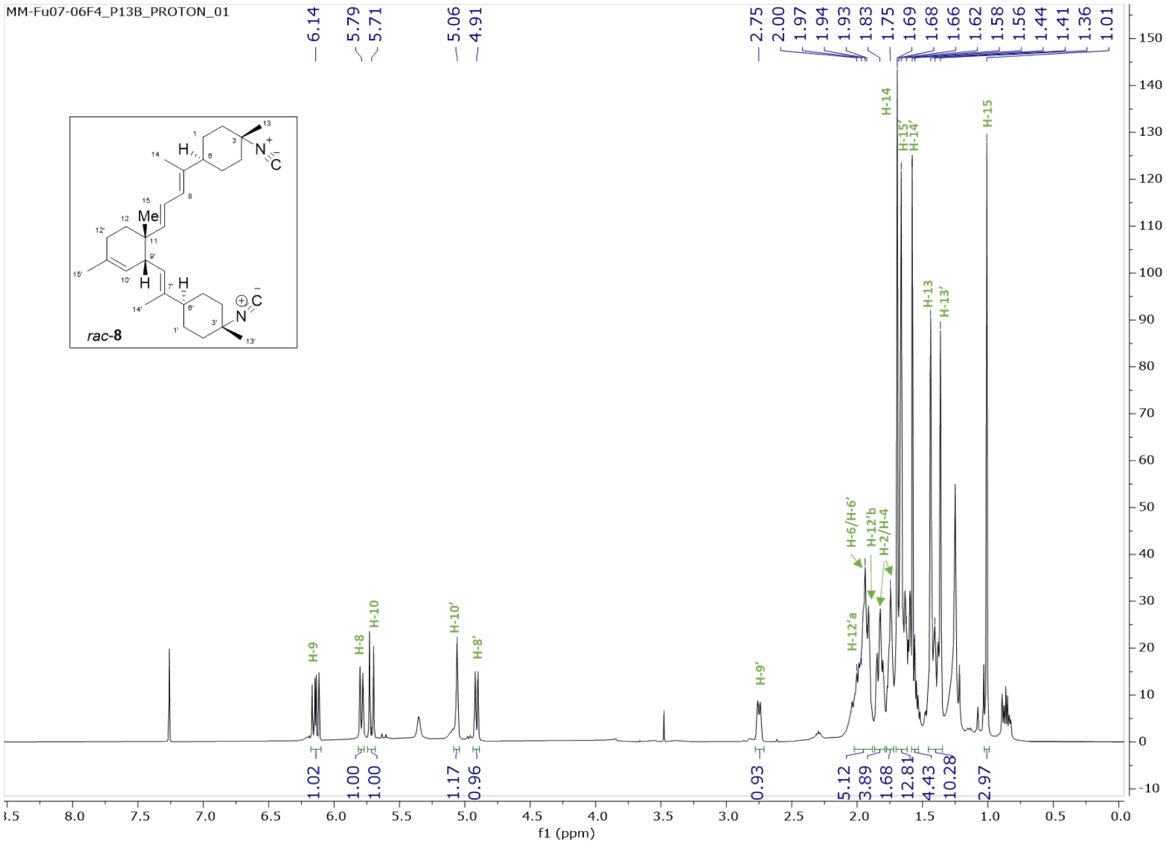

Figure S55. ^{1}H-NMR spectrum of *cis*-dimer theonellin isocyanide (***rac*-8**) at 600 MHz in $CDCl_3$

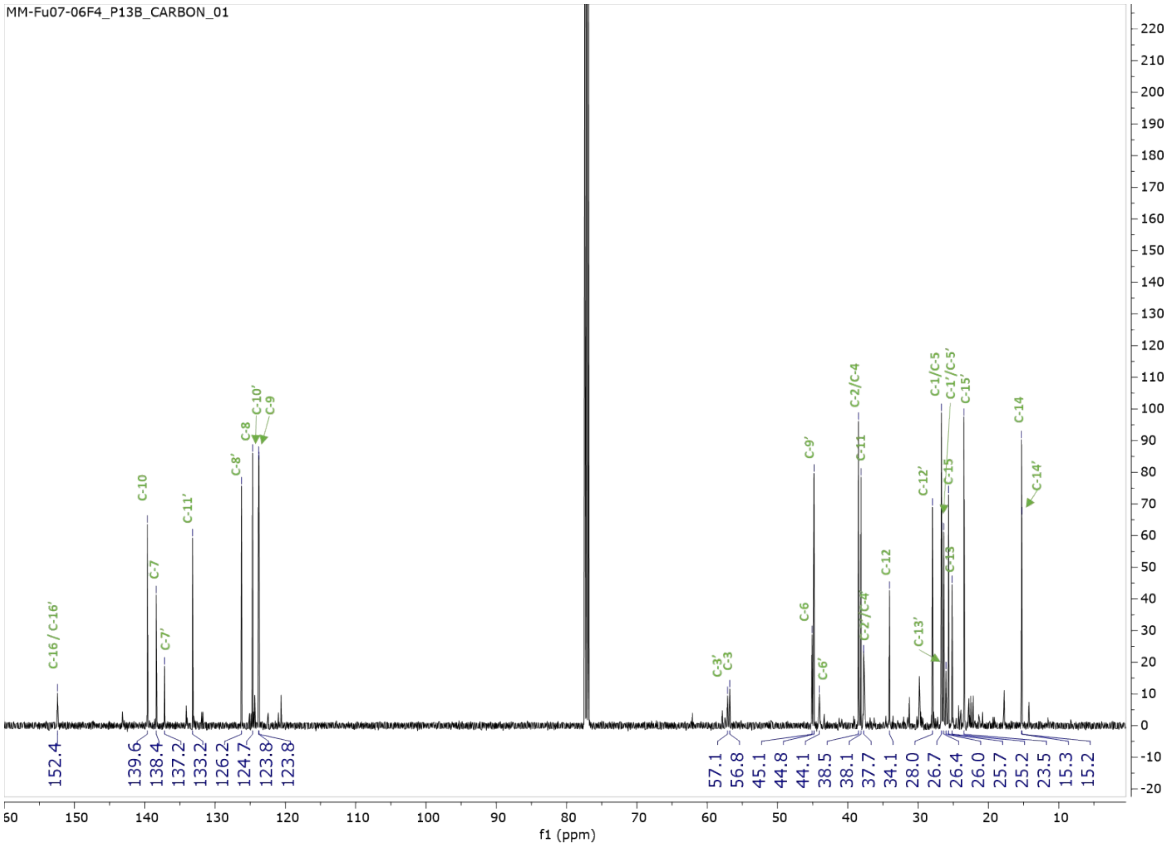

Figure S56. ^{13}C-NMR spectrum of *cis*-dimer theonellin isocyanide (***rac*-8**) at 150 MHz in $CDCl_3$

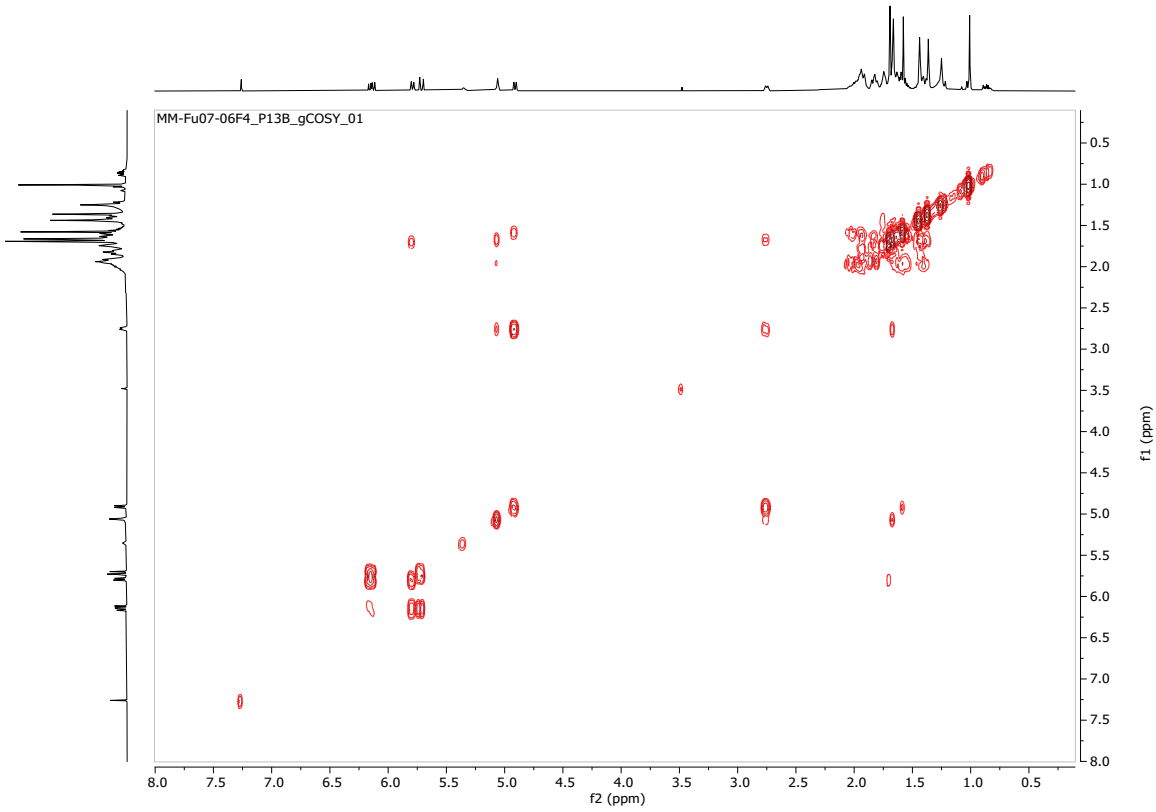

Figure S57. COSY spectrum of cis-dimer theonellin isocyanide (***rac*-8**) at 600 MHz in $CDCl_3$

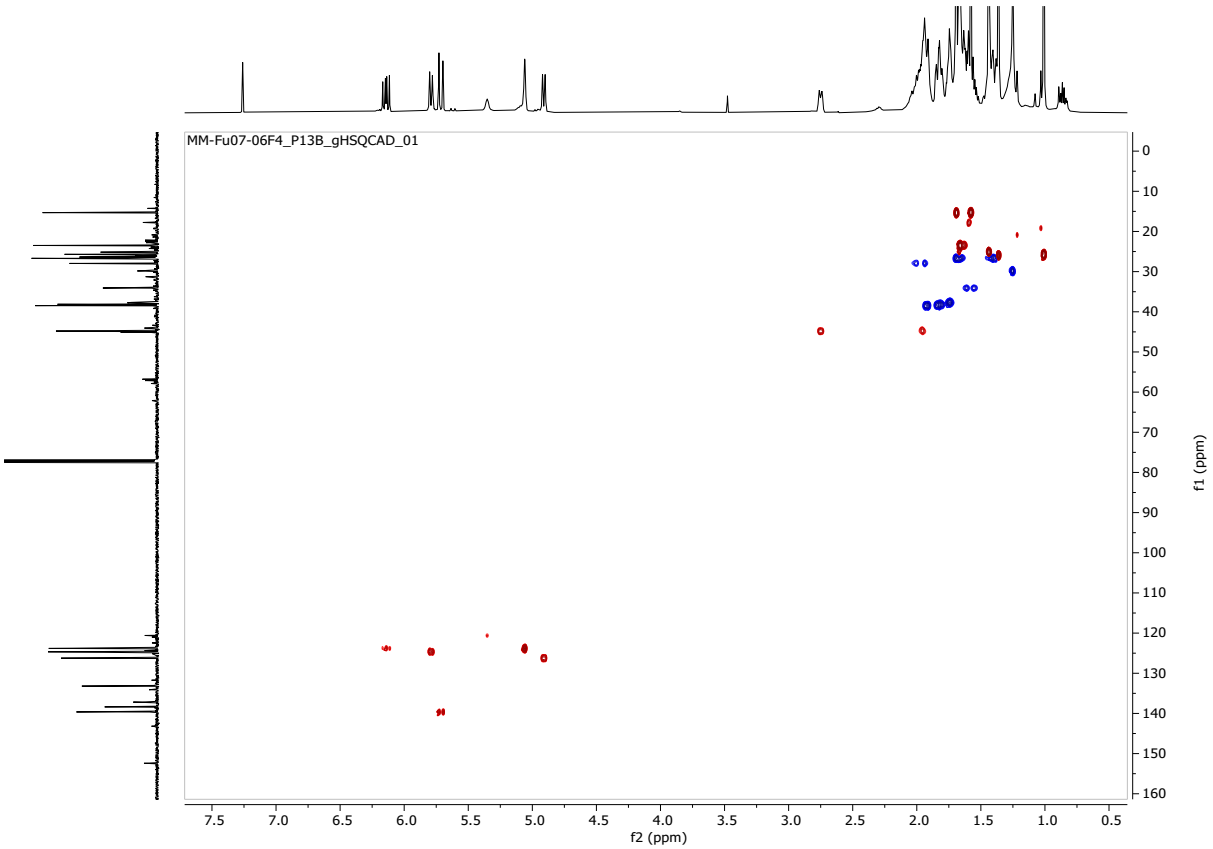

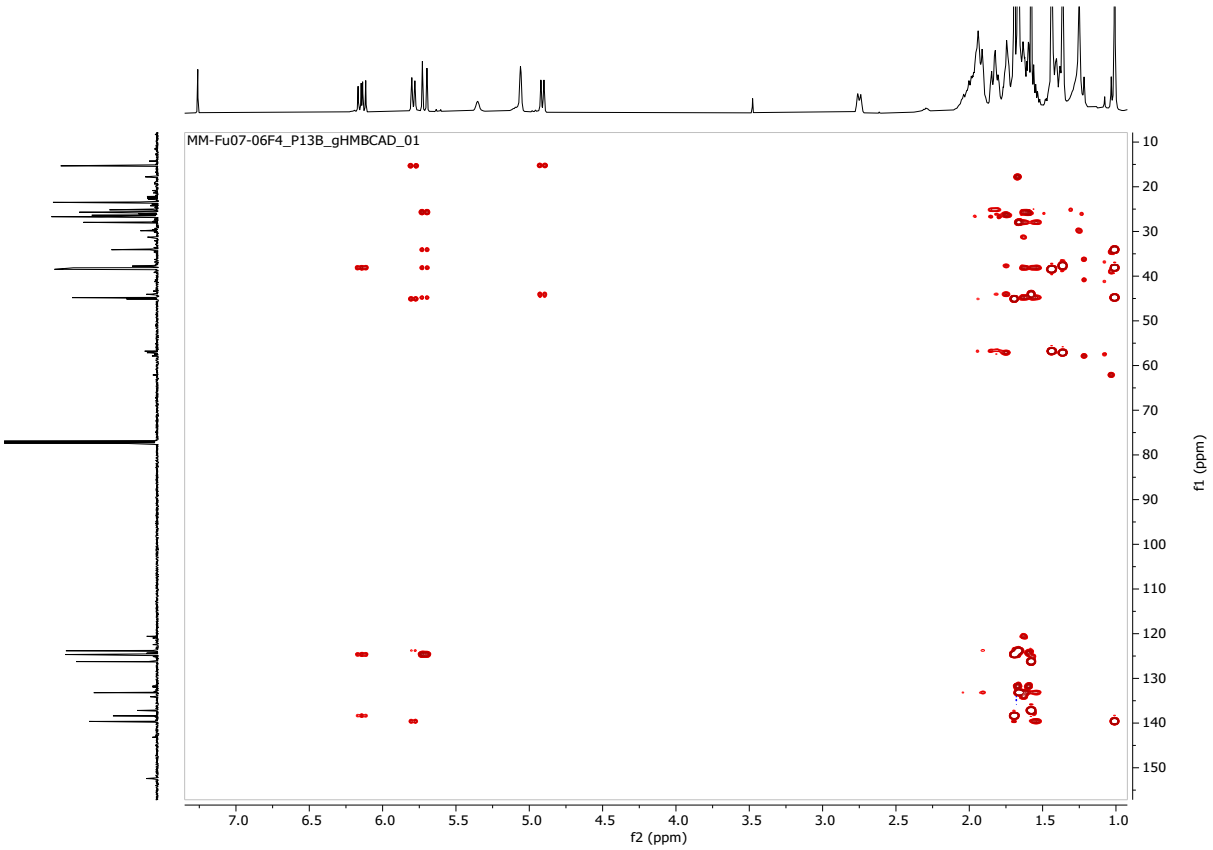

Figure S58. HSQC spectrum of *cis*-dimer theonellin isocyanide (***rac*-8**) at 600 MHz in $CDCl_3$

Figure S59. HMBC spectrum of *cis*-dimer theonellin isocyanide (***rac*-8**) at 600 MHz in $CDCl_3$

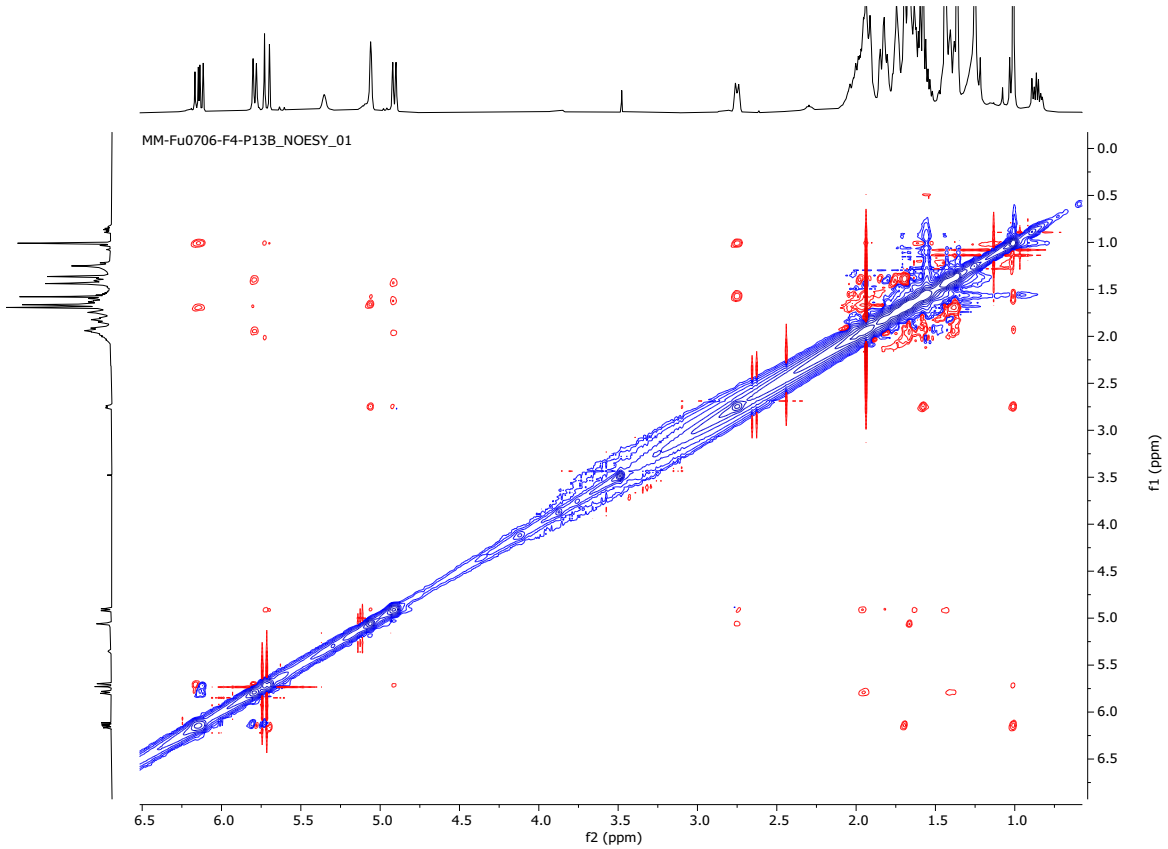

Figure S60. NOESY spectrum of *cis*-dimer theonellin isocyanide (***rac*-8**) at 600 MHz in $CDCl_3$

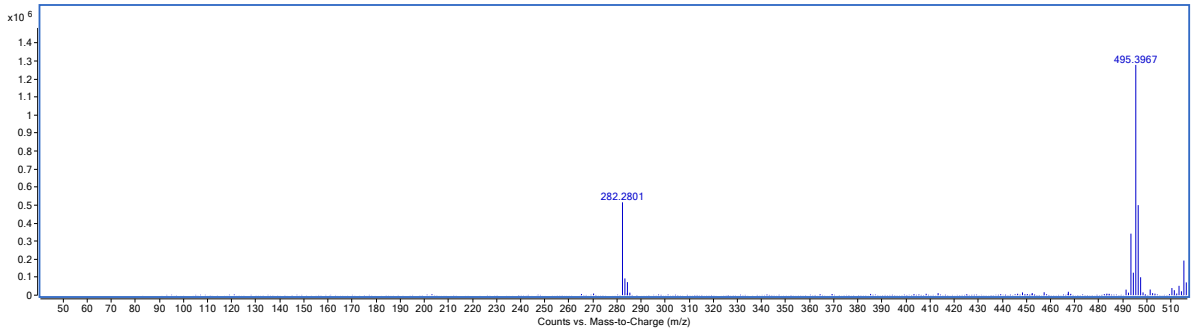

Figure S61. (+)-HRESIMS spectrum of *cis*-dimer theonellin formamide (***rac*-9**)

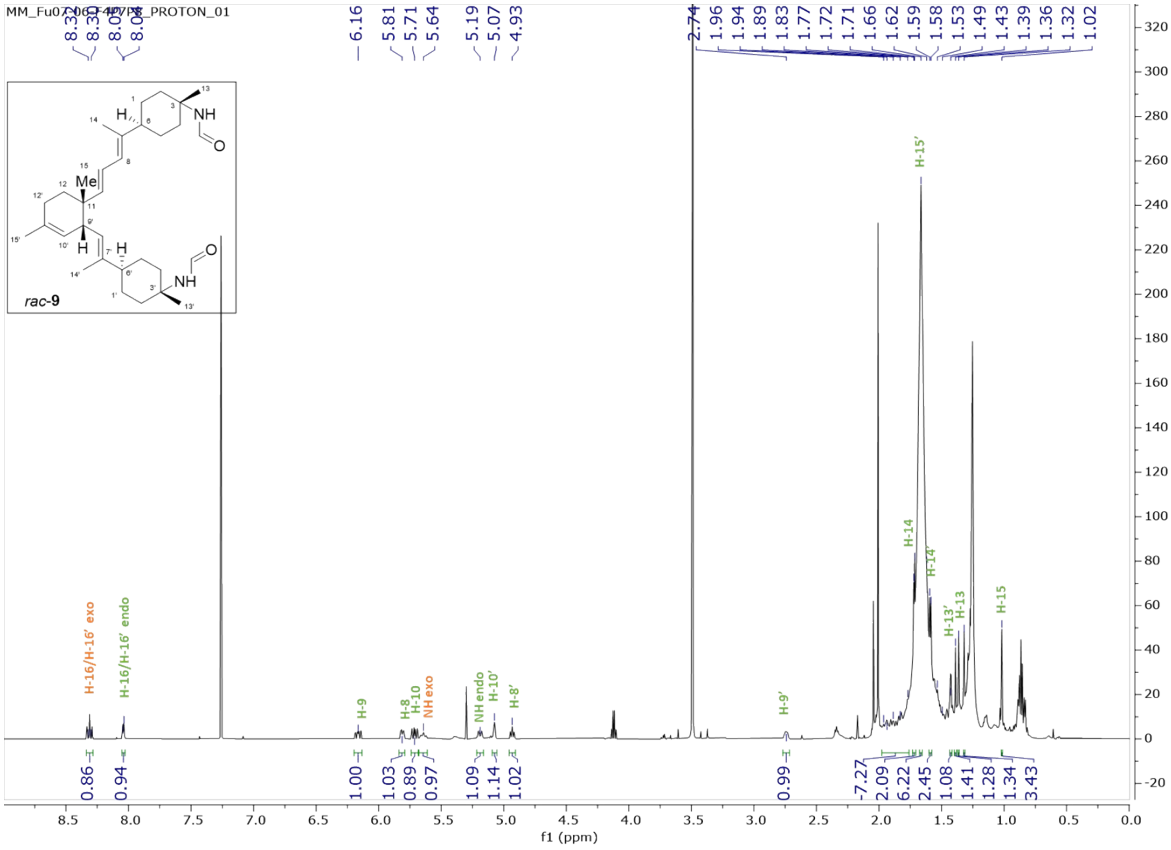

Figure S62. ^{1}H-NMR spectrum of *cis*-dimer theonellin formamide (***rac*-9**) at 600 MHz in $CDCl_3$

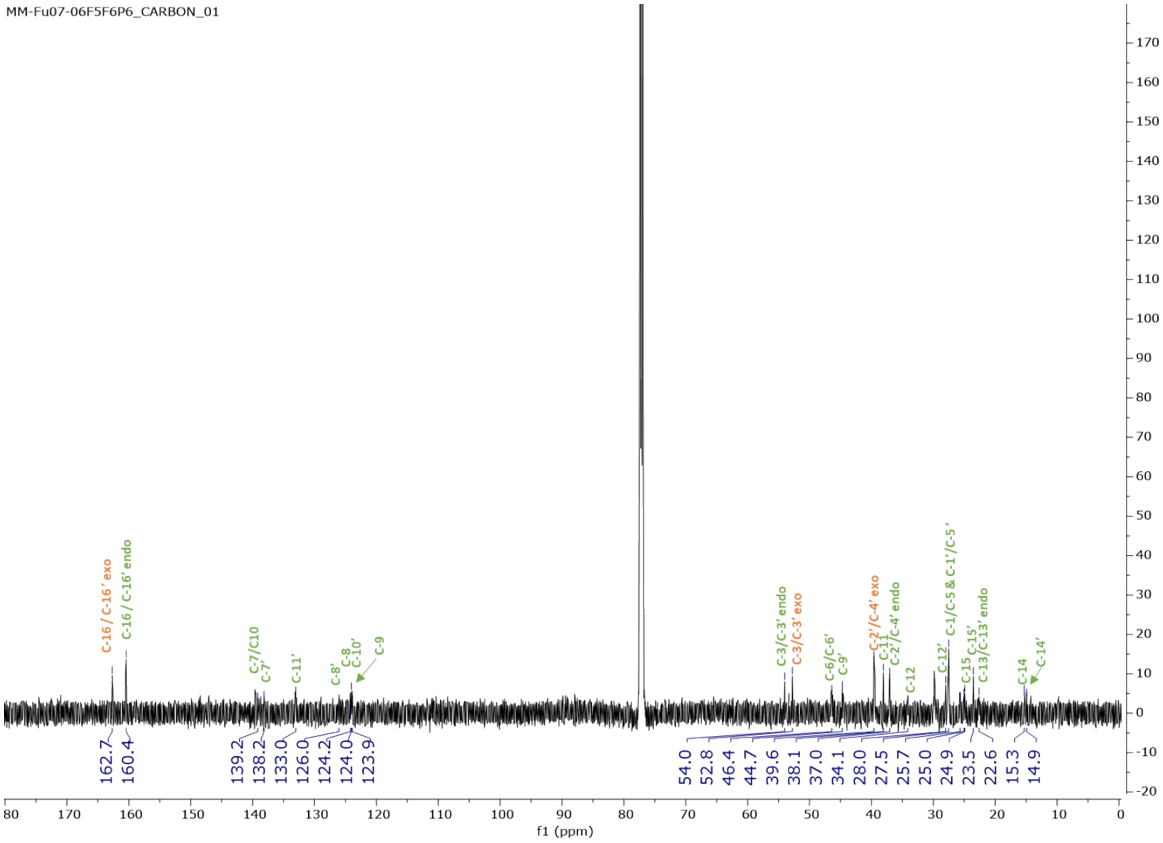

Figure S63. ^{13}C-NMR spectrum of *cis*-dimer theonellin formamide (***rac*-9**) at 150 MHz in $CDCl_3$

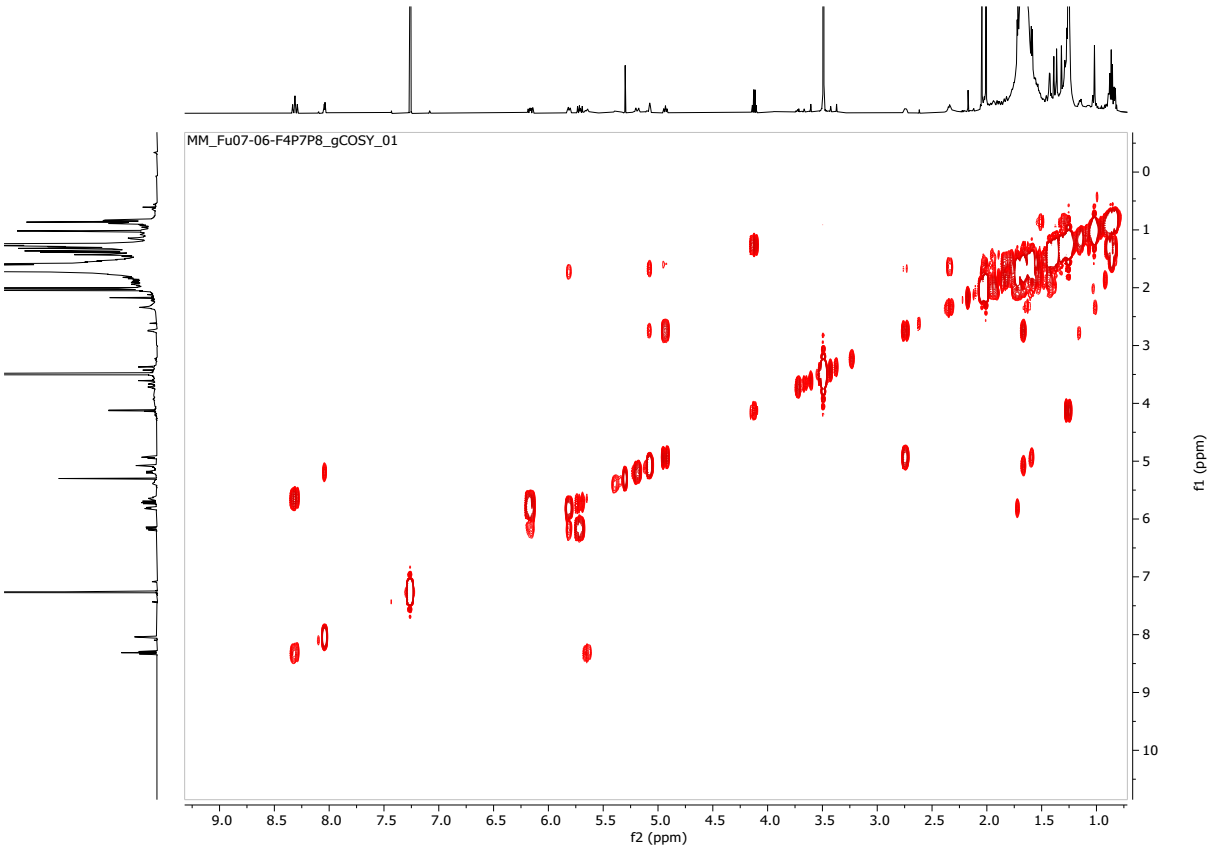

Figure S64. COSY spectrum of *cis*-dimer theonellin formamide (***rac*-9**) at 600 MHz in $CDCl_3$

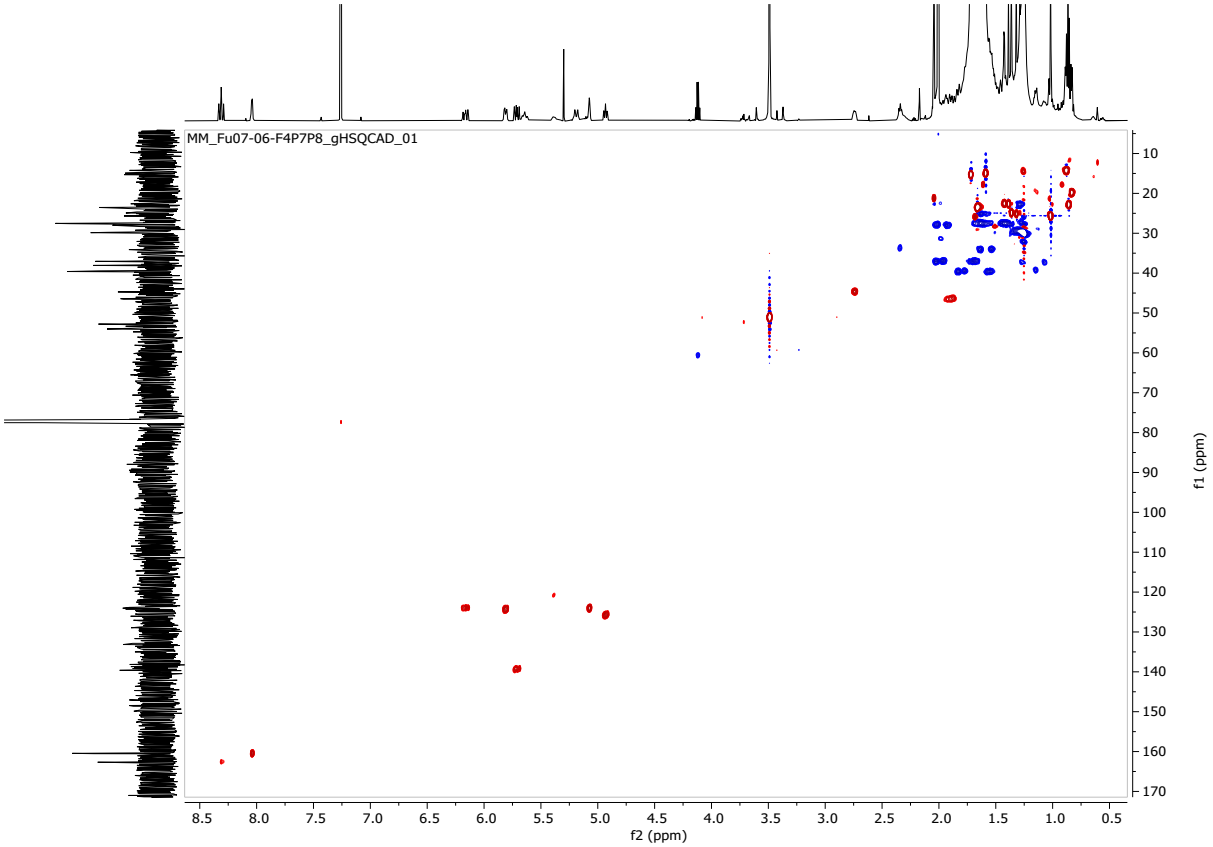

Figure S65. HSQC spectrum of *cis*-dimer theonellin formamide (***rac*-9**) at 600 MHz in $CDCl_3$

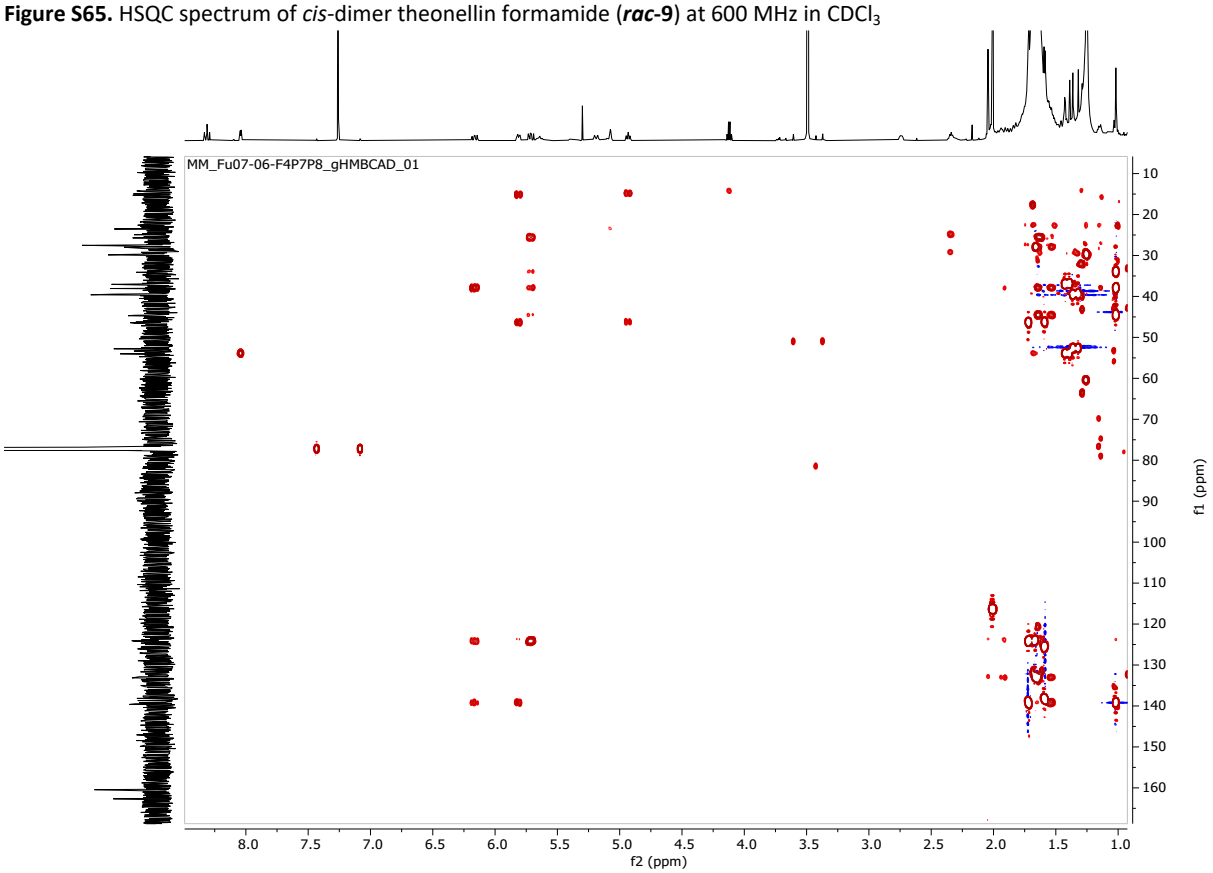

Figure S66. HMBC spectrum of *cis*-dimer theonellin formamide (***rac*-9**) at 600 MHz in $CDCl_3$

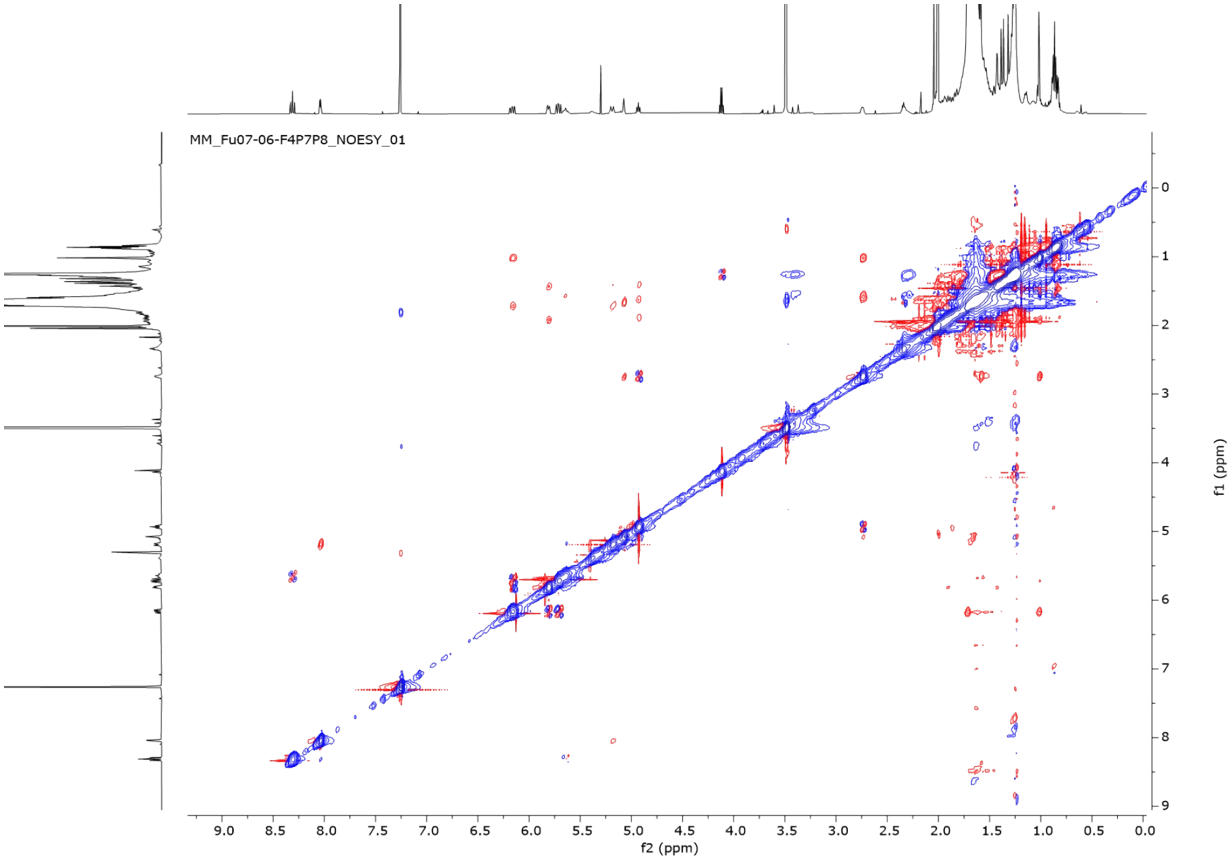

Figure S67. NOESY spectrum of *cis*-dimer theonellin formamide (***rac*-9**) at 600 MHz in $CDCl_3$

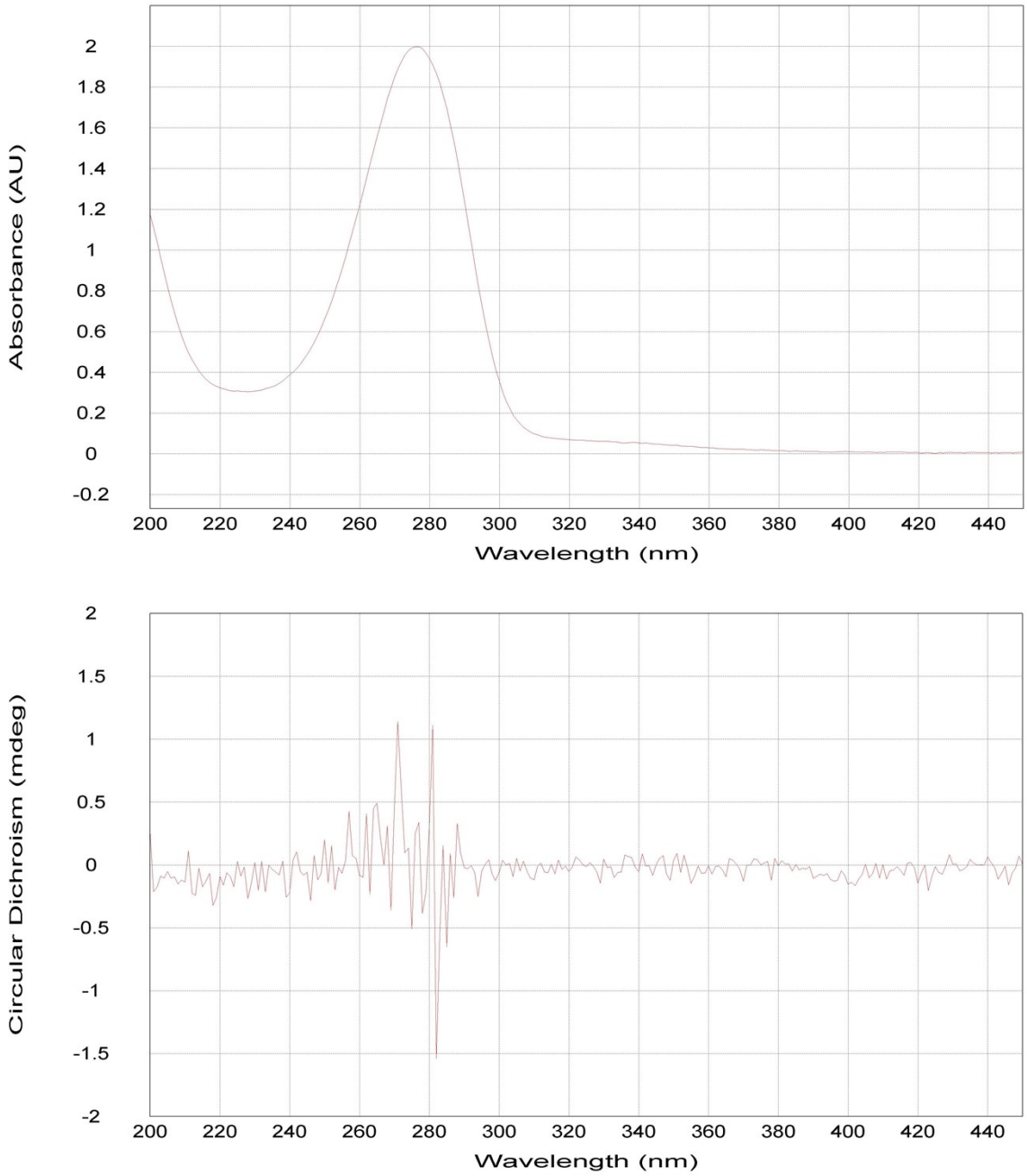

Figure S68. Absorbance and ECD spectra of bubaridin A (*rac*-**1**)

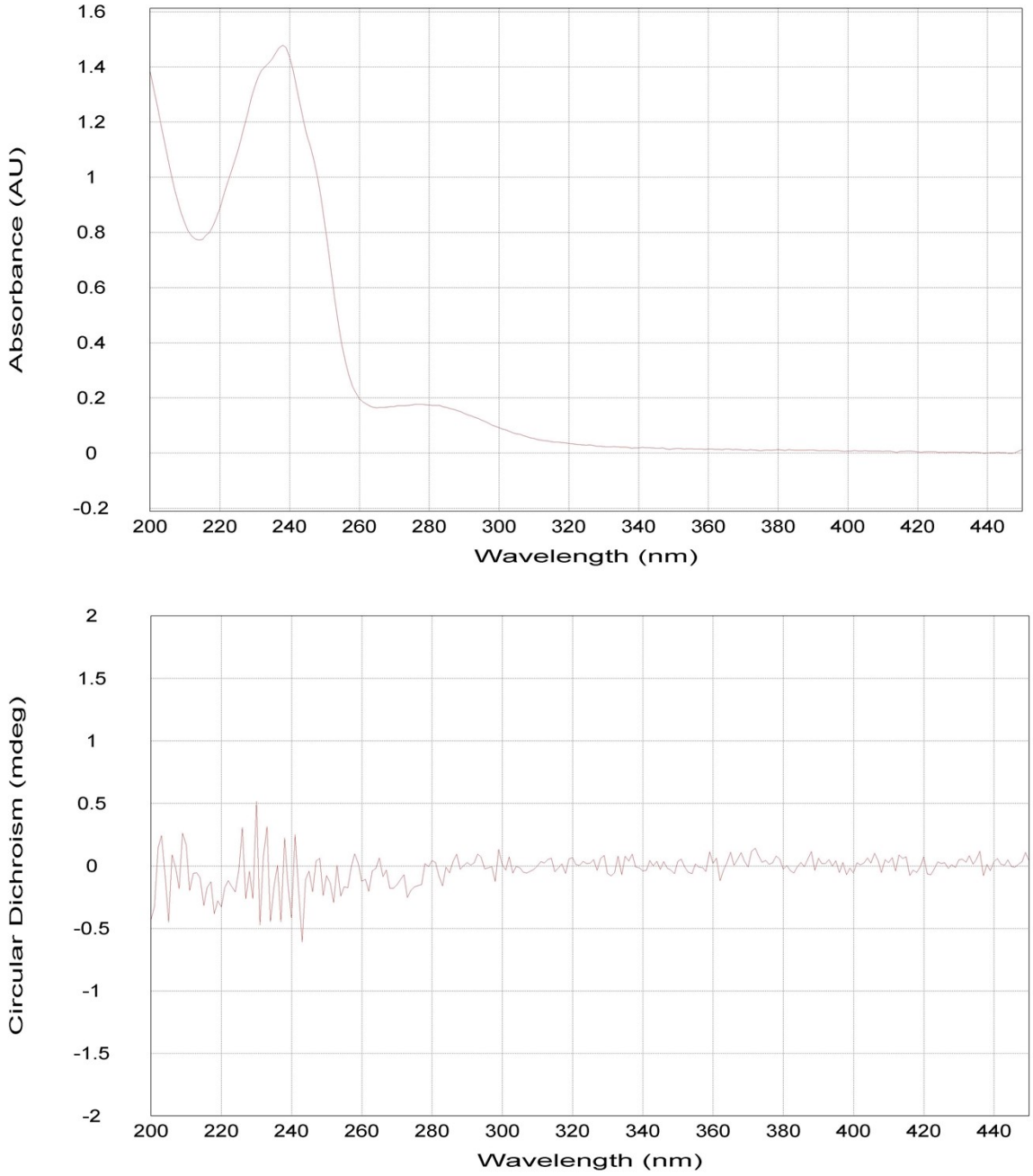

Figure S69. Absorbance and ECD spectra of bubaridin B (*rac*-**2**)

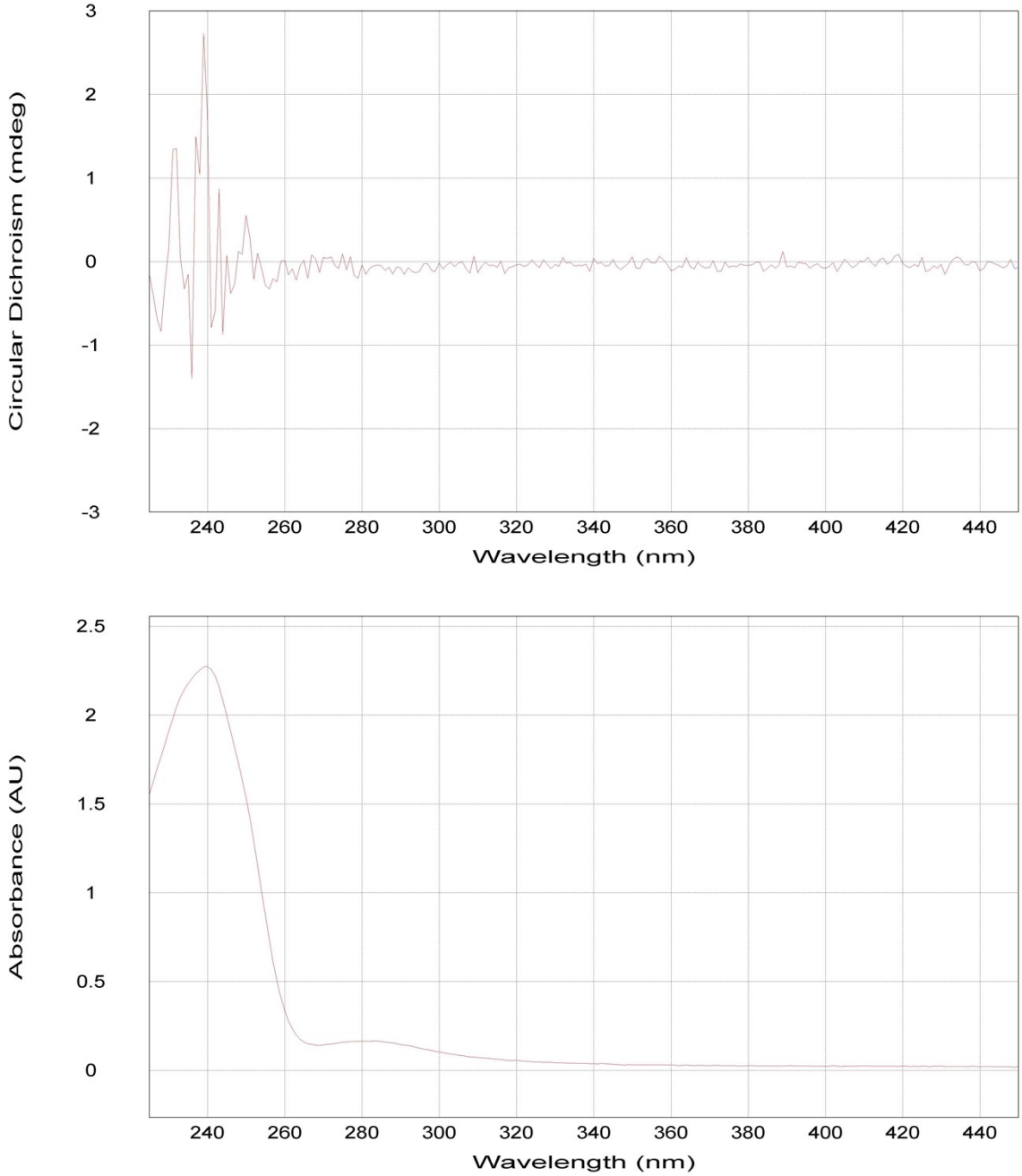

Figure S70. Absorbance and ECD spectra of bubaridin C (*rac*-**3**)

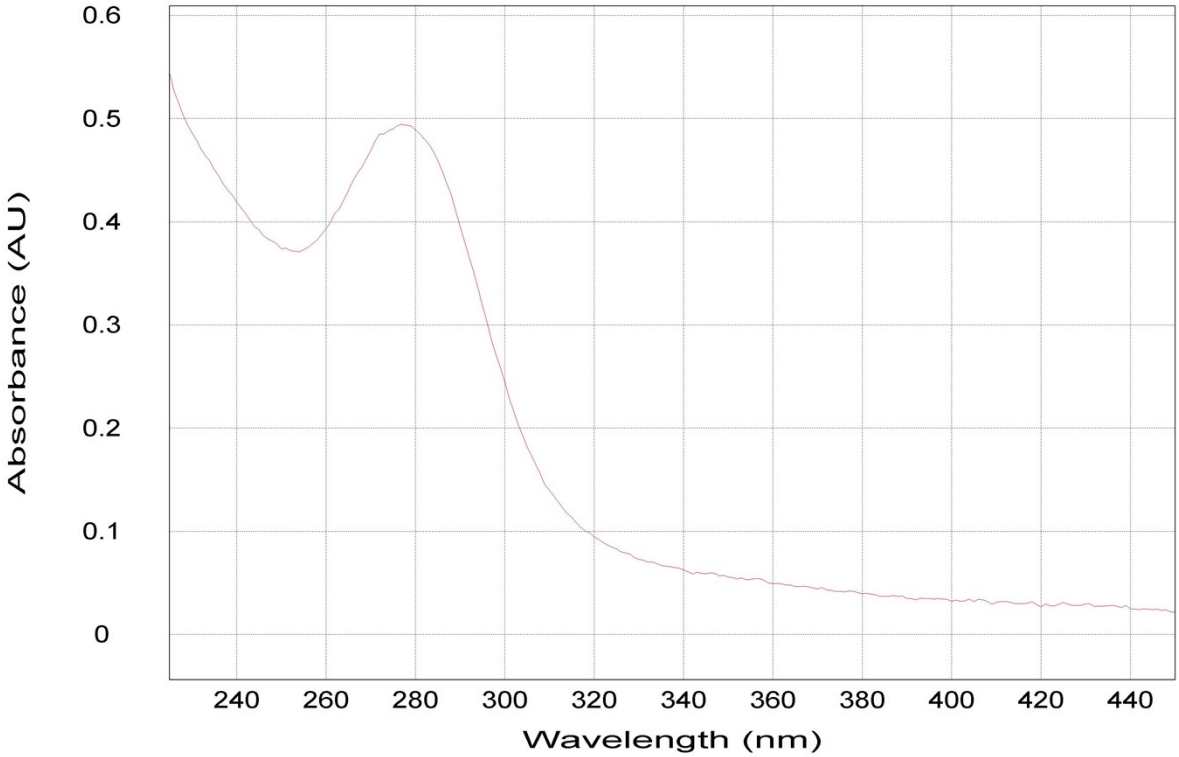

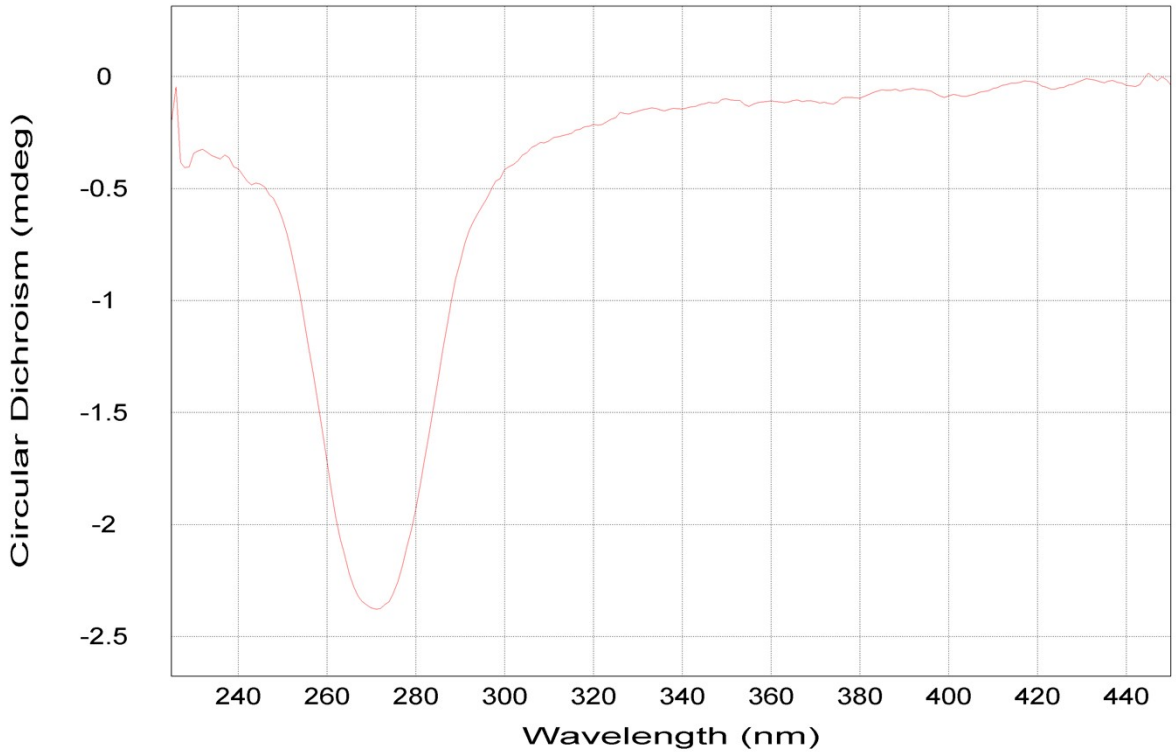

Figure S71. Absorbance and ECD spectra of bubaridin D and 11-*epi*-bubaridin D (*rac*-**4** and *rac*-*epi*-**4**)

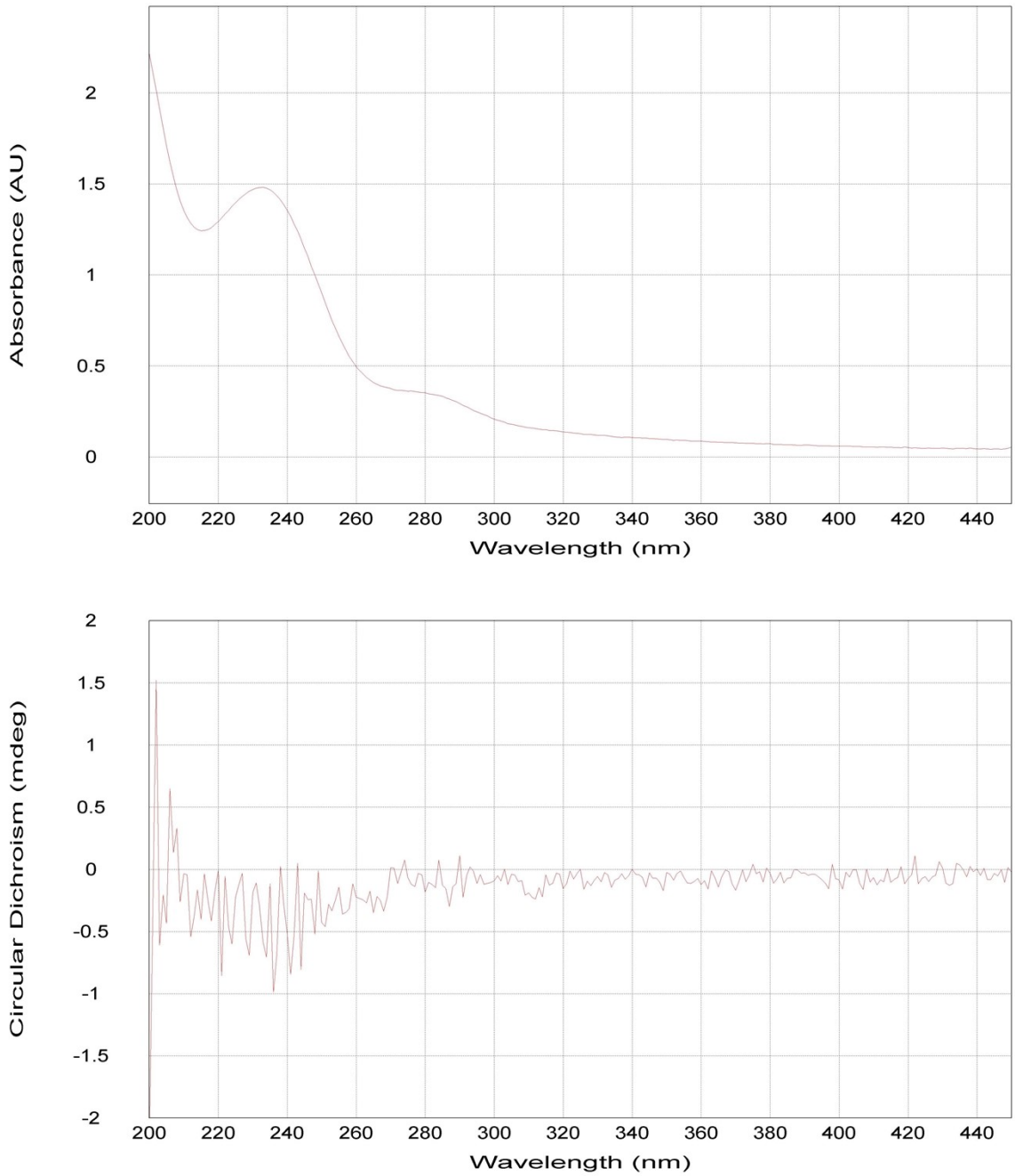

Figure S72. Absorbance and ECD spectra of bubaridin E (*rac*-**5**)

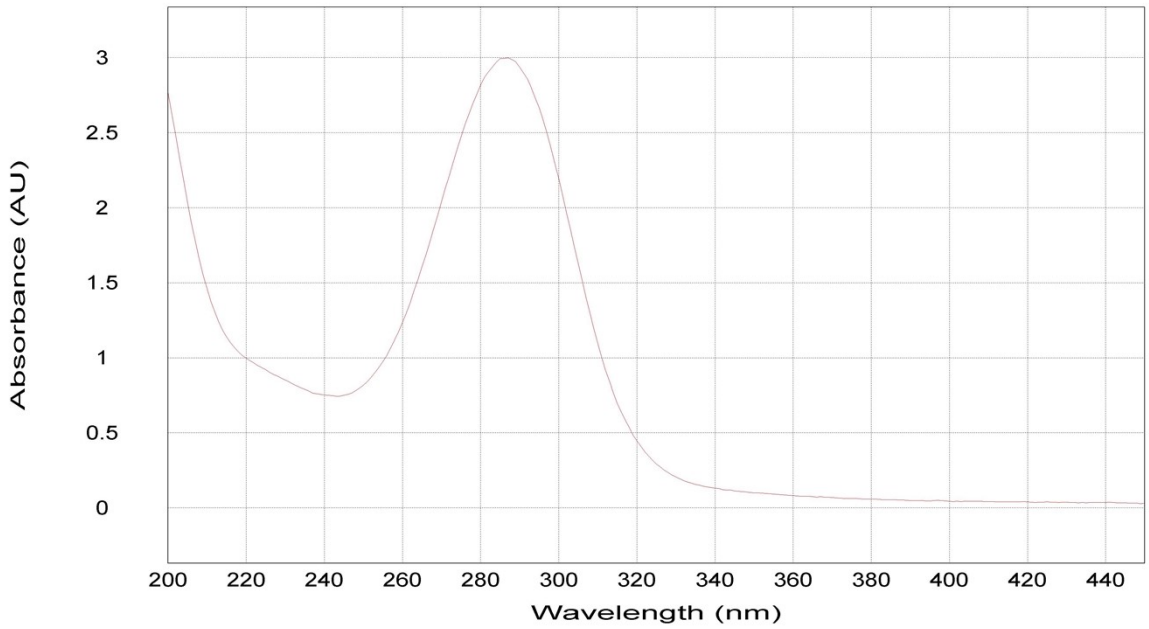

Figure S73. Absorbance spectra of bubaridin F (*rac*-**6**)

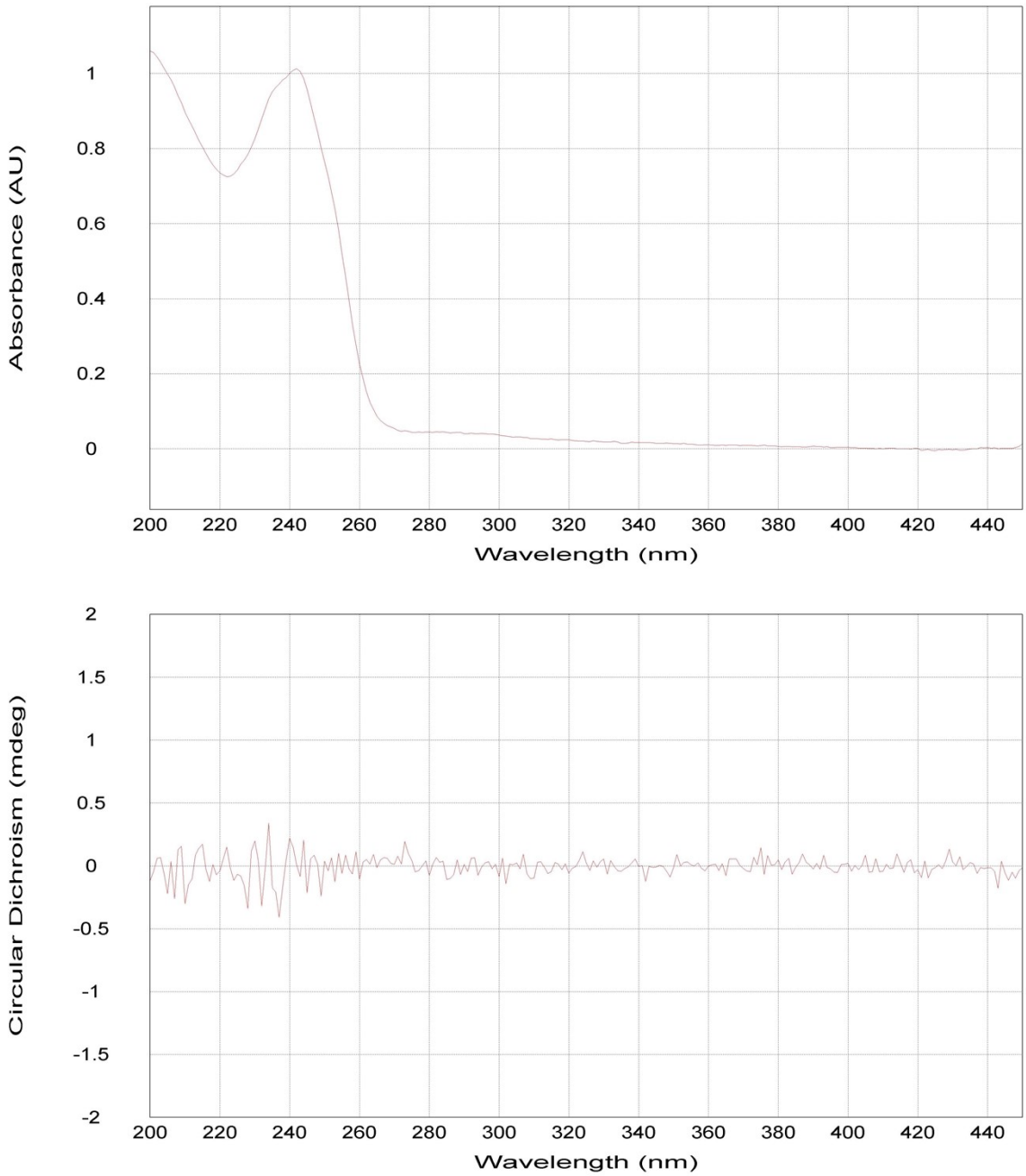

Figure S74. Absorbance and ECD spectra of *trans*-dimer theonellin isocyanide (*rac*-**7**)

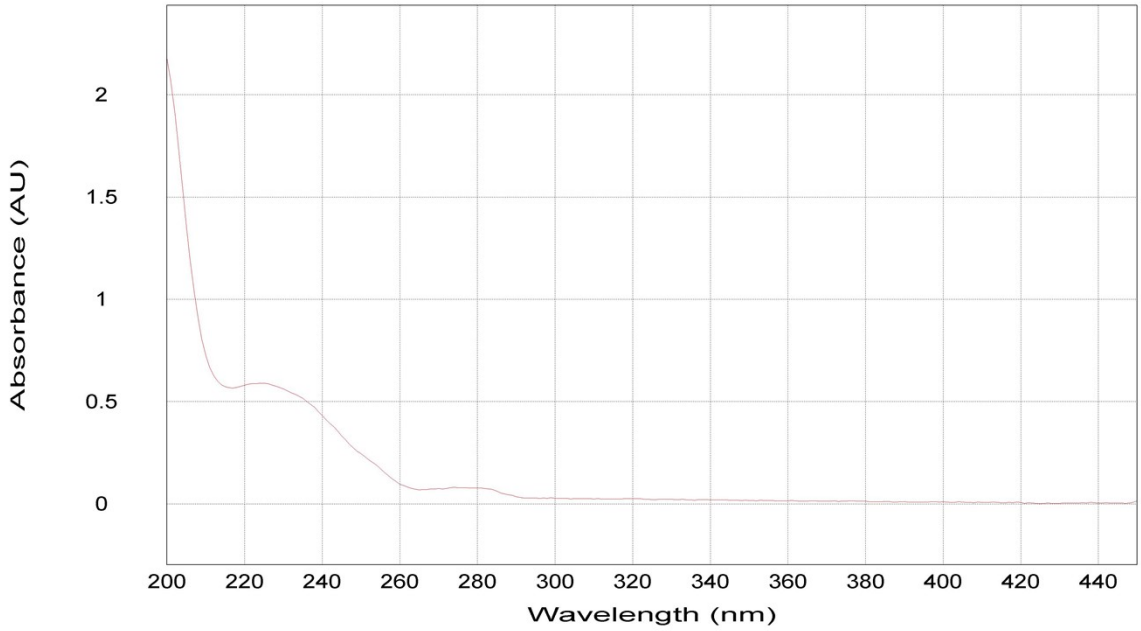

Figure S75. Absorbance and ECD spectra of *cis*-dimer theonellin isocyanide (*rac*-**8**)

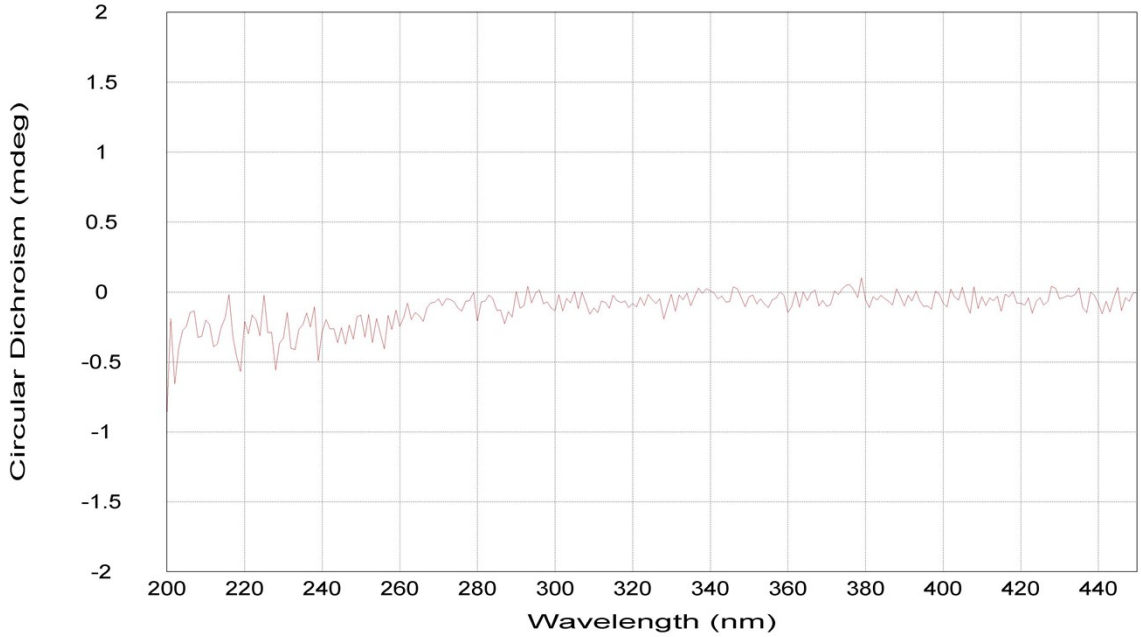

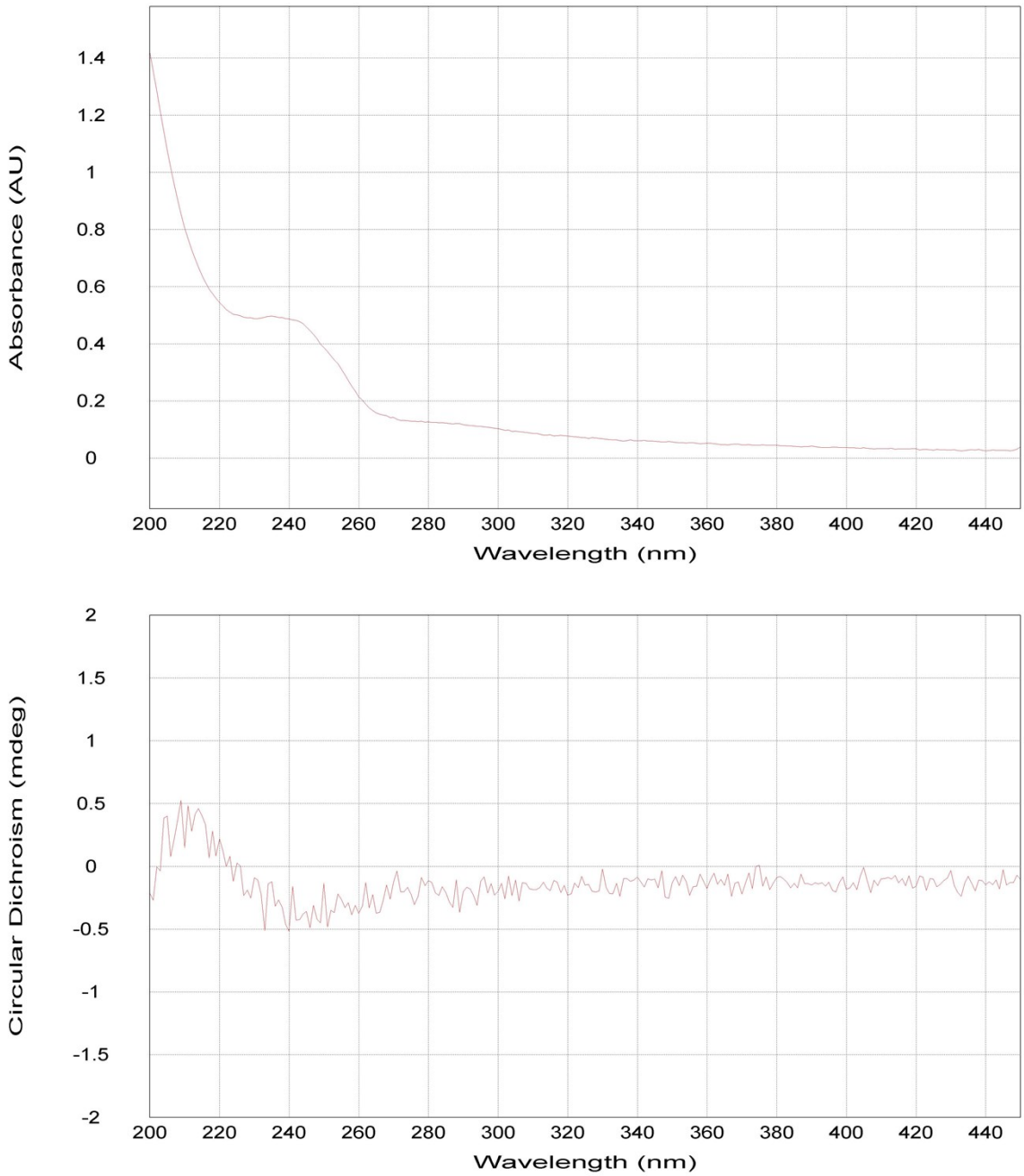

Figure S76. Absorbance and ECD spectra of *cis*-dimer theonellin formamide (*rac*-**9**)

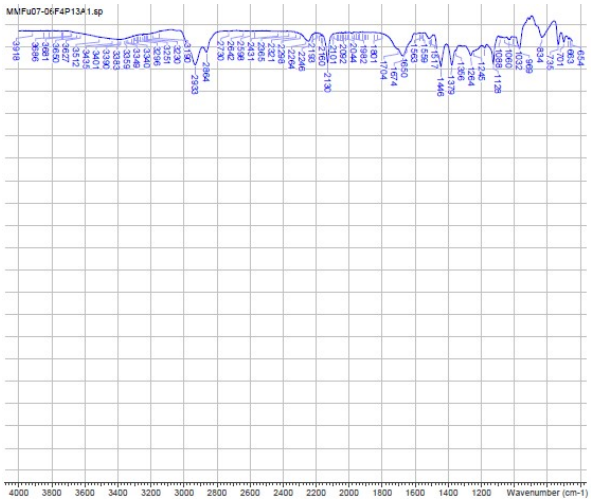

Figure S77. FT-IR spectra of *trans*-dimer theonellin isocyanide (*rac*-**7**)

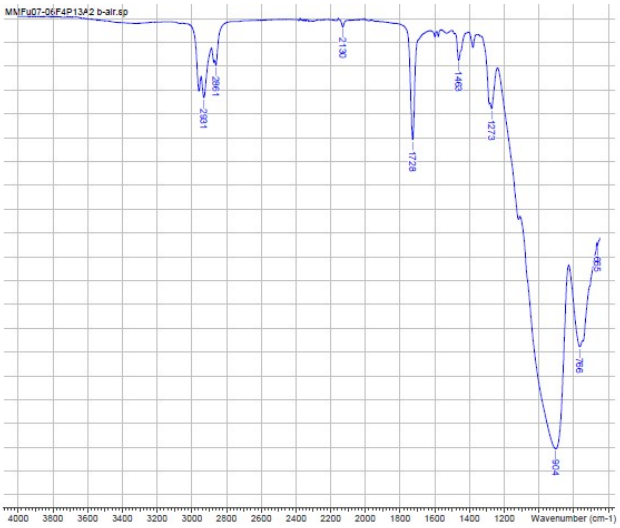

Figure S78. FT-IR spectra of *cis*-dimer theonellin isocyanide (*rac*-**8**)

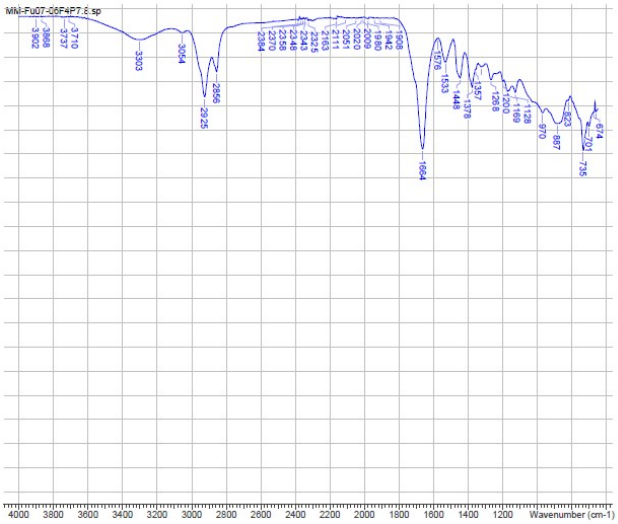

Figure S79. FT-IR spectra of *cis*-dimer theonellin formamide (*rac*-**9**)

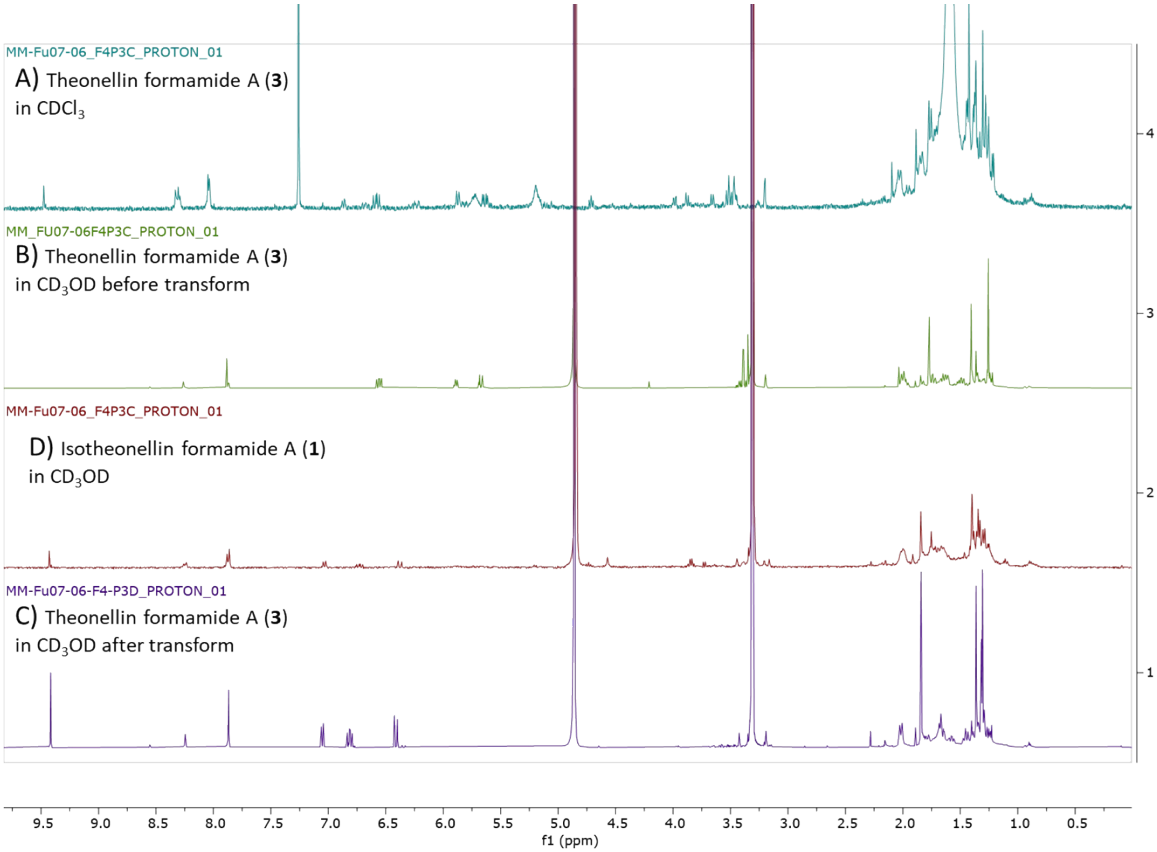

Figure S80. ^{1}H-NMR spectra comparison of the transformation of compound bubaridin C (**3**) into bubaridin A (**1**).

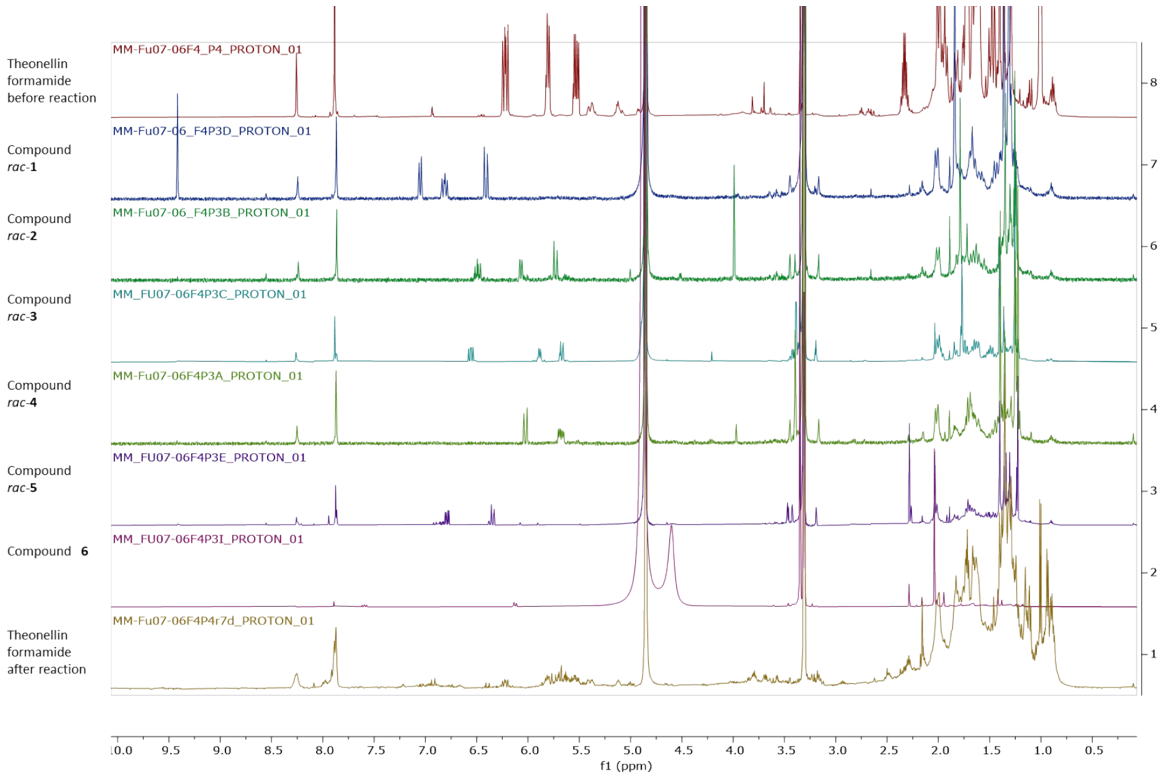

Figure S81. ^{1}H-NMR spectra comparison of the reactivity test performed with theonellin formamide (before and after air exposure in acidic conditions) and the compounds isolated (**1-6**) in CD_3OD.

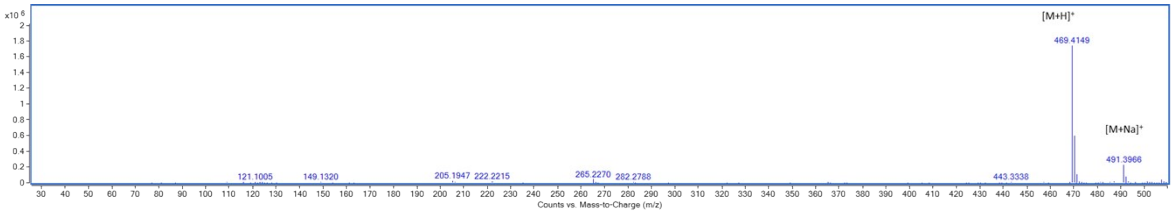

Figure S82. (+)-HRESIMS spectrum of N,N'-bis[(6R,7S)-7-amino-7,8-dihydro-α-bisabolen-7-yl]

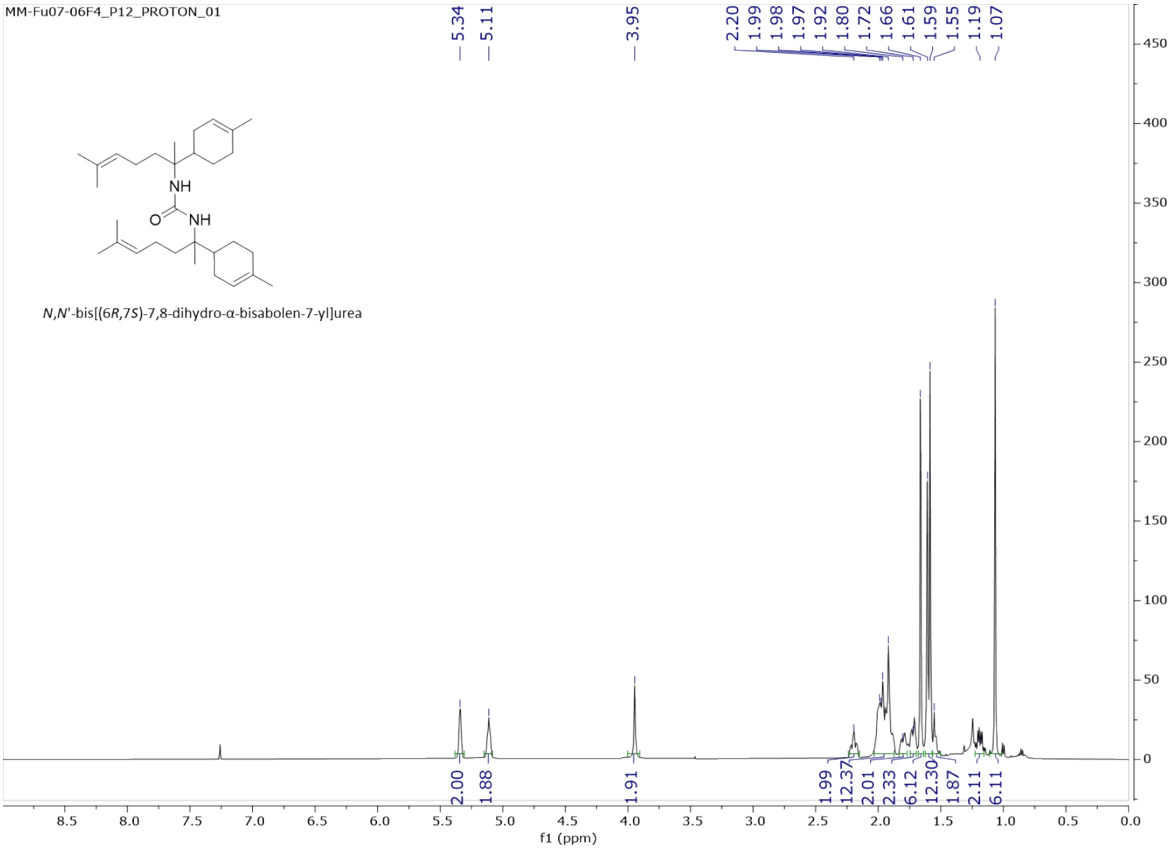

Figure S83. ^{1}H-NMR spectrum of N,N'-bis[(6R,7S)-7-amino-7,8-dihydro-α-bisabolen-7-yl] at 600 MHz in $CDCl_3$

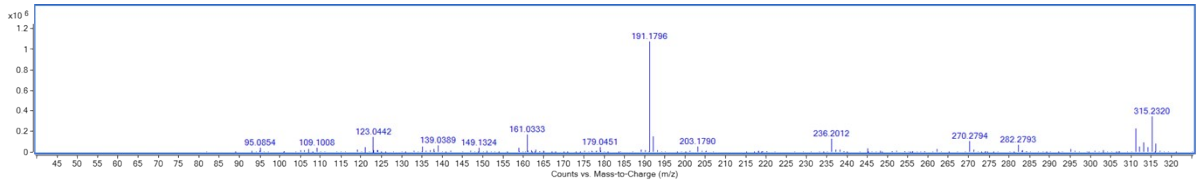

Figure S84. (+)-HRESIMS spectrum of aureol

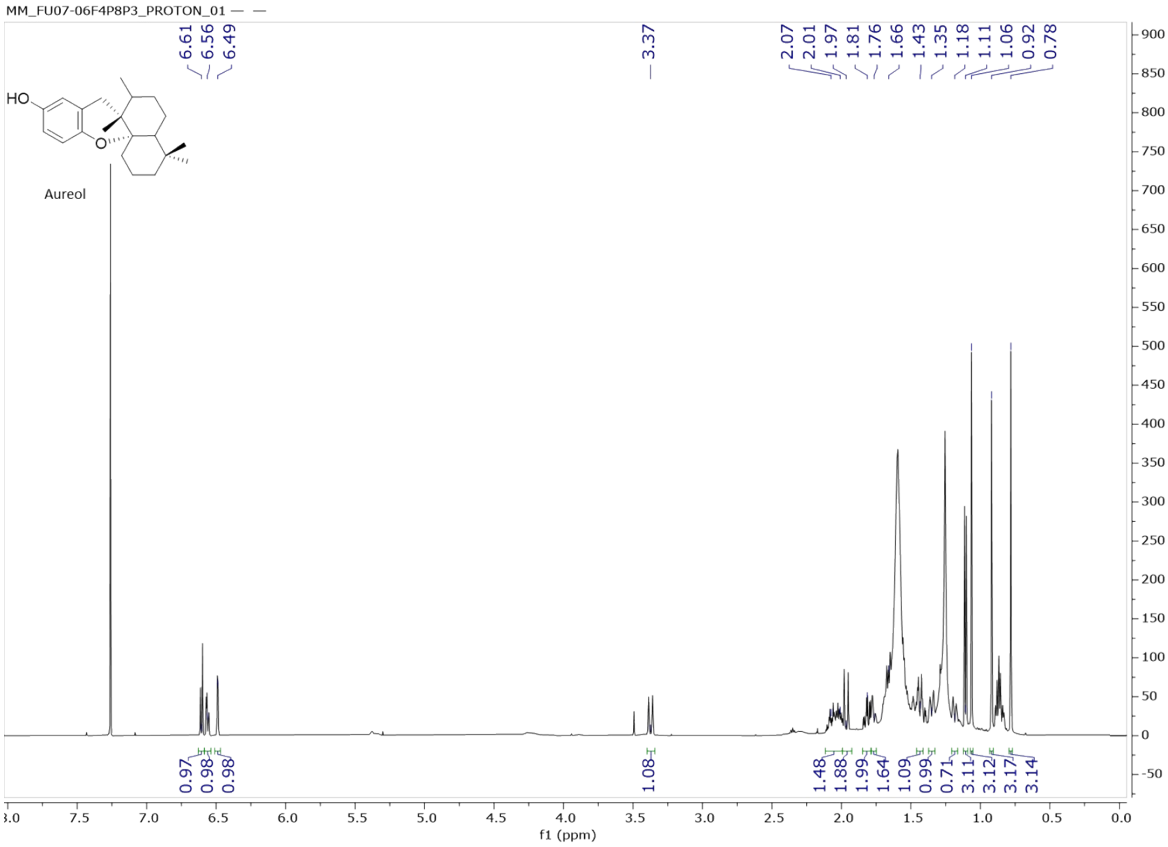

Figure S85. ^{1}H-NMR spectrum of aureol at 600 MHz in $CDCl_3$

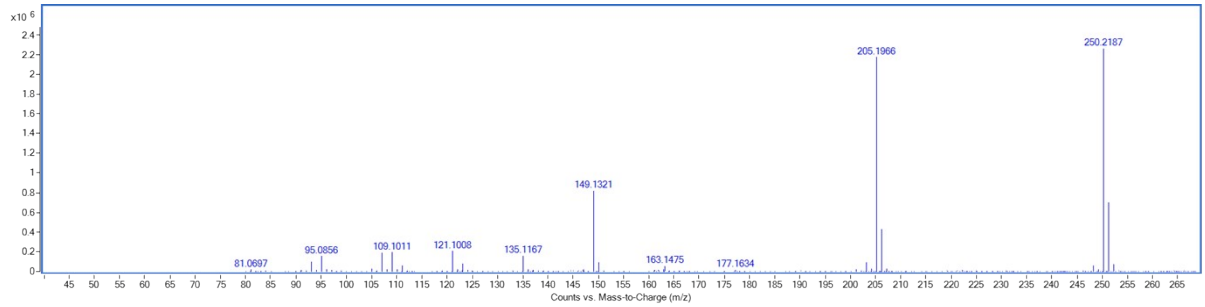

Figure S86. (+)-HRESIMS spectrum of theonellin formamide

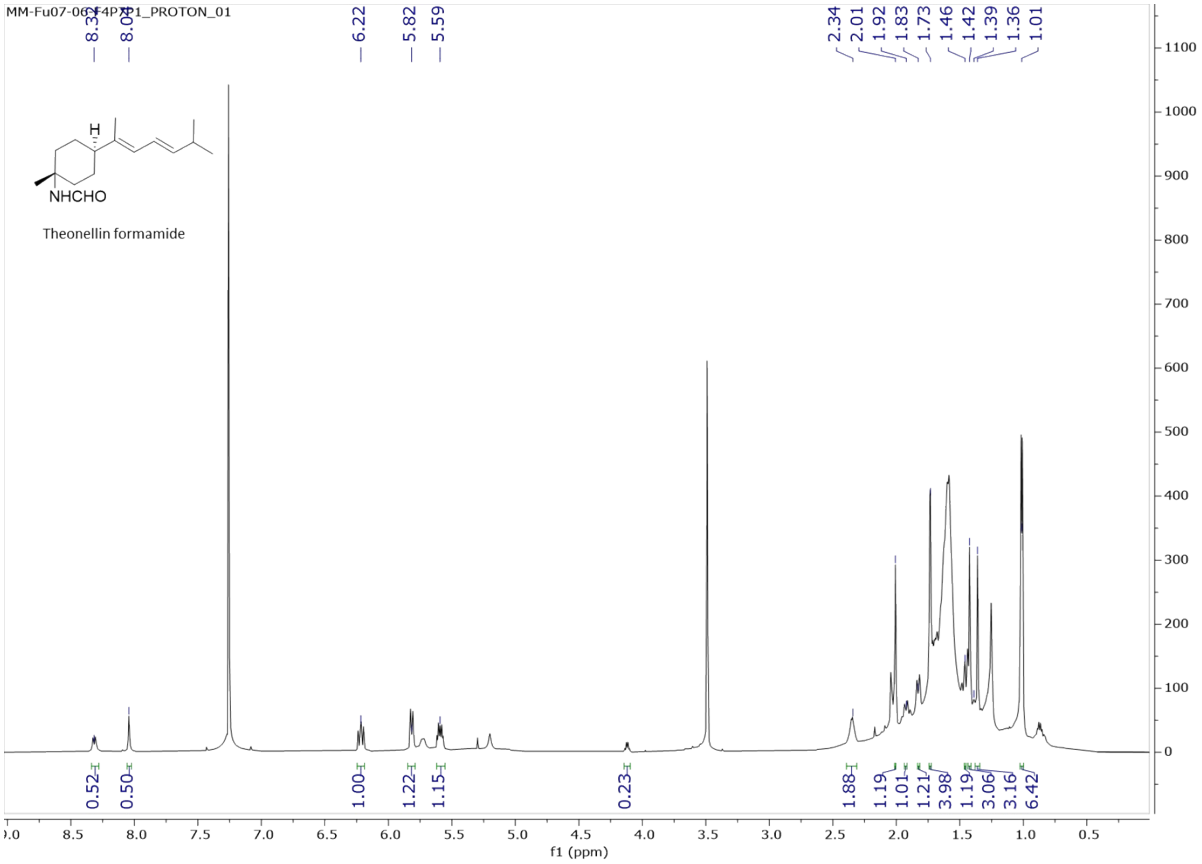

Figure S87. ^{1}H-NMR spectrum of theonellin formamide at 500 MHz in $CDCl_3$

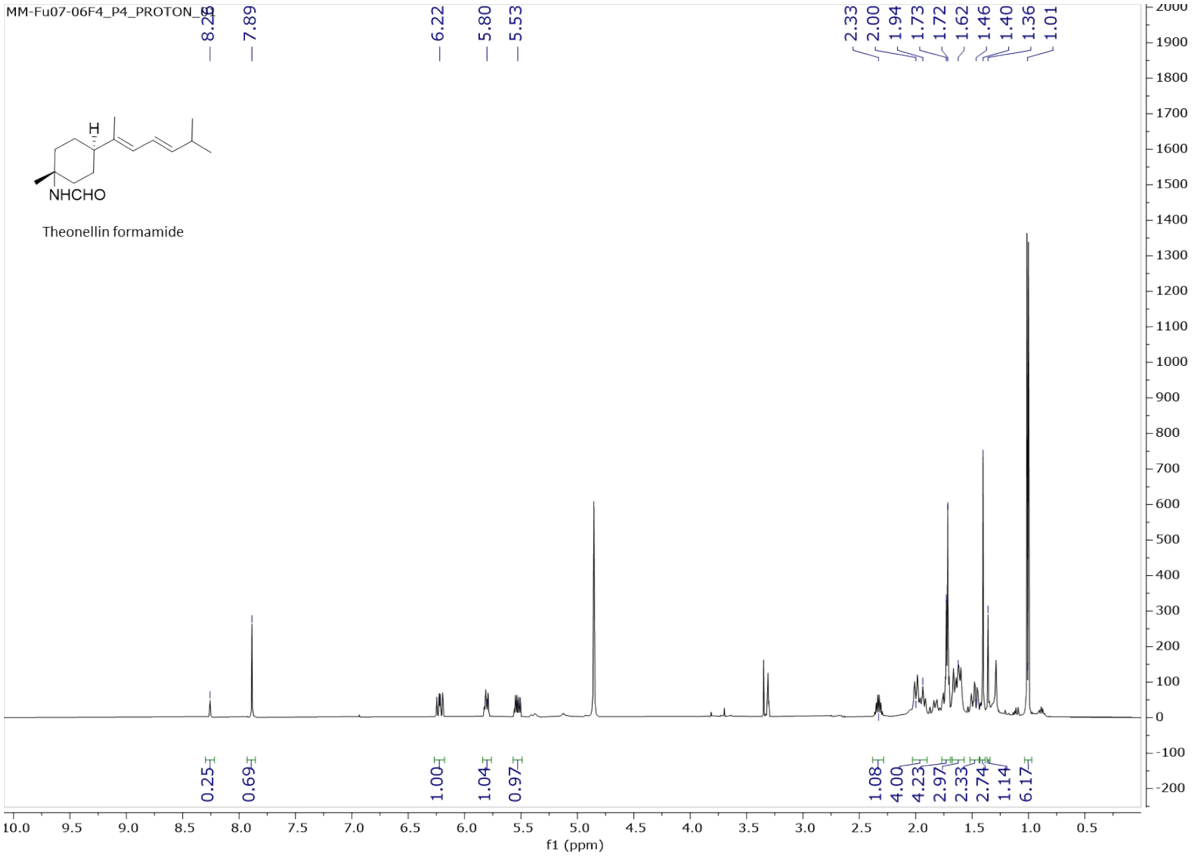

Figure S88. ^{1}H-NMR spectrum of theonellin formamide at 500 MHz in CD_3OD

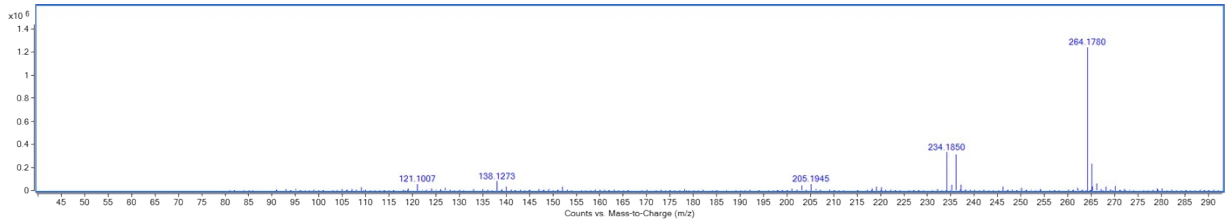

Figure S89. (+)-HRESIMS spectrum of 7-isothiocyanato-7,8-dihydro-α-bisabolene

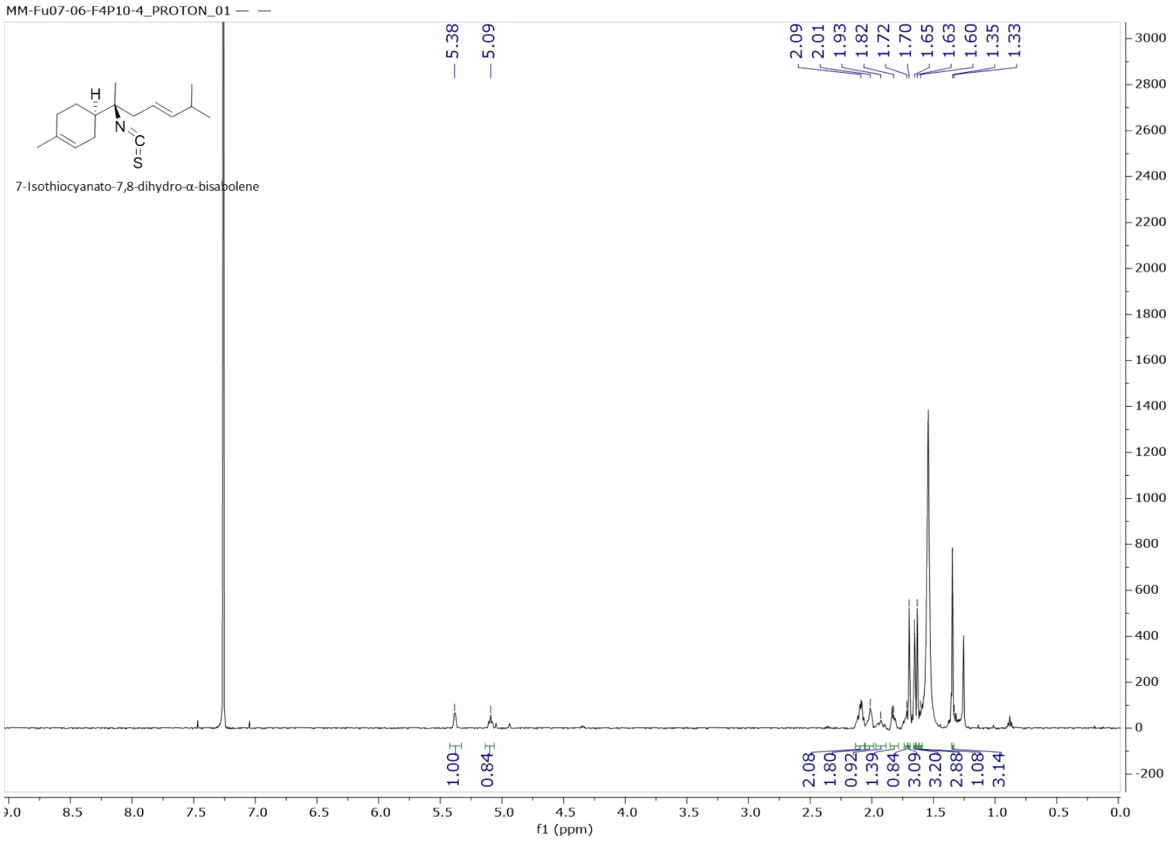

Figure S90. ^{1}H-NMR spectrum of 7-isothiocyanato-7,8-dihydro-α-bisabolene at 500 MHz in $CDCl_3$

SUPPLEMENTARY INFORMATION

TARA PACIFIC CONSORTIUM

The members of the Tara Pacific Consortium are as follows: Planes S. (1), Allemand D. (2), Agostini S. (15), Armstrong E. (20), Audrain S. (12), Aury J.-M. (20), Banaig B. (1), Barbe V. (20), Belser C. (20), Beraud E. (2), Boissin E. (1), Bonnival E. (22), Boss E. (13), Bourdin G.(13), Bourgois E. (12), Bowler C. (25), Carradec Q. (20), Cassar N. (27, 28), Cohen N. R. (30), Conan P. (10), Cronin D. R. (19), da Silva O. (17), de Vargas C. (22), Djerbi N. (3), Dolan J. R.(17), Dominguez Herta G. (19), Douville E. (14), Du J. (19), Filée J. (32), Flores J. M. (8), Forcioli D. (3), Friedrich R. (26), Furla P. (3), Galand P. E. (11), Ghiglione J.-F. (10), Gilson E. (3), Gorsky G. (17), Guinther M. (15), Hae¨ntjens N. (13), Henry N. (22), Hertau M. (12), Hochart C. (11), Hume B. C. C. (4), Iwankow G. (1), John S. G. (29), Karp-Boss L. (13), Kelly R. L. (29), Kitano Y. (16), Klinges G. (21), Koren I. (8), Labadie K. (20), Lancelot J. (12), Lang-Yona N. (9), Lê-Hoang J. (20), Lemee R. (17), Lin Y. (27), Lombard F. (17), Marie D. (22), McMind R. (3), Miguel-Gordo M. (24), Trainic M. (8), Monmarche D. (12), Moulin C. (12), Mucherie Y. (12), Noel B. (20), Ottaviani A. (3), Paoli L. (7), Pedrotti M.-L. (17), Pesant S. (23), Pogoreutz C. (4), Poulain J. (20), Pujo-Pay M. (10), Reverdin G. (31), Reynaud S. (2), Romac S. (22), Röthig T. (5), Rottinger E. (3), Rouan A. (3), Ruscheweyh H.-J. (7), Salazar G. (7), Sullivan M. B. (18), Sunagawa S. (7), Thomas O. P. (24), Troublé R. (12), Vardi A. (9), Vega-Thunder R. (21), Voolstra C. R. (4), Wincker P. (20), Zahed A. (19), Zamoum T. (3), Ziegler M. (6), and Zoccola D. (2) on behalf of the consortium Tara Pacific. With (1) PSL Research University: EPHE-UPVD-CNRS, USR 3278 CRIOBE, Université de Perpignan, France; (2) Centre Scientifique de Monaco, Principality of Monaco; (3) Université Côte d'Azur, CNRS, Inserm–IRCAN; (4) Department of Biology, University of Konstanz, Konstanz, Germany; (5) Aquatic Research Facility, Environmental Sustainability Research Centre, University of Derby, Derby, United Kingdom; (6) Department of Animal Ecology & Systematics, Justus Liebig University, Giessen, Germany; (7) Department of Biology, Institute of Microbiology and Swiss Institute of Bioinformatics, ETH Zürich, Zürich, Switzerland; (8) Weizmann Institute of Science, Dept. Earth and Planetary Science, Israel; (9) Weizmann Institute of Science, Dept. Plant and Environmental Science, Israel; (10) Sorbonne Université, CNRS, LOMIC, Observatoire Océanologique de Banyuls; (11) Sorbonne Université, CNRS, LECOB, Observatoire Océanologique de Banyuls; (12) Tara Ocean Foundation, Paris, France; (13) School of Marine Sciences, University of Maine, United States of America; (14) Laboratoire des Sciences du Climat et de l'Environnement, LSCE/IPSL, CEA-CNRS-UVSQ, Université Paris-Saclay, France; (15) Shimoda Marine Research Center, University of Tsukuba, Shizuoka, Japan; (16) National Institute of Environmental Science, Japan; (17) Sorbonne Universite´, Institut de la Mer de Villefranche sur mer, Laboratoire d'Océanographie de Villefranche, France; (19) The Ohio State University, Departments of Microbiology and Civil, Environmental and Geodetic Engineering, Columbus, Ohio, United States of America and The Ohio State University, Departments, Columbus, Ohio, United States of America; (20) Ge´nomique Me´tabolique, Genoscope, Institut François Jacob, CEA, CNRS, Univ Evry, Université Paris-Saclay, Evry, France; (21) Oregon State University, Department of Microbiology, Oregon, United States of America; (22) Sorbonne Université, CNRS, Station Biologique de Roscoff, AD2M, UMR 7144, ECOMAP, Roscoff, France; (23) PANGAEA, Data Publisher for Earth and Environment Science, Bremen, Germany &MARUM—Center for Marine Environmental Sciences, Universität Bremen, Bremen, Germany; (24) Marine Biodiscovery Laboratory, School of Chemistry and Ryan Institute, National University of Ireland, Galway, Ireland; (25) Institut de Biologie de l'Ecole Normale Supérieure (IBENS), Ecole normale supérieure, CNRS, INSERM, Université PSL, Paris, France; (26) World Courier, an AmerisourceBergen Company, Russelsheim, Germany; (27) Division of Earth and Ocean Sciences, Duke University, Durham, North Carolina, United States of America; (28) Laboratoire des Sciences de l'Environnement Marin (LEMAR), UMR 6539 UBO/ CNRS/IRD/IFREMER, Institut Universitaire Européen de la Mer (IUEM), Brest, France; (29) Department of Earth Sciences, University of Southern California, Los Angeles, California, United States of America; (30) Marine Chemistry and Geochemistry Department, Woods Hole Oceanographic Institution; (31) Institut Pierre Simon Laplace, CNRS/IRD/MNHN (LOCEAN)Sorbonne-Université Paris Cedex 05, France; (32) Laboratoire Evolution, Génomes, Comportement et Ecologie, CNRS/Université Paris-Saclay, Avenue de la Terrasse, Gif sur Yvette, France. S. Planes and D. Allemand are joint scientific directors of Tara Pacific.